TRANSPORTATION RESEARCH RECORD 715

Pavement Distress, Evaluation, and Performance

TRANSPORTATION RESEARCH BOARD

COMMISSION ON SOCIOTECHNICAL SYSTEMS
NATIONAL RESEARCH COUNCIL

NATIONAL ACADEMY OF SCIENCES
WASHINGTON, D.C. 1979

The Transportation Research Board is an agency of the National Research Council, which serves the National Academy of Sciences and the National Academy of Engineering. The Board's purpose is to stimulate research concerning the nature and performance of transportation systems, to disseminate information that the research produces, and to encourage the application of appropriate research findings. The Board's program is carried out by more than 150 committees and task forces composed of more than 1800 administrators, engineers, social scientists, and educators who serve without compensation. The program is supported by state transportation and highway departments, the major administrations of the U.S. Department of Transportation, the Association of American Railroads, and other organizations interested in the development of transportation.

The Transportation Research Board operates within the Commission on Sociotechnical Systems of the National Research Council. The Council was organized in 1916 at the request of President Woodrow Wilson as an agency of the National Academy of Sciences to enable the broad community of scientists and engineers to associate their efforts with those of the Academy membership. Members of the Council are appointed by the president of the Academy and are drawn from academic, industrial, and governmental organizations throughout the United States.

The National Academy of Sciences was established by a congressional act of incorporation signed by President Abraham Lincoln on March 3, 1863, to further science and its use for the general welfare by bringing together the most qualified individuals to deal with scientific and technological problems of broad significance. It is a private, honorary organization of more than 1000 scientists elected on the basis of outstanding contributions to knowledge and is supported by private and public funds. Under the terms of its congressional charter, the Academy is called upon to act as an official–yet independent–advisor to the federal government in any matter of science and technology, although it is not a government agency and its activities are not limited to those on behalf of the government.

To share in the task of furthering science and engineering and of advising the federal government, the National Academy of Engineering was established on December 5, 1964, under the authority of the act of incorporation of the National Academy of Sciences. Its advisory activities are closely coordinated with those of the National Academy of Sciences, but it is independent and autonomous in its organization and election of members.

Transportation Research Record 715
Price $4.20
Edited for TRB by Mary McLaughlin

modes
1 highway transportation
4 air transportation

subject area
24 pavement design and performance

Transportation Research Board publications are available by ordering directly from TRB. They may also be obtained on a regular basis through organizational or individual affiliation with TRB; affiliates or library subscribers are eligible for substantial discounts. For further information, write to the Transportation Research Board, National Academy of Sciences, 2101 Constitution Avenue, N.W., Washington, DC 20418.

Library of Congress Cataloging in Publication Data
National Research Council. Transportation Research Board.
Pavement distress, evaluation, and performance.

(Transportation research record; 715)
1. Pavements–Evaluation–Addresses, essays, lectures. 2. Pavements–Testing–Addresses, essays, lectures. I. Title. II. Series.
TE7.H5 no. 715 [TE250] 380.5'08s [625.8'028]
ISBN 0-309-02962-7 ISSN 0361-1981 79-607814

Sponsorship of the Papers in This Transportation Research Record

GROUP 2–DESIGN AND CONSTRUCTION OF TRANSPORTATION FACILITIES
Eldon J. Yoder, Purdue University, chairman

Pavement Design Section
Carl L. Monismith, University of California, Berkeley, chairman

Committee on Rigid Pavement Design
Ronald L. Hutchinson, U.S. Army Engineer Waterways Experiment Station, chairman
Kenneth J. Boedecker, Jr., William E. Brewer, William J. Carson, James I. Clark, Bert E. Colley, Donald K. Emery, Jr., Wade L. Gramling, Yang H. Huang, T. J. Larsen, B. Frank McCullough, Robert G. Packard, Frazier Parker, Jr., Thomas J. Pasko, Jr., Dwight E. Patton, Karl H. Renner, Surendra K. Saxena, Don L. Spellman, T. C. Paul Teng, William A. Yrjanson

Committee on Surface Properties–Vehicle Interaction
Don L. Ivey, Texas A&M University, chairman
Glenn G. Balmer, Frederick E. Behn, John C. Burns, A. Y. Casanova III, Robert D. Ervin, Michael W. Fitzpatrick, Kenneth D. Hankins, Carlton M. Hayden, Rudolph R. Hegmon, Kenneth J. Law, David C. Mahone, James A. Matthews, W. E. Meyer, Thomas H. Morrow, Jr., W. Grigg Mullen, Arthur H. Neill, Jr., Bayard E. Quinn, John J. Quinn, J. Reichert, Hollis B. Rushing, Richard K. Shaffer, Elson B. Spangler, James C. Wambold, E. A. Whitehurst, Ross G. Wilcox

Committee on Pavement Condition Evaluation
K. H. McGhee, Virginia Highway and Transportation Research Council, chairman
Michael I. Darter, Edwin J. Dudka, Karl H. Dunn, Asif Faiz, Wouter Gulden, William H. Highter, W. Ronald Hudson, L. B. R. Hunter, Don H. Kobi, J. W. Lyon, Jr., R. D. Pavlovich, William A. Phang, Bayard E. Quinn, Freddy L. Roberts, Albert F. Sanborn III, Lawrence L. Smith, Paul N. Sonnenburg, Herbert F. Southgate, Elson B. Spangler, Robert J. Weaver, Loren M. Womack

Committee on Theory of Pavement Design
Ralph C. G. Haas, University of Waterloo, chairman
G. H. Argue, Yu T. Chou, Santiago Corro Caballero, Michael I. Darter, Paul J. Diethelm, David C. Esch, Fred N. Finn, Per E. Fossberg, W. Ronald Hudson, Lynne H. Irwin, Ali S. Kemahli, William J. Kenis, Ramesh Kher, Robert L. Lytton, Carl L. Monismith, Leon M. Noel, Robert G. Packard, Dale E. Peterson, James F. Shook, William T. Stapler, Ronald L. Terrel, Kornelis Wester, E. B. Wilkins

Committee on Strength and Deformation Characteristics of Pavement Sections
Richard D. Barksdale, Georgia Institute of Technology, chairman
S. F. Brown, Jim W. Hall, Jr., Amir N. Hanna, R. G. Hicks, Frank L. Holman, Jr., Ignat V. Kalcheff, Bernard F. Kallas, William J. Kenis, Thomas W. Kennedy, Kamran Majidzadeh, Fred Moavenzadeh, Lutfi Raad, Quentin L. Robnett, Jatinder Sharma, Eugene L. Skok, Jr., Ronald L. Terrel, Peter J. Van de Loo

Lawrence F. Spaine, Transportation Research Board staff

Sponsorship is indicated by a footnote at the end of each report. The organizational units and officers and members are as of December 31, 1978.

Contents

Structural Distress Mechanisms in Continuously Reinforced Concrete Pavement

Michael I. Darter, Department of Civil Engineering, University of Illinois at Urbana-Champaign
Scott A. LaCoursiere, Illinois Department of Transportation, Dixon
Scott A. Smiley, Brown and Root, Inc., Houston, Texas

A study of distress types and mechanisms in continuously reinforced concrete pavement in Illinois is reported. The major purpose of the study was to determine types and amounts of distress so that improved maintenance and design procedures could be developed. The approximately 1979 km (1230 miles) of Interstate highway surveyed consisted of 18- to 25-cm (7- to 10-in) slabs over granular and stabilized subbases. Edge punchouts, steel ruptures, D-cracking, blowups, joint failures, lug rotation, longitudinal cracking, construction-related distress, pumping, and shoulder deterioration were found. Since the edge punchout is the major structural distress, its mechanism was studied in depth. Heavy truck loads, excess free moisture, deicing salts, construction practice, and poor aggregate quality in the slab are the major causes of distress. Slab thickness and foundation support have a very significant effect on the development of structural distress. D-cracking is causing severe deterioration on several projects. Overall, the performance of the thicker [23- to 25-cm (9- to 10-in)] slabs has been excellent under heavy truck traffic, but a number of thinner [18- to 20-cm (7- to 8-in)] sections have performed poorly and are showing an accelerated rate of distress development over time. The amount of distress that is expected to occur in the future indicates a need for more efficient and durable ways of maintaining continuously reinforced concrete pavement and for revised design procedures.

A study of the occurrence of edge punchouts in continuously reinforced concrete pavement (CRCP) in Illinois has been conducted. The purpose of the study was to determine the amount of this type of distress and the specific mechanism that causes it. This study represents part of the first phase of an overall effort aimed at the development of optimal maintenance procedures for CRCP. A comprehensive study of all types of distress in CRCP is provided elsewhere (1).

The state of Illinois has constructed 3226 equivalent two-lane km (2000 two-lane miles) of CRCP on the Interstate highway system. A detailed condition survey was conducted on 1979 km (1230 miles), or 132 projects. These projects range in age from 5 to 15 years. Slab thickness ranges from 18 to 25 cm (7 to 10 in). The subbases were initially granular but since about 1965 have been stabilized with asphalt or cement. Both deformed rebar and welded wire fabric have been used as reinforcement. Many of the projects that are located on heavily traveled routes are approaching or have exceeded their design traffic and are showing significant distress at an increasing rate.

DESCRIPTION OF EDGE PUNCHOUTS

Edge punchouts, the major structural distress found in CRCP, occur when a portion of the concrete slab near the outside edge of the truck lane between two closely spaced transverse cracks breaks off and subsequently punches downward. Edge punchouts have only occurred along the outer edge of the truck lane. A type of punchout that occurs in the center of the lane is caused by other factors (generally lack of consolidation) and should not be confused with edge punchouts, which are caused primarily by traffic load and loss of support.

An edge punchout is first characterized by a loss of aggregate interlock at one or two cracks that are usually spaced less than 122 cm (48 in) apart. The crack or cracks begin to fault and spall slightly, and this causes the portion of the slab between the closely spaced cracks to act essentially as a cantilever beam. As heavy truck loads continue, a short, longitudinal crack forms between the two transverse cracks about 61-152 cm (24-60 in) from the pavement edge. Eventually, the transverse cracks break down further, the steel ruptures, and the pieces of concrete punch downward into the subbase and subgrade, causing a very serious traffic hazard. There is generally evidence of pumping and settlement—and sometimes extensive pumping—near edge punchouts. If it is not repaired, the distressed area will expand in size to adjacent transverse cracks and become quite large.

FIELD RESULTS

Edge punchouts per kilometer versus total accumulated 80-kN [18 000-lb (18-kip)] equivalent single-axle loads (ESALs) in the outside truck lane are plotted for all 18- to 25-cm (7- to 10-in) projects in Figures 1-3. This value was computed for each project by adding the number of observed edge punchouts plus those previously patched in the truck lane of the project and dividing by the length of the project.

All CRCP slab thicknesses show an increase in punchouts per kilometer as traffic loads accumulate. For any given traffic level, the thicker the CRCP slab is, the fewer the edge punchouts that occur. Figure 4 shows a comparative plotting of the mean curves for each CRCP thickness. These curves should be considered overall averages only since there is a large scatter in the data about each curve. In addition to the relation between the thickness of the CRCP slab and the number of edge punchouts, the data show that the amount of distress increases curvilinearly with repeated traffic loadings.

The relative performance of each CRCP thickness with respect to the total number of 80-kN ESAL applications can also be plotted as shown in Figure 5. This figure shows 80-kN ESALs (in the truck lane) versus the cumulative percentage of projects that have more than 0 punchouts/km. More than 70 percent of all 18-cm (7-in) thick projects have some punchouts after 4 million 80-kN ESALs. After 8 million, almost 70 percent of all 20-cm (8-in) thick projects have some punchouts, whereas only 45 percent of 23-cm (9-in) thick projects show punchouts. After as many as 10 million or more 80-kN ESALs, 0 percent of the 25-cm (10-in) thick projects show edge punchouts.

Another distribution shows that almost 70 percent of the 20-cm-thick projects show punchouts after 8

Figure 1. Traffic loadings versus edge punchouts for 18-cm-thick CRCP.

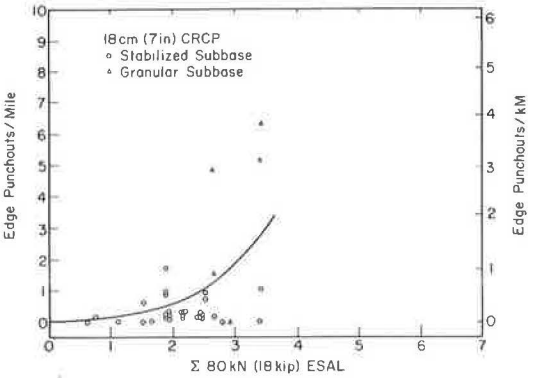

Figure 2. Traffic loadings versus edge punchouts for 20-cm-thick CRCP.

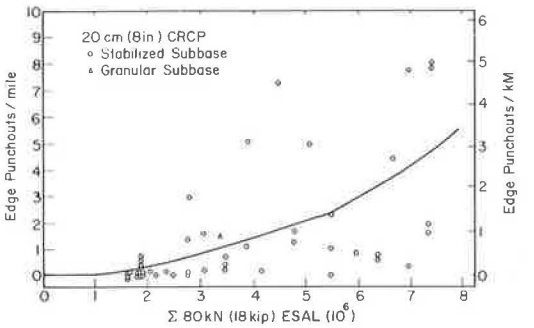

Figure 3. Traffic loadings versus edge punchouts for 25- and 23-cm-thick CRCP.

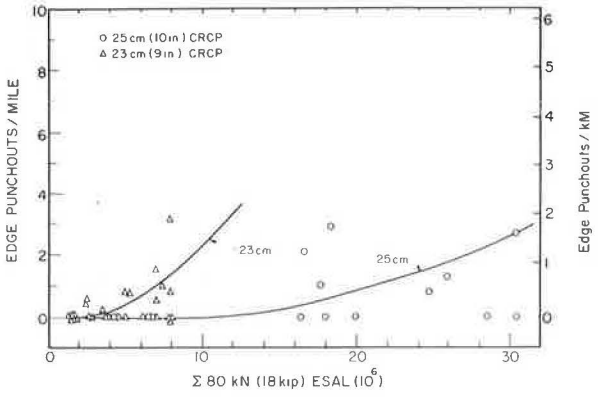

million 80-kN ESALs, 38 percent show more than 0.6 punchout/km (1 punchout/mile), 21 percent more than 1.2 punchouts/km (2 punchouts/mile), and 9 percent more than 3.7 punchouts/km (6 punchouts/mile). The proportion of projects that show punchouts increases with accumulated traffic loadings.

STRESS ANALYSIS

A stress analysis was conducted by using a finite-element computer program developed and validated at the University of Illinois (2). The program is capable of determining stresses and deflections in CRCP that has full support or that shows a loss of subgrade support attributable to pumping. Parameters such as slab thickness, subgrade support, transverse crack spacing

Figure 4. Traffic loadings versus mean edge punchouts for 18-, 20-, 23-, and 25-cm-thick CRCP.

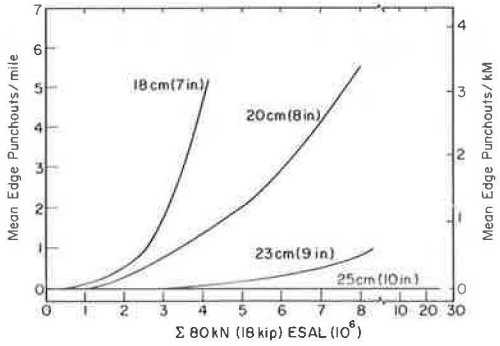

Figure 5. Relative performance of each CRCP thickness with > 0 edge punchouts.

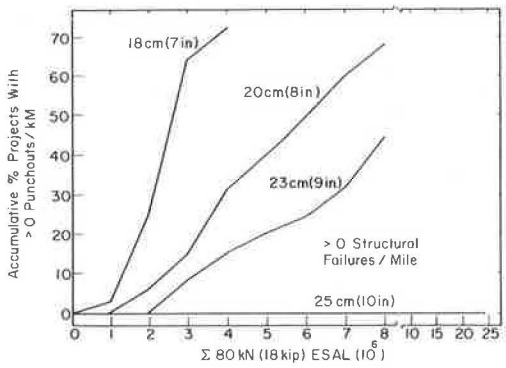

and load-transfer efficiency, and the lateral position of load were studied. The program output gives stresses at the top and bottom of the slab and the deflection of each node as they correspond to a grid system determined by the user.

The critical stress that causes edge punchouts occurs when the wheel of a truck is located near the slab edge. Figure 6 shows a high tensile stress occurring at the top of the slab at a distance T from the edge of the pavement. This stress is highly dependent on the amount of load transfer across the transverse cracks. It would occur when there is no such load or moment transfer. This would be representative of the slab only after the transverse cracks have opened up and aggregate interlock is lost and some of the reinforcement has ruptured. This effect is shown in Figure 6, where the maximum transverse stress is computed over a range of crack spacing for full and zero load transfer across the transverse cracks. The transverse stress becomes considerably greater as crack spacing shortens and load transfer is lost.

Critical tensile stress depends on several pavement and load variables and on the distance T, which is also variable. Results show that, as the outside wheel load is moved inward from the edge of the pavement just 30 cm (12 in), not only does the critical stress decrease by 50 percent but also the maximum stress moves from 91 to 122 cm (36 to 48 in) from the slab edge.

Figure 7 shows that slab thickness has a very significant effect on critical stresses as the maximum tensile stress increases by 76 percent, from 1758 kPa (255 lbf/in^2) for a 25-cm (10-in) slab to 3096 kPa (449 lbf/in^2) for an 18-cm (7-in) slab. Note that the location of the maximum stress is 91 cm (36 in) from the slab edge. The relative effect of slab thickness on edge

Figure 6. Effect of load transfer across transverse cracks and crack spacing on critical transverse tensile stress in CRCP slab.

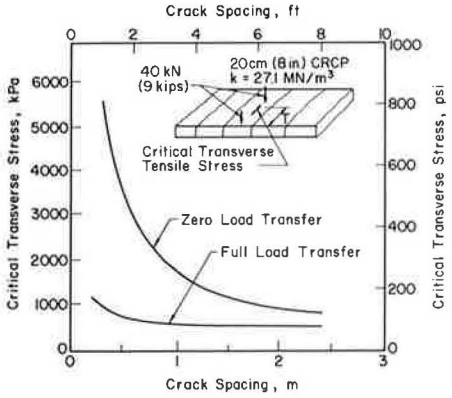

Figure 7. Effect of slab thickness on maximum tensile stress.

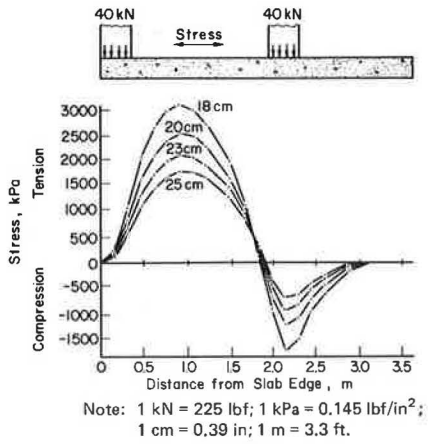

Note: 1 kN = 225 lbf; 1 kPa = 0.145 lbf/in^2; 1 cm = 0.39 in; 1 m = 3.3 ft.

Figure 8. Effect of crack spacing on maximum tensile stress with zero load transfer across transverse cracks.

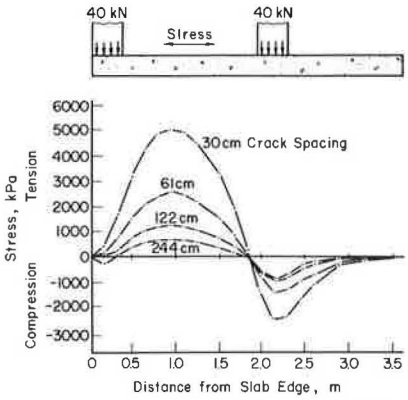

Note: 1 kN = 225 lbf; 1 kPa = 0.145 lbf/in^2; 1 cm = 0.39 in; 1 m = 3.3 ft.

Figure 9. Effect of erodibility on maximum tensile stress and its distance from slab edge.

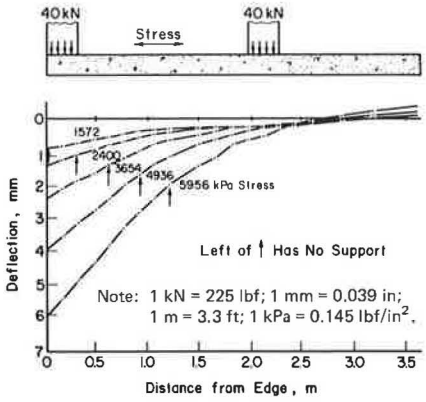

Note: 1 kN = 225 lbf; 1 mm = 0.039 in; 1 m = 3.3 ft; 1 kPa = 0.145 lbf/in^2.

punchouts is shown in Figure 4. Thus, increased slab thickness has a considerable effect on reducing critical stress, which in turn results in a reduction of edge punchouts.

As Figure 8 shows, crack spacing has the most dramatic effect on stress. For a 20-cm (8-in) thick slab over a foundation k-value of 54.2 N/cm^3 (200 lbf/in^3), the maximum tensile stress increases from 731 kPa (106 lbf/in^2) at a crack spacing of 244 cm (96 in) to 5069 kPa (735 lbf/in^2) at a crack spacing of 30 cm (12 in). This is important because many edge punchouts occur in areas where there is "cluster cracking"—the formation of several cracks at an average spacing of about 30-61 cm (12-24 in). Again, note that the maximum stress occurs 91 cm (36 in) from the slab edge.

The majority of edge punchouts have occurred between cracks spaced 30-91 cm apart, and the short, longitudinal crack has usually occurred 61-152 cm (24-60 in) from the slab edge. In most cases in which the longitudinal crack has formed at greater distances from the edge—i.e., 152 cm—there had been extensive pumping, which indicated loss of support (see Figure 9). Very seldom has an edge punchout occurred where cracks were spaced 122 cm (48 in) or more apart or where a longitudinal crack was less than 61 cm or more than 152 cm from the slab edge. This is illustrative of the fact that the tensile stress under the inner wheel is much less than that under the outer wheel near the slab edge.

Changing the k-value from 13.5 N/cm^3 (50 lbf/in^3), which is typical of a fine-grained, saturated soil subgrade, to 135.5 N/cm^3 (500 lbf/in^3), which is typical of a stabilized subbase over a granular subgrade, decreases the transverse stress by 34 percent. Figure 9 shows the effect of loss of subgrade support along the slab edge. As the loss of support increases, in addition to the increase in deflections and the movement of the point of maximum stress inward from the pavement edge, the stresses increase dramatically [52 percent for a 30-cm (12-in) loss of support].

Field observations and past experience have indicated that a granular subbase has a high tendency to pump under moisture and load conditions in Illinois. This pumping causes a loss of support along the edge, increased stresses, and higher potential for edge punchouts. The results shown in Figure 1 indicate that the only sections of 18-cm (7-in) thick CRCP that had more than 1.2 punchouts/km (2 punchouts/mile) were those sections with a granular subbase that pumped. Sections constructed with a stabilized subbase contained fewer edge punchouts.

The effect of a good foundation support can be seen by observing the performance of a project on I-70 that was constructed in 1967. The westbound lane was constructed by placing the CRCP slab over an old jointed reinforced concrete slab that was overlayed with asphalt concrete. No edge punchouts have occurred in this lane. The eastbound lane was constructed with a typical stabilized subbase over a new alignment. Almost 3 punchouts/km (5 punchouts/mile) have occurred in the eastbound lane. Traffic was heavy in both directions

Figure 10. Crack pattern and deflections at cores 2 and 4.

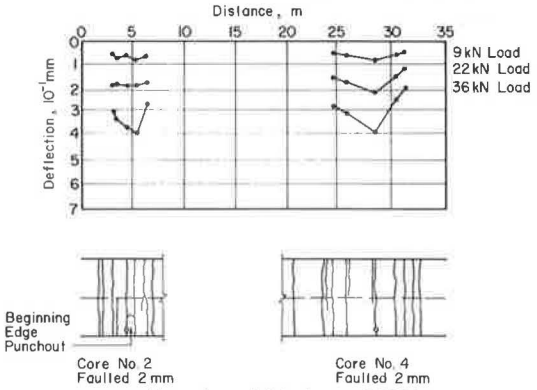

Figure 11. Crack pattern and deflections at cores 1 and 3.

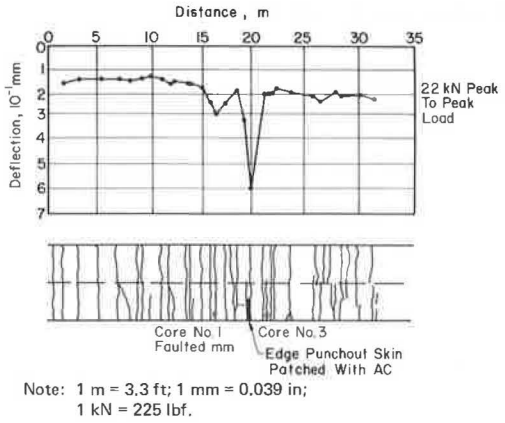

and approximately equivalent (6.7 million 80-kN ESALs). The effect of the underlying portland cement concrete (PCC) slab in providing increased support is evident. In addition, local maintenance personnel indicated that, on several projects that had an above-average number of punchouts, the stabilized subbase had deteriorated and loss of support was a major cause.

STUDY OF DEFLECTIONS AND CORES

One project on I-57 has experienced many edge punchouts. It was believed that studying deflections and core samples might help in determining the causes. A vibratory deflection device (road rater) owned by the Illinois Department of Transportation that can apply up to 35.5 kN (8000-lbf) peak-to-peak vibratory load was used. Deflections were taken continuously over a 61-m (200-ft) section and at four other sections within a test area of 198 m (650 ft). Core samples were taken at four locations that corresponded with certain of the areas of deflection measurement. The cores were taken approximately 30 cm (12 in) from the slab edge in an attempt to sample the second reinforcing bar. Figures 10 and 11 show the CRCP crack pattern and deflections and the locations of the cores taken.

Core 1 was taken at what appeared to be a typical tight crack. It was noticed that this crack had twice the deflection of the immediately adjacent cracks. On further examination, it was found that the crack had faulted approximately 1 mm (0.04 in), and it was decided to take a core sample. The rebar was corroded nearly all the way through, and considerable concrete was missing around the bar (thus only minimal aggregate interlock was present).

Core 2 was taken at a crack that typified the beginning stages of an edge punchout. The crack had faulted 2 mm (0.08 in), and the deflection was high at the punchout. A short, longitudinal crack had formed approximately 152 cm (60 in) from the edge, and the transverse crack spacing was 63 cm (25 in). Again, there was extensive rebar corrosion and concrete deterioration in the core.

Core 3 was taken over a very tight crack. It was believed that there would be no corrosion or deterioration. The crack became microscopic just below the surface of the slab, and the core had to be broken apart to observe the steel that was not corroded. The deflection at this crack was similar to that at other tight cracks.

Core 4 was taken over a crack that had spalled considerably but had not yet opened extensively. Results showed that the rebar had ruptured and there was a void in the concrete around the rebar as in cores 1 and 2. The rebar was necked down on both ends as a result of corrosion.

These results and other observations made during patching operations indicate that, when a crack shows any faulting at all [i.e., as little as 1 mm (0.04 in)], it is reasonable to assume either that corrosion has been significant enough to reduce the cross-sectional area of steel or that there has been a considerable loss of aggregate interlock. Deflections were markedly greater at each of the three locations that had faulted than they were at immediately adacent cracks where there was no faulting. The high deflections are also an indication of a void under the slab. Water was introduced into core holes 1, 2, and 4 for 10 min by means of a hose connected to a water barrel. The water never filled up the holes. Thus, there must have been extensive voids at these locations. The cement-aggregate-mixture (CAM) subbase could not be cored at any of the four holes (it disintegrated during coring).

It is believed that deflections can be used to locate areas that may be in early stages of distress. For future study, however, it should be noted that the magnitude of load needed to get adequate information is relatively high. As Figure 10 shows, a vibratory load of 8.9 kN (2000 lbf) does not adequately produce deflections that will indicate the true loss of support. Thus, it is recommended that peak-to-peak loads of 22.2 kN (5000 lbf) or more be used so that distressed areas can be located.

MECHANISM OF EDGE PUNCHOUTS

The development of the typical edge punchout in CRCP is a complex phenomenon that may have more than one basic cause. The following analysis is based on field observations of many edge punchouts and the information given above.

A localized loss of support beneath the slab that results in relatively high deflection is the primary causative factor in edge punchouts. Deflections measured near the point of initiation of a punchout were invariably much higher than those in the adjoining CRCP. Loss of support had occurred in several ways, including accumulation of free moisture in a "soft" localized subgrade area, localized disintegration of a stabilized subbase course, and localized pumping of a stabilized or granular subbase course. High deflection will result in increased stress in the reinforcement under

load and also greater vertical shear that must be carried across a transverse crack. Experimental studies have shown that the wider the crack is the sooner the aggregate interlock will break down across the crack under repeated loadings (3). Other factors in addition to high localized deflections may cause a widening of the crack, including high tensile stress in the steel at the crack as a result of drying shrinkage or cold temperatures (4). An inadequate overlap of the reinforcing steel may prevent the transfer of all of the stress from one bar to another, allowing the bars to pull apart and resulting in an open crack. A loss of bond between the steel and the concrete in the vicinity of a crack would allow the stresses and strains in the steel to be applied over a longer length and result in greater crack width. The latter two causes have been verified in a report by Lepper and Kim (5).

Once a transverse crack has opened up somewhat, repeated heavy traffic loads may eventually break down the aggregate interlock (6, 7). In a study conducted by Colley and Humphrey (3), the load-transfer capabilities of aggregate-interlock systems for certain variables—including width of crack opening, thickness of concrete slab, magnitude of load, foundation support, and type of aggregate—were investigated. For a 23-cm (9-in) slab over 15 cm (6 in) of gravel base when the crack opening is 2 mm (0.065 in), the effectiveness of load transfer is reduced to 25 percent after only 400 000 load cycles. A more rapid deterioration occurs for an 18-cm (7-in) pavement.

As the aggregate interlock continues to break down, slight faulting and spalling of the crack appear near the slab edge. Continued traffic loadings reduce aggregate interlock even more, increasing both deflections and the critical transverse tensile stress at the top of the slab. The reinforcing steel, of course, resists the crack opening and faulting. But as aggregate interlock is lost, more and more of the vertical shear is transferred to the reinforcement, which eventually may rupture.

Corrosion may also have an effect. Whenever crack width becomes great enough to admit moisture, corrosion of the reinforcement may begin. Results obtained from National Cooperative Highway Research Program (NCHRP) Project 1-15 (4) indicate that crack width need not be very great since cracks with an opening as small as 0.6 mm (0.023 in) allowed enough moisture to reach the reinforcement to cause "minor" corrosion. The NCHRP report also shows that cracks wider than about 0.6 mm allowed rapid infiltration of surface water and caused "heavy" corrosion of the reinforcement. Corrosion was found at many distress areas where the reinforcing bars were necked down across a wide transverse crack. Observation and discussion with various maintenance personnel also indicated that corrosion of rebars at failed areas was common in some areas. However, the performance of CRCP in areas where no deicing salt is used indicates that edge punchouts occur even without corrosion. Thus, corrosion is believed to have an effect only after a crack has opened. The corrosion that does occur has two effects: It reduces the cross-sectional area of steel reinforcement, and its expansive forces fracture the concrete surrounding the steel and cause it to spall. Thus, as cores 1, 2, and 4 show, there is a void around the steel.

Then, because of increasing transverse tensile stresses and accumulated fatigue damage, a longitudinal crack eventually forms between the two transverse cracks. Under additional traffic loading, the aggregate interlock wears away completely, the steel begins to rupture at the outer bar near the slab edge, and the outside portion of the slab begins to depress into the subbase. Once the block of concrete begins to punch downward, pumping accelerates so that more and more support is lost under the slab, and fatigue may cause more longitudinal cracking, faulting, and spalling. The area eventually expands so much that a large patch is required. It is noted that, because fatigue, corrosion, loss of aggregate interlock, and pumping all increase with time and traffic, the occurrence of edge punchouts also accelerates with age and traffic.

EFFECTS OF DRAINAGE ON DISTRESS

One of the major factors that contributes to several types of distress is free moisture within the CRCP structure. Several recent studies have concluded that free water, largely in the form of surface infiltration of precipitation, is a primary causative or accelerating factor in many structural distresses (8-10). Most of the CRCPs surveyed had a "bathtub" cross section in which stabilized subbase and shoulders completely encased the CRCP slab. In addition, the slab-shoulder longitudinal joint is nearly always wide open and unsealed so that most precipitation that falls on the traffic lane can readily infiltrate the joint. The free water that infiltrates this joint does not have a flow path by which to escape and thus becomes entrapped. Many examples have been seen in which, at a low point in the profile, water "bleeds" out of the longitudinal joint and can be seen standing in the joint for several days after a rainstorm. This free water can thus saturate both the concrete and the subbase for long periods of time during the year. Some of the older designs used a granular subbase. The basic moisture-flow pattern of the bathtub design, however, is not changed since dense-graded gravel is essentially as impervious as the stabilized subbase.

One of the major results of this free water surrounding the CRCP slab is pumping. A heavy wheel puts high pressure on the free water beneath the slab, which causes the water to move violently in any available direction. This water thrust under high pressure, repeated over many truck loads, eventually leads to disintegration of the subbase and shoulder. This phenomenon of water pumping from the longitudinal joint has been observed several times after rainstorms on various projects. Pumping of fine soil has been observed on the shoulder surface of CRCP with stabilized subbase. CRCP with granular subbase has shown much greater pumping, however. A major result of pumping is a loss of support under the pavement edge. This loss of support causes high stresses and deflections, both of which lead to accelerated occurrence of punchouts. Recognizing this problem, the Illinois Department of Transportation (DOT) has installed in some sections longitudinal edge drains that, according to local maintenance personnel and the limited data given in Table 1, have generally had a beneficial effect. These drains have decreased the number of punchouts by an average of 24 percent for these projects.

TRAFFIC LOADINGS

Most of the Interstate highways in Illinois that are included in this study are very heavily trafficked truck routes. A comparison of this traffic with that on routes in other states shows that these Illinois routes carry as much heavy truck traffic as most states or more (11). The volume and weight of truck traffic have increased sharply during the 1960s and 1970s (1). The amount of overloadings is also believed to be large.

Table 1. Effect of longitudinal edge subdrains on distress in Illinois CRCP.

Highway	Subdrains	Number of Projects	Age (years)		Mean Punchouts per Kilometer
			Projects	Subdrains	
I-57	With	5	8	7	1.1
	Without	3	9		1.6
I-74	With	1	11	11	1.0
	Without	1	11		1.3
I-80	With	1	9	2	1.6
	Without	1	9		2.1

Note: 1 km = 0.62 mile.

Data were obtained from enforcement weight tickets for a few months on the freeway system in Chicago during 1975. Single-axle weights ranged up to 169 kN (38 000 lbf), and tandem-axle weights ranged up to 249 kN (56 000 lbf) (1).

Truck-traffic volume and weight can be expressed in 80-kN (18 000-lb) ESALs. The total accumulated 80-kN ESALs for each project range from less than 1 million to 30 million on the Stevenson Expressway in Chicago. The following table gives the range in traffic loadings at various Illinois locations:

Location	Total 80-kN ESALs on Heaviest-Traveled Truck Lane (000 000s)	Age (years)	80-kN ESALs per Year (000 000s)
I-94 Chicago	16.6	6	2.8
I-55 Chicago	30.0	15	2.0
I-57 Champaign	2.6	8	0.3
I-80 Joliet	8.0	8	0.9
I-70 Vandalia	6.0	10	0.6
I-57 Mt. Vernon	2.9	10	0.3
I-74 North Peoria	2.2	7	0.3
I-70 Marshall	3.5	6	0.6

The design 80-kN ESAL for each slab thickness, assuming typical foundation conditions, is as follows (1 cm = 0.39 in):

Slab Thickness (cm)	Design 80-kN ESAL (000 000s)
18	2.1
20	4.8
23	10.0
25	20.5

The 18-cm (7-in) CRCP is no longer constructed by the Illinois DOT.

Assuming these design limits with actual accumulated traffic, 46 percent of the kilometers of CRCP has surpassed its design traffic limits even though the mean age is only nine years. After 100 percent design traffic life was reached, the serviceability index should have dropped to 2.5. However, because permanent patching restores rideability almost to the original smoothness, the projects are well above this serviceability level. The use of the serviceability-performance approach to design is questionable because extensive patching could keep a CRCP above the 2.5 almost indefinitely. However, maintenance cost and lane downtime would become very high. Discussions with maintenance engineers show that, whenever projects require more than 1.8 patches/km (3 patches/mile), keeping up with the necessary repairs becomes very difficult and lane closures become excessive. A more rational design approach would be to design the CRCP for an acceptable number of edge punchouts that could be determined from economic and other studies. The data obtained in this study could be used to develop updated design procedures.

CONCLUSIONS

1. The edge punchout occurs between two closely spaced transverse cracks near the edge of the travel lane and is the result of a combination of factors. The mechanism of development was analyzed by using a finite-element structural computer program. The location of critical stress, which was found at the top of the slab and transverse across the slab, should be used to design against the punchout. Critical stress was affected mostly by transverse crack spacing and load transfer, slab thickness, and loss of support along the slab edge (from pumping) in addition to repeated truck loadings. These results were generally verified through numerous field observations. The occurrence of edge punchouts by thickness of slab was approximately as follows (1 cm = 0.39 in):

Slab Thickness (cm)	CRCP with Edge Punchouts (%)
18	72
20	64
23	44
25	40

The thicker slabs had much heavier truck traffic.

2. The rate of occurrence of edge punchouts in CRCP is highly dependent on traffic loadings. As loads accumulate, the number of edge punchouts increases at an increasing rate (see Figure 4). In the Illinois projects truck traffic has been much heavier than expected, and many projects (46 percent) are approaching or have exceeded their design traffic life long before reaching their normal 20-year age (the mean age is 9 years).

3. The placement of edge subdrains has reduced the rate of occurrence of distress by about 24 percent on a few available comparative projects (Table 1).

4. The structural design of CRCP needs revision. The use of the serviceability-performance concept is believed not to be valid since continuous patching can keep the pavement in operation almost indefinitely although at a very high maintenance cost and considerable lane downtime. Design should be based on prediction of the occurrence of an acceptable amount of structural distress.

5. The repair of distress in CRCP is a very difficult, time-consuming, and expensive operation and has become a major concern in several districts where 18- and 20-cm (7- and 8-in) thick CRCP carries heavy truck traffic. Thus, there is a great need for less costly and more durable procedures for maintaining CRCP. Research is currently under way at the University of Illinois, and many experimental patches have been placed (12).

ACKNOWLEDGMENT

This paper was prepared by the Department of Civil Engineering in the Engineering Experiment Station, University of Illinois at Urbana-Champaign, in cooperation with the Illinois Department of Transportation and the Federal Highway Administration, U.S. Department of Transportation, as part of a project of the Illinois Cooperative Highway Research Program.

REFERENCES

1. S. A. LaCoursiere, M. I. Darter, and S. A. Smiley. Performance of CRCP in Illinois. Federal Highway Administration, U.S. Department of Transportation, Rept. FHWA-IL-UI-172, 1978.
2. A. M. Tabatabaie. ILLI-SLAB Finite Element Program for Structural Analysis of Concrete Pavement Systems. Department of Civil Engineering, Univ. of Illinois at Urbana-Champaign, 1978.
3. B. E. Colley and H. A. Humphrey. Aggregate Interlock at Joints in Concrete Pavements. HRB, Highway Research Record 189, 1967, pp. 1-18.
4. B. F. McCullough, A. Abou-Ayyash, W. R. Hudson, and J. Randall. Design of Continously Reinforced Concrete Pavements for Highways. NCHRP Project 1-15, Final Rept., 1975.
5. H. A. Lepper and J. B. Kim. Tests of Reinforcement Splices for Continuously Reinforced Concrete Pavement. HRB, Highway Research Record 60, 1963, pp. 116-139.
6. D. L. Spellman, J. H. Woodstrom, and B. F. Neal. Faulting of Portland Cement Concrete Pavements. HRB, Highway Research Record 407, 1972, pp. 1-9.
7. W. Gulden. Pavement Faulting Study. Georgia Department of Transportation, Project 7104, Final Rept., 1975.
8. R. D. Barksdale and R. G. Hicks. Drainage Considerations to Minimize Distress at the Pavement-Shoulder Joint. Proc., International Conference on Concrete Pavement Design, Purdue Univ., West Lafayette, IN, 1977.
9. H. R. Cedergren. Drainage of Highway and Airfield Pavements. Wiley, New York, 1974.
10. Guidelines for the Design of Subsurface Drainage Systems for Highway Structural Sections. Federal Highway Administration, U.S. Department of Transportation, Rept. FHWA-RD-72-30, 1972.
11. M. I. Darter and E. J. Barenberg. Zero-Maintenance Pavements: Results of Field Studies on the Performance Requirements and Capabilities of Conventional Pavement Systems. Federal Highway Administration, U.S. Department of Transportation, Rept. FHWA-RD-76-105, 1976.
12. D. J. Maxey, M. I. Darter, and S. A. Smiley. Evaluation of CRCP Patching. TRB, Transportation Research Record, 1979 (in preparation).

Publication of this paper sponsored by Committee on Rigid Pavement Design.

Response and Distress Models for Pavement Studies

J. Brent Rauhut and Freddy L. Roberts, Austin Research Engineers, Inc., Austin, Texas
Thomas W. Kennedy, University of Texas at Austin

Results of a detailed study to select mathematical and other models for the prediction of significant distress for flexible, composite, and rigid pavements are presented. Rigid pavements were subdivided for study into nonreinforced jointed concrete pavements (JCP), jointed reinforced concrete pavements (JRCP), and continuously reinforced concrete pavements (CRCP). The models selected are to be used in establishing optimal material properties for zero-maintenance pavements. The published results of field surveys and other experience were used to identify, for each type of pavement, distresses that cause considerable maintenance or loss of serviceability. Material properties that influence the occurrence of significant distresses were then identified, and theoretical or empirical models were selected to predict these distresses by using material properties and other engineering parameters. The distresses found to be most significant for these studies were (a) fatigue cracking for all types of pavement, (b) rutting and reduced skid resistance for flexible and composite pavements, (c) reflection cracking for composite pavements, (d) low-temperature cracking for flexible pavements, (e) spalling for all rigid pavements, (f) faulting for JCP and JRCP, (g) low-temperature and shrinkage cracking for JRCP and CRCP, and (h) punchouts and steel rupture for CRCP. The models considered, the context in which they are to be used, their attributes and limitations, and those finally selected for the study of specific distress for specific pavement types are briefly described.

The Federal Highway Administration (FHWA) research project on Material Property Requirements for Zero-Maintenance Pavements has as its goal the identification of material properties that will provide optimal performance in flexible, rigid, or composite premium or zero-maintenance pavements. This goal is to be accomplished through a combination of empirical and theoretical studies. The published results of field surveys, notably those of Darter and Barenberg (1) and McCullough and others (2), and other experience were used to identify, for each type of pavement, distresses that cause significant loss of serviceability or require significant maintenance. Material properties that influence the occurrence of significant distress were then identified, and theoretical or empirical models were selected to predict these distresses by using material properties and other engineering parameters. A detailed account of these studies appears elsewhere (3).

This paper reports the results of studies of contemporary mathematical models to select those most capable of predicting the distresses of interest in terms of the significant material properties. It includes identification and brief descriptions of the distress models considered and tabular identification of the significant distresses by (a) pavement type, (b) the material properties considered to affect the occurrence of each distress, and (c) the distress model selected to predict each distress.

MODELS OF PAVEMENT RESPONSE AND DISTRESS

There are many models of pavement response that predict stresses and strains in a pavement structure. They all assume linear elasticity, and most fall into two categories: those that basically analyze an elastic plate sup-

ported by springs (or a semidense liquid) and those that analyze a layered system with individual elastic properties. Included in this group of models are the Westergaard equations, elastic layer theory, discrete-element slab theory, and finite-element theory. Some versions of these models also consider nonlinearity in materials response through iteration on nonlinear stress-strain curves furnished as input. None of these models are distress models, but they predict pavement behavior under loads. Environmental effects are also considered by some of the models in terms of their effects on the input variables.

By building on this capability for predicting pavement responses, more sophisticated models such as VESYS A (4) and PDMAP (5) for flexible pavements and RPOD (6) and JCP-1 (7) for rigid pavements have been developed to relate load-induced stresses or strains to distress and thus become predictive models for distress. These models are generally available for predicting only fatigue cracking and rutting for flexible and composite pavements and only fatigue cracking for rigid pavements. Other computer-based analytical procedures (2, 5, 8-12) have been developed for predicting cracking that results from changes in volume as temperature decreases.

This leaves other distresses—such as faulting and spalling at joints and cracks—without theoretical or analytical models. For such cases, models may not be mathematical but simply a set of qualitative factors that can be used to predict distress in an approximate manner.

All promising analytical models were studied concurrently with the identification of significant distresses and related material properties. The more promising models have been used, and limited preliminary sensitivity analyses have been conducted both to check out the models and to gain insight into the importance of various material properties to the distress they predict. The results of these model studies were reviewed, and the models that best predict each type of distress were selected.

These models of pavement structure and distress are discussed below in relation to five types of pavements: flexible, composite, and plain jointed concrete pavement (JCP); jointed reinforced concrete pavement (JRCP); and continuously reinforced concrete pavement (CRCP). The available models for the specific type of pavement under discussion are listed, and the model selections are discussed.

MODELS OF PAVEMENT STRUCTURE THAT USE ELASTIC THEORY

The three general types of computer programs or models of pavement structure that are available include models based on elastic layer theory, plate theory (Westergaard equations, discrete-element slab theory, and two-dimensional finite-element models), and three-dimensional finite-element theory. Excellent discussion and comparisons of these theories are presented by Crawford and Katrona (13). Three-dimensional finite-element programs are very expensive to use and are generally used only for very special problems. The version produced by Huang and Wang (14) has been specialized into two dimensions on Winkler springs and is very similar in final matrix formulation to discrete-element slab theory. Comparisons of results reported by Darter (7) for the Huang and Wang finite-element program and for the same sets of data from the discrete-element SLAB program indicate almost identical results except where vagaries of input or boundary conditions cause differences.

Elastic layer theory has the capability of analyzing many pavement systems, but edge or corner stresses for rigid slabs cannot be directly simulated because of the inherent assumption in elastic layer theory that wheel loads are applied to a surface with infinite horizontal dimensions. This is generally a satisfactory assumption for flexible pavements and for interior wheel loadings for rigid pavements.

Obviously, these theories have their capabilities, strong points, and limitations. Neither the finite-element program of Huang and Wang nor the discrete-element slab theory developed by Hudson and others satisfactorily models the supporting soil. Vesic and Saxena (15) have shown that a constant modulus of subgrade reaction k does not permit accurate predictions of stresses and deflections. The Huang and Wang finite-element model and the discrete-element models also assume that vertical deformations do not occur in the rigid slab and thus that the predicted bending stresses at the top and bottom of the slab are identical, which in reality they are not. These theories do, however, provide capabilities for defining discrete boundaries, varying the bending stiffness of the slab from point to point, simulating cracks in the slab and joints between slabs, creating void spaces in the support for the slab, and calculating curling stresses.

One of the attributes of elastic layer theory is that all the layers in the pavement structure can be characterized individually so that their separate effects on pavement responses can be studied. Elastic layer theory spreads predicted stresses and strains with depth in a more realistic fashion than do the "plate models" discussed above, and it is relatively more economical to operate. The primary limitations of elastic layer theory are its inability to define any horizontal boundaries or to simulate very directly the existence of variations in stiffness in the pavement structure, cracks in the surface, or voids under the surface layer. Despite these limitations, however, elastic layer theory and the distress models that use it as a model of pavement structure offer very useful capabilities for comprehensive study of the various layer materials in this project.

Since elastic layer theory clearly represented one of the models to be used, it was necessary to compare the various computer codes that are available and to select those most suited to project needs. Schnitter (16) compared computer output from the ELSYM5, LAYER1S, LAYIT, and BISAR programs for several typical problems over a range of conditions and got essentially the same results from all programs, usually within 1 percent and with a maximum difference of only 3 percent. The most economical program was LAYER5, but it is capable of handling only one wheel load at a time. Of the computer codes considered, ELSYM5 and BISAR can handle multiple loads. ELSYM5 is more economical to operate than BISAR, and five layers are generally sufficient for most problems. BISAR, however, can consider both variable friction at its interfaces and a horizontal load applied at the surface, so it may be useful for special studies.

ELSYM5 serves as the pavement-structure model for the system of rutting prediction used by Monismith and others (17) and for the RPOD program (6). PDMAP (5) uses an elastic layer program called NLAYER, which as the name implies can consider any reasonable number of layers. The Shell method (18) uses BISAR as its structural model. VESYS A (4) uses an elastic layer code that is limited to three layers derived from an early Chevron program.

DISTRESS MODELS FOR FLEXIBLE PAVEMENTS

The distress models studied and considered for use in this project for flexible pavements were as follows:

Type of Distress	Model
Rutting	Shell method (18) VESYS A (4) PDMAP (5) Rutting subsystem, Monismith and others (17) DEVPAV (19) OPAC (20) and WATMODE (21) Huschek rutting-prediction method (22)
Fracture cracking	Shell method VESYS A PDMAP OPAC and WATMODE
Low-temperature cracking	VESYS A PDMAP Shahin-McCullough model (8,9) OPAC and WATMODE
Reduced skid resistance	Studies by Stietle and McCullough (23) Studies by Rauhut and McCullough (24)

None of these models considers all four types of distress, and only VESYS A, PDMAP, OPAC, and WATMODE consider rutting, fracture cracking, and low-temperature cracking. The Shell method considers rutting and fatigue cracking. All of the rest consider only the distress under which they are listed.

Because the Shell method was specifically developed to use hand calculations, many of the complexities have been simplified. All rutting is assumed to occur in the asphalt concrete layer, and all strains in base, subbase, and subgrade are assumed to be elastic. However, Shell research indicates that rutting is limited to surface layers when the surface thickness exceeds about 13 cm (5 in) whereas some rutting occurs in underlying layers for thicknesses less than 13 cm (25). Results from the Shell circular test track indicate that rut depth is no longer a function of surface layer thickness (26) for surfaces thicker than 13 cm. In spite of these conflicting data, the procedure assumes that all rutting occurs in the surface layer and that rutting or rut depth is proportional to the thickness of the surface layer.

The Shell research on fatigue cracking of asphalt concrete materials (27) compared the results of "wheel tracking tests" on instrumented asphalt concrete slabs supported by elastic subgrade and beam fatigue tests for a variety of mixes. This work provides excellent insight into the stages of fatigue cracking and crack propagation in a supported slab as opposed to a nonsupported beam. It and the work reported by Van Dijk and Visser (28) also provide valuable data on the energy approach to prediction of fatigue life used in the Shell method. Shell's approach was to provide a design procedure for limiting radial strain in the bottom of the asphalt concrete layer to an acceptable level by using hand computations. Although the fatigue characterizations of materials obtained by using the energy approach are arrived at differently from those obtained in standard laboratory testing, linear summation of cycle ratios (Minor's hypothesis) is used as in other models to estimate damage or the percentage of the fatigue life that has been consumed at any point in time. Consequently, there appears to be no advantage to using the analytical procedures in the Shell method to predict fatigue life, but several references (18,27,28) contain extensive information for developing the fatigue characterizations of the materials.

VESYS A is an improved version of VESYS IIM, a distress model that has been discussed in great detail in the literature (29,30). The capabilities added to VESYS IIM to produce VESYS A were (a) seasonal modification of material properties, (b) incremental breakdown of axle-load distribution by tire radius and corresponding tire pressure, and (c) a low-temperature-cracking model. The details of these revisions and the improvements in the idealization of flexible pavements are discussed by Rauhut and Jordahl (4).

VESYS A is a sophisticated computer code that accepts some 23 control variables and 44 independent variables that describe a flexible pavement structure, the traffic loadings it endures, and, through input of pavement temperatures and seasonal materials characterization, the environment in which it exists. VESYS A then predicts fatigue cracking, rut depth, slope variance, present serviceability index, and expected service life as functions of time correlated with truck traffic. Distress from fatigue cracking is predicted by using the classical fatigue equation and linear summation of cycle ratios (Minor's hypothesis) as well as probability theory to consider the variability of the input parameters on the predictions of damage caused by axle-load distribution and traffic rate. Rutting is calculated as the difference in predicted total and elastic displacements at the surface. The procedure used is very similar to that proposed by Monismith and others (17). In VESYS A, the permanent strains in the layers are accumulated through separate solutions in which the layer stiffnesses are modified; the permanent deformations in the layers are calculated separately and added together to predict the change in displacement at the surface in the Monismith procedure.

The low-temperature-cracking model used in VESYS A was developed by Haas and Hajek (11) by using multiple-regression equations from data on pavements in Canada. The independent variables used were age of the pavement, thickness of the bituminous layers, type of subgrade soil in a numerical code, winter design temperature, and stiffness of the original asphalt cement. Although this model does a relatively acceptable job of predicting low-temperature cracking, other models such as the COLD program and the Shahin and McCullough models include more detailed consideration of material properties.

Currently, VESYS A is perhaps the most complete model of distress in flexible pavements. It considers a broad range of material properties in its distress subsystems. Some of the input variables, such as those for the permanent deformation characterization of materials, are relatively new to the engineering profession, but considerable data have been accumulated on these variables for a variety of materials and sources.

The term PDMAP stands for probabilistic distress models for asphalt pavement. The distress models included are for fatigue cracking and rutting. The low-temperature-cracking distress model is actually a separate computer program called COLD. Models for both fatigue-cracking distress and rutting in PDMAP are based on multiple regressions on data from the AASHO Road Test, but they depend on an elastic layer structural model to predict needed pavement responses. Complete descriptions of PDMAP and COLD and their development are given by Finn and others (5).

The rutting model for PDMAP predicts the seasonal rate of rutting for permanent deformation per equivalent load application. Seasonal changes in the elastic constants used for the various layers are considered as rutting accumulates with time. The rutting predictions are displayed at different confidence levels on the basis of the stochastic characteristics of the elastic materials characterizations.

The model of fatigue distress is very similar to that

used in most fatigue predictions except that a term has been added to consider the effects of asphalt concrete stiffness.

It is believed that the model of rutting distress has some limitations that restrict its value to research. These are the following:

1. The regression model is based entirely on elastic material properties and elastic responses and includes no permanent deformation characterization of the materials at all. Consideration of the permanent deformation characteristics of materials in this regression model is entirely implicit and would only apply directly to those materials in the pavements of the AASHO Road Test.
2. The three regression coefficients in the model for the rate of rutting prediction are based entirely on AASHO Road Test materials and conditions and, according to Christison (10), require reestablishment for use under other conditions.

The design subsystem presented by Monismith and others (17) estimates the amount of permanent deformation or rutting that results from repeated traffic loading. Relations between applied stress and permanent strain defined by repeated-load triaxial compression tests are used for fine-grained soils, granular materials, and asphalt concrete. Stresses that result from wheel loads are estimated through use of one of the ELSYM computer programs. The stresses in turn permit estimation of permanent deformation in each layer of a specific pavement: The permanent strain at a number of points within the layer is computed so as to define strain variations with depth, and then the products of the average permanent strains and the corresponding differences in depths between the locations at which the strains were determined are summed. Total rut depth is estimated by summing the contributions from each layer.

Although this is a fairly straightforward, promising method, two serious drawbacks limit its use:

1. The materials characterizations are complex and require a very detailed test program to arrive at the values of the many parameters included in the equations.
2. Laborious hand calculations are required for large factorial studies.

Since both this rutting prediction model and that of VESYS A effectively accumulate the permanent deformations in each layer as permanent displacement at the surface, similar results are to be expected if the permanent deformation characterizations are based on the same test data.

DEVPAV is a finite-element program that has been under development by Kirwan and others (19) for some years in Ireland. In addition to the usual loading information, the permanent deformation characterizations are apparently based on multiple-regression studies.

The equation for permanent strain contains temperature, number of load cycles, and applied stress as independent variables. Kirwan and others compared calculated and measured rut depths for the Shell (31) and Nottingham Test Tracks and reported that the computed values of rut depth were in all cases substantially higher than those actually measured but that the shapes of the plots of rut depth versus applications were similar. General use of this model is limited because materials characterizations for permanent deformations are available only for the two materials recorded by Kirwan and others (19), and the finite-element program has been revised so that the lateral strain of one column of elements is prevented from affecting the adjoining column.

OPAC is a system of pavement design developed for the province of Ontario, Canada, by Meyer and Haas (20) and others. It has been further developed into a later form called the Waterloo model of distress estimation (WATMODE) (21). Both models predict distresses from rutting, fatigue cracking, and low-temperature cracking.

These models are generally based on statistical correlations between laboratory tests on materials from the Brampton and Ste. Anne Test Roads in Ontario and measured roadway responses. The correlations between predicted and measured distress are very good for those road tests but may not be generally applicable to more temperate climates. These procedures can be used in other locations and with different materials only after careful validation. However, there are some very useful developments in WATMODE (3, 20).

The Huschek method (22) is very similar to that of Monismith and others (17) described above except that the structural model is the elastic layer program BISAR and the permanent deformation characterization for asphalt concrete is based on cyclic creep compliance tests. Rutting is again predicted by summing the permanent deformations in the separate layers, as done by Monismith and others and indirectly by VESYS A. Calculated results from this procedure compared reasonably well with rutting measurements taken on a test road near Zurich, Switzerland.

The Shahin and McCullough model for prediction of low-temperature or thermal cracking, which is described in detail elsewhere (8, 9), includes separate models for pavement temperature, thermal stress, low-temperature cracking, and thermal fatigue cracking. The model for thermal fatigue cracking grew out of the realization that thermal cracking of asphalt concrete pavements occurs in the more temperate zones of the United States as well as in the northern zones that have relatively lower temperatures. Study has attributed this occurrence of thermal cracking at relatively low levels of strain to the fatigue effects of daily temperature cycling. In this context, the cracking predicted by the COLD program might then be thought of as "one-cycle fatigue cracking" because of relatively much higher strains that would not require repetitive loading to produce a failure.

Comparisons between measured and calculated low-temperature cracking from the Shahin and McCullough model for the Ste. Anne and Ontario Test Roads and a runway in Fairbanks, Alaska, are given by Shahin (9). The predictions were reasonable considering the variability in occurrence of low-temperature cracking in the field; i.e., significant differences in the amount of cracking are generally found between apparently identical sections for the same environmental conditions.

Most of the literature on skid resistance is concerned with the magnitudes of skid numbers for different types of pavements and the reductions in measured skid numbers over periods of time. Steitle and McCullough (23) have reported statistical relations between measured skid numbers, number of vehicle applications (in which trucks and automobiles are counted equally), a "field constant" for each aggregate that depends on its polishing characteristics under traffic, and a skid number taken after a specific number of vehicle applications. The values for the field constants can only be produced by long-term studies. Fortunately, some values are available and represent a limited basis for considering the general effects of abrasive wear of surface aggregates on reductions in skid resistance.

A careful evaluation indicates that none of the models discussed above have better capabilities for predicting rutting and fatigue cracking distress than VESYS A. Since none of the other models offered any apparent

advantage over VESYS A for prediction of these two distresses, the VESYS system was selected because it predicts both distresses and because considerable information on permanent deformation characterizations for a range of materials is available for study.

The COLD program was not selected because it predicts only the point at which a crack will occur and when. It does not predict crack spacing or area cracked, both of which may be obtained from the other two low-temperature-cracking models considered.

The Haas and Hajek model for low-temperature cracking is based on Canadian data only but has been found to correlate reasonably for some pavements in North America. The Shahin and McCullough model has a much more thorough theoretical base and offers much more generality, but the Haas and Hajek model is relatively simpler to use and can be used independently while VESYS A is used for studies of rutting and fatigue-cracking distress.

The study by Steitle and McCullough on the effects of aggregate polishing (23) can be used to study loss of skid resistance, but the field data necessary to the study are so limited that only qualitative results can be expected.

DISTRESS MODELS FOR COMPOSITE PAVEMENTS

The choice of models for prediction of distress is much more limited for composite pavements than for flexible pavements. A composite pavement is considered to be one that has a flexible surface over a very stiff subbase, composed of either a portland cement concrete (PCC) pavement layer or a portland-cement-treated granular base layer. Although the studies of composite pavements will be similar to those of flexible pavements, special modeling will be required since the strongest pavement layer does not occur at the surface. For instance, distress from rutting and reduced skid resistance can be studied by using the same models as those used for flexible pavements, but the fatigue model must be capable of considering fatigue in the more rigid underlying layer of PCC or cement-treated base. In addition, the serious problem of reflection cracking in the surface layer, induced by movements of the underlying layer at the joints or cracks, introduces a need for an additional and entirely different model.

The distress models reviewed and considered for use in studying composite pavements are as follows:

1. For rutting distress, VESYS A;
2. For fatigue-cracking distress, (a) computer program ELSYM5 for predicting stresses and strains at the bottom of the flexible and rigid layers, supplemented by fatigue relations, and (b) RPOD (6, 32); and
3. For reflection-cracking distress, RFLCR1 (6).

Reduced skid resistance is to be studied concurrently with the flexible pavement study. Since none of the available models have been developed specifically for predicting rutting in composite pavements, VESYS A will be used with one minor revision.

The RPOD program was developed by Austin Research Engineers specifically for the design of either flexible or rigid overlays for rigid pavements and includes a model for fatigue-cracking distress that uses ELSYM5 as a model of pavement structure. The alternatives for study of fatigue-cracking distress are (a) modify ELSYM5 to add a model for fatigue-cracking distress to the present model of pavement structure or (b) bypass most of RPOD's subroutines to use only the ELSYM5 model of pavement structure and its model of fatigue-cracking distress. A study of the staff and computation time involved indicated that it would be more economical to modify ELSYM5, so that approach was selected.

RFLCR1 is the only available model for predicting reflection cracking. It includes analysis of two types of distress mechanisms: (a) a form of reflection cracking in the overlay caused by horizontal movements of the rigid slab in response to temperature and moisture changes and (b) shear cracking caused by differential vertical movements at joints or cracks in the underlying rigid pavements.

DISTRESS MODELS FOR RIGID PAVEMENTS

Rigid pavements include JCP, JRCP, and CRCP. Since the steel provided in JRCP or CRCP is neither positioned properly nor of sufficient quantity to provide additional structural capacity, a common model of pavement structure can be used for the prediction of stresses and strains in JRCP, CRCP, and JCP. As a result, the studies of fatigue-cracking distress can be combined for the three types of pavements. Since the distress mechanisms for faulting at cracks and joints and joint spalling are also essentially the same for JRCP and JCP, these distresses can also be studied simultaneously.

Thermal cracking and shrinkage cracking are generally not serious problems for JCP if the joint spacings are short. Future designs should not include joint spacing any greater than 4.5 m (15 ft) if the recommendations of Darter for zero-maintenance pavements (7) are followed. Since longer joint spacings are sometimes used for JRCP, thermal and shrinkage cracking should be considered. The only models available for predicting this distress in a JRCP are a computer program called JRCP-1 (34) and an improved version called JRCP-2 (unless the classical subgrade drag theory is considered).

The fatigue-cracking model for JRCP may also be used for CRCP, but the distinctive nature of CRCP also requires special distress models for thermal and shrinkage cracking. The only relatively complete models developed specifically for the analysis of CRCP are the CRCP-1 program developed by McCullough and others (2) and CRCP-2, an improved version of CRCP-1 developed by Ma (34). Follow-up studies by Strauss (35) and others at the Center for Highway Research of the University of Texas at Austin offer additional statistical insight into the effects of material properties on CRCP distress.

There are several models of pavement structure that could be used to predict stresses and strains for fatigue-cracking analysis. Several of these have already been discussed. Because of the limitations of plate theory, elastic layer theory is considered to be the appropriate model of pavement structure when one wants to consider all pavement layers, but the special capabilities of the discrete-element and finite-element models can also be used for special studies.

Although the JCP-1 program is subject to the same limitations as the Huang and Wang model (14) on which it is based, JCP-1 was also considered as a potential fatigue-cracking model. JCP-1 provides fatigue and serviceability data for a design procedure developed by Darter and Barenberg for JCP (7). Multiple-regression equations based on analytical solutions from the Huang and Wang finite-element program predict pavement stress for an 80-kN [18 000 lb (18-kip)] axle load with the outside tire on the outer 15.4 cm (6 in) of the slab. The procedure also includes prediction of daytime and nighttime curling stresses and their superposition with stresses created by wheel loads. A very detailed

fatigue-cracking model is then applied to predict fatigue damage.

The approach of including the effects of curling and accumulating fatigue damage separately by day and by night to more accurately apply the effects of curling during these periods is considered to be excellent. The emphasis given to the greater importance of wheel loads near the slab edge because of the magnitudes of stresses they create is also considered to be significant. The procedure is based, however, on certain "built-in" assumptions that limit its general applicability to these studies; therefore, it was not selected as a primary model. A detailed discussion of JCP-1 and reasons for its limited use appear elsewhere (3).

The dimensional changes in a CRCP caused by drying shrinkage of the concrete and temperature variation after curing were investigated by McCullough and others, and the design method using the CRCP-1 program was developed in their study (2). This computer program was subsequently improved by Ma (34) and designated CRCP-2.

The spacing of transverse cracks that occur naturally in CRCP is perhaps the most important variable that affects the behavior of the pavement. Relatively large distances between cracks result in a greater accumulation of drag forces from the subgrade as a result of frictional resistance, thus producing high steel stress at the crack and wide crack widths. Closer crack spacing reduces frictional restraint and thus steel stress and crack width. It is clear that the transverse cracks in CRCP are caused by the thermal contraction and shrinkage of the concrete slab. The one-dimensional axial model used in this method is the only available rational model that considers the internal forces caused by the difference in thermal coefficient between the concrete and the steel material and is therefore a valuable tool for the analysis of CRCP.

In 1959, the Texas Highway Department began the Falls-McClennan County Project to evaluate the performance of CRCP. Intensive surveys of crack spacing were conducted at ages that varied from 20 d to 15 years. The results of the survey were compared with the CRCP-2 computer prediction, and the good correlation obtained indicates that this method gives reasonable predictions.

The JRCP-2 program developed by Rivero-Vallejo and McCullough (33) uses many of the concepts developed for CRCP-1, but the geometry and boundary conditions for the JRCP-2 model are considerably different from those for CRCP-2. JRCP-2 also considers the stresses in the concrete and reinforcing steel with time and location. These stresses are affected by the frictional resistance of the subbase; the stiffness, tensile strength, and shrinkage coefficient of the concrete; temperature drops anticipated over time; slab length; percentage of reinforcement; bar diameter; the yield stress and elastic modulus of the steel; the unit weight of the concrete; and the ages at which cracking is to be considered. Given this information, JRCP-2 will theoretically proceed with analysis until the first crack forms and then restructure the problem for subsequent consideration for the formation of a second crack between the joint and the first crack. The output includes the time when the first crack is formed, concrete stress, steel stress, joint width,

Table 1. Distresses, related material properties, and distress models selected for flexible pavement, composite pavement, JRCP, and JCP.

Type of Pavement	Distress	Material Properties That Significantly Affect Distress	Model Selected for Distress Studies
Flexible	Fatigue cracking	Fatigue constants $K_1(T)$, $K_2)T$) for AC surface Stiffness modulus for AC surface Stiffness modulus for base materials	VESYS A
	Rutting	Stiffness modulus for AC surface Permanent deformation parameters for AC surface Stiffness modulus for subgrade soil Permanent deformation parameters for subgrade soil	VESYS A
	Low-temperature cracking	Coefficient of thermal expansion for AC Stiffness modulus for AC Tensile strength for AC	Shahin and McCullough low-temperature-cracking model
	Reduced skid resistance	Abrasive wear potential	Study separate from primary factorial study
Composite	Reflection cracking	Stiffness modulus for AC overlay Thermal coefficient for existing pavement Creep modulus for AC overlay	RFLCR1
	Fatigue cracking	Stiffness modulus for PCC or cement-treated base Fatigue constants for AC overlay or PCC Stiffness modulus for AC overlay	ELSYM5*
	Rutting	Permanent deformation parameters for AC overlay Stiffness modulus for AC overlay	VESYS A
	Reduced skid resistance	Abrasive wear	Concurrent with study for flexible pavement
JRCP	Low-temperature and shrinkage cracking	Tensile strength for PCC Thermal coefficient Shrinkage coefficient	JRCP-2
	Fatigue (transverse or corner cracking)	Fatigue constants for PCC Stiffness modulus for PCC Stiffness modulus for subbase material	ELSYM5*
	Faulting at cracks		Study separate from primary factorial study
	Joint spalling	Volume-change characteristics for PCC surface Tensile strength for PCC Stiffness modulus for PCC	Study separate from primary factorial study
JCP	Fatigue cracking	Fatigue constants for PCC Stiffness modulus for PCC Stiffness modulus for subbase materials	ELSYM5* (concurrent with studies for JRCP and CRCP)
	Joint faulting	Erodibility of subbase Erodibility of subgrade Tensile strength of PCC	Study separate from primary factorial study
	Joint spalling		Concurrent with study for JRCP

*Stresses predicted by ELSYM5 are essentially interior slab stresses and will be multiplied by a stress factor to approximate slab edge stresses.

Table 2. Distresses, responses to thermal and shrinkage cracking, related material properties, and distress models selected for CRCP.

Distress	Response to Thermal and Shrinkage Cracking That Can Be Optimized to Minimize Distress	Material Properties That Significantly Affect Distress	Model Proposed for Sensitivity Analysis
Fatigue cracking	-	Fatigue constants for PCC Stiffness modulus for PCC Stiffness modulus for subbase	ELSYM5[a] (concurrent with study for JRCP)
Low-temperature and shrinkage cracking	-	Thermal coefficient for PCC Shrinkage coefficient for PCC Tensile strength for PCC	CRCP-2
Punchouts, crack spalling, and steel rupture	Crack width and spacing[b]	Thermal coefficient for PCC Shrinkage coefficient for PCC Tensile strength for PCC	CRCP-2 (concurrent with study for low-temperature and shrinkage cracking for CRCP)

[a]Stresses predicted by ELSYM5 are essentially interior slab stresses and will be multiplied by a stress factor to approximate slab edge stresses.
[b]Narrow cracks generally do not spall, and punchouts do not generally occur except when crack spacing is close. Since crack width and spacing are negatively correlated, only one must be optimized.

and crack width as a function of time and the same data for second cracks if they are formed.

It is believed that JRCP-2 is the only thorough model available for the study of the effects of material properties on drying shrinkage and thermal cracking in JRCP. Unfortunately, our use of the model indicates that the computer program is not completely debugged and that it does not predict cracking or correctly predict stresses in concrete and steel. Consequently, the predictions for crack widths are questionable. But since it appears to be theoretically correct and is the only suitable model for JRCP, it has been selected for study of JRCP distresses assuming correction of its deficiencies.

SUMMARY OF RESULTS

Tables 1 and 2 give the distresses, material properties, and models selected for flexible pavements, composite pavements, JRCP, JCP, and CRCP. Some distresses have not been assigned a specific model because no suitable mathematical models for prediction of these distresses were found. These distresses will be studied separately from the factorial study, and the optimal material properties for them will be considered in the optimization.

ACKNOWLEDGMENT

The work presented in this paper was accomplished by a team including Thomas W. Kennedy, J. Brent Rauhut, Freddy L. Roberts, Harvey J. Treybig, W. Ronald Hudson, B. Frank McCullough, Fred N. Finn, James Ma, and Lee Jane Ream. Appreciation is extended to Carl L. Monismith for his ideas on models and for his review and discussion of distresses and material properties.

Support for the project was provided by the Office of Research and Development of the Federal Highway Administration. We are grateful for the technical coordination provided by Ken Clear and William Kenis and also for the time and efforts they expended in participating in technical discussions and meetings with project staff.

REFERENCES

1. M. I. Darter and E. J. Barenberg. Zero-Maintenance Pavements Requirements and Capabilities of Conventional Pavement Systems. Federal Highway Administration, U.S. Department of Transportation, Interim Rept. FHWA-RD-76-105, April 1976.
2. B. F. McCullough, A. Abou-Ayyash, W. R. Hudson, and J. P. Randall. Design of Continuously Reinforced Concrete Pavements for Highways. NCHRP Project 1-15, 1975.
3. J. B. Rauhut, F. L. Roberts, and T. W. Kennedy. Models and Significant Material Properties for Predicting Distresses in Zero-Maintenance Pavements. Federal Highway Administration, U.S. Department of Transportation, Rept. FHWA-RD-78-84, Sept. 1978.
4. J. B. Rauhut and J. R. Jordahl. Effects on Flexible Highways of Increased Legal Vehicle Weights Using VESYS IIM. Federal Highway Administration, U.S. Department of Transportation, Final Rept. FHWA-RD-77-134, Jan. 1978.
5. F. N. Finn, C. Saraf, R. Kulkarni, K. Nair, W. Smith, and A. Abdullah. Development of Pavement Structural Subsystems. NCHRP Project 1-10B, Final Rept., Feb. 1977.
6. H. J. Treybig, B. F. McCullough, P. Smith, and H. Von Quintus. Overlay Design and Reflection Cracking Analysis for Rigid Pavements: Volume 1—Development of New Design Criteria. Federal Highway Administration, U.S. Department of Transportation, Final Rept. FHWA-RD-77-66, Jan. 1978.
7. M. I. Darter. Design of Zero-Maintenance Plain Jointed Concrete Pavement: Volume 1—Development of Design Procedures. Department of Civil Engineering, Univ. of Illinois at Urbana-Champaign, Rept. ZM-2-77, June 8, 1977.
8. M. Y. Shahin. Prediction of Low-Temperature and Thermal Fatigue Cracking of Bituminous Pavements. Univ. of Texas, Ph.D. dissertation, Aug. 1972.
9. M. Y. Shahin. Design System for Minimizing Asphalt Concrete Thermal Cracking. Proc., 4th International Conference on Structural Design of Asphalt Pavements, Univ. of Michigan, Ann Arbor, Aug. 1977.
10. J. T. Christison. Response of Asphalt Pavements to Low Temperature. Univ. of Alberta, Ph.D. dissertation, 1972.
11. R. C. G. Haas. A Method for Designing Asphalt Pavements to Minimize Low-Temperature Shrinkage Cracking. Asphalt Institute, College Park, MD, Jan. 1973.
12. F. Rivero-Vallejo and B. F. McCullough. Drying Shrinkage and Temperature Drop Stresses in Jointed Reinforced Concrete Pavement. Center for Highway Research, Univ. of Texas at Austin, Rept. 177-1, Aug. 1975.
13. J. E. Crawford and M. G. Katrona. State-of-the-Art for Prediction of Pavement Response. U.S.

Army Engineer Waterways Experiment Station, Vicksburg, MS, Rept. FAA-RD-75-183, Sept. 1975.
14. Y. H. Huang and S. T. Wang. Finite-Element Analysis of Concrete Slabs and Its Implications for Rigid Pavement Design. HRB, Highway Research Record 466, 1973, pp. 55-69.
15. A. S. Vesic and S. K. Saxena. Analysis of Structural Behavior of AASHO Road Test Rigid Pavements. NCHRP, Rept. 97, 1970.
16. O. Schnitter. Comparison of Stresses, Strains, and Deflections Calculated with Various Layer Programs. Univ. of Texas at Austin, Pavement Design Course Term Project, Spring 1977.
17. C. L. Monismith, K. Inkabi, C. R. Freena, and D. E. McLean. A Subsystem to Predict Rutting in Asphalt Concrete Pavement Structures. Proc., 4th International Conference on Structural Design of Asphalt Pavements, Univ. of Michigan, Ann Arbor, Vol. 1, Aug. 1977.
18. A. I. M. Claessen, J. M. Edwards, P. Sommer, and P. Uge. Asphalt Pavement Design—The Shell Method. Proc., 4th International Conference on Structural Design of Asphalt Pavements, Univ. of Michigan, Ann Arbor, Vol. 1, Aug. 1977.
19. R. W. Kirwan, M. N. Snaith, and T. E. Glynn. A Computer-Based Subsystem for the Prediction of Pavement Deformation. Proc., 4th International Conference on Structural Design of Asphalt Pavements, Univ. of Michigan, Ann Arbor, Vol. 1, Aug. 1977.
20. F. R. P. Meyer and R. C. G. Haas. A Working Design Subsystem for Pavement Deformation in Asphalt Pavements. Proc., 4th International Conference on Structural Design of Asphalt Pavements, Univ. of Michigan, Ann Arbor, Vol. 1, Aug. 1977.
21. F. R. P. Meyer, A. Cheetham, and R. C. G. Haas. A Coordinated Method for Structural Distress Predictions in Asphalt Pavements. Presented at Annual Meeting, AAPT, Lake Buena Vista, FL, Feb. 1978.
22. S. Huschek. Evaluation of Rutting Due to Viscous Flow in Asphalt Pavements. Proc., 4th International Conference on Structural Design of Asphalt Pavements, Univ. of Michigan, Ann Arbor, Vol. 1, Aug. 1977.
23. D. C. Steitle and B. F. McCullough. Skid Resistance Considerations in the Flexible Pavement Design System. Texas Highway Department; Texas Transportation Institute, Texas A&M Univ.; and Center for Highway Research, Univ. of Texas at Austin, Res. Rept. 123-9, April 1972.
24. J. B. Rauhut and B. F. McCullough. Development of Guideway Skid Control Requirements for Dual Mode Vehicle Systems. Austin Research Engineers, Inc, Austin, TX, Jan. 1974.
25. P. Uge and P. J. van de Loo. Permanent Deformation of Asphalt Mixes. Proc., Canadian Technical Asphalt Assn., Vol. 19, 1974.
26. J. Pfeiffer and P. M. Van Doormaal. The Rheological Properties of Asphaltic Bitumen. Journal of Institution of Petroleum Technologists, No. 22, 1963.
27. W. Van Dijk. Practical Fatigue Characterization of Bituminous Mixes. Presented at Annual Meeting, AAPT, Phoenix, Feb. 1975.
28. W. Van Dijk and W. Visser. The Energy Approach to Fatigue for Pavement Design. Presented at Annual Meeting, AAPT, San Antonio, Feb. 1977.
29. J. B. Rauhut, J. C. O'Quin, and W. R. Hudson. Sensitivity Analysis of FHWA Structural Model VESYS II. Federal Highway Administration, U.S. Department of Transportation, Rept. FHWA-RD-76-24, March 1976.
30. W. J. Kenis. Predicted Design Procedures—A Design Method for Flexible Pavements Using the VESYS Structural Subsystem. Proc., 4th International Conference on Structural Design of Asphalt Pavements, Univ. of Michigan, Ann Arbor, Vol. 1, Aug. 1977.
31. A. Hofstra and A. J. G. Klomp. Permanent Deformation of Flexible Pavements Under Simulated Road Traffic Conditions. Proc., 3rd International Conference on the Structural Design of Asphalt Pavements, Vol. 1, London, 1972.
32. H. J. Treybig, B. F. McCullough, P. Smith, and H. Von Quintus. Overlay Design and Reflection Cracking Analysis for Rigid Pavements: Volume 2—Design Procedures. Federal Highway Administration, U.S. Department of Transportation, Rept. FHWA-RD-77-67, Aug. 1977.
33. F. Rivero-Vallejo and B. F. McCullough. Drying Shrinkage and Temperature Drop Stresses in Jointed Reinforced Concrete Pavement. Center for Highway Research, Univ. of Texas at Austin, Rept. 177-1, Aug. 1975.
34. J. C. M. Ma. CRCP-2: An Improved Computer Program for the Analysis of Continuously Reinforced Concrete Pavement. Univ. of Texas at Austin, Master's thesis, Aug. 1977.
35. P. Strauss, B. F. McCullough, and W. R. Hudson. Continuously Reinforced Concrete Pavements: Structural Performance and Design Construction Variables. Center for Highway Research, Univ. of Texas at Austin, Res. Rept. 177-7, May 1977.

Publication of this paper sponsored by Committee on Theory of Pavement Design.

Distresses and Related Material Properties for Premium Pavements

Thomas W. Kennedy, University of Texas at Austin
Freddy L. Roberts and J. Brent Rauhut, Austin Research Engineers, Inc., Austin, Texas

In order for zero-maintenance pavements to be constructed, the materials from which they are built must withstand severe stresses without suffering extensive distress. In evaluating the conditions for which zero-maintenance pavements must be designed, it is necessary to clearly define and categorize these distresses, determine their causes, and rank the material properties that affect each distress in order of importance. The process used to prioritize these distresses and the material properties related to them is described, and a set of definitions on which this process is based is presented. The result of this effort is a minimum set of distresses and material properties that affect those distresses that must be considered in designing zero-maintenance pavements. Categories of distress noted in field surveys were ranked based on these definitions and processes. Only distresses that occur in premium pavements were included in the analysis, and each was evaluated to determine its impact on meeting the requirements for zero-maintenance pavements. The evaluations presented are subjective but were developed by using the experience of the project staff and sensitivity analyses based on models that predict distress. A detailed set of distresses and major material properties that affect those distresses are given for rigid, flexible, and composite premium pavements.

For several years, the Federal Highway Administration (FHWA) has pursued multiple research studies aimed at producing premium pavement structures for heavily traveled routes. The intent of these efforts has been to minimize maintenance, which not only disrupts traffic flow but also creates hazards and high user costs. The goal is the development of pavement structures that will be maintenance-free for 20 years and require only routine maintenance for 10-20 years thereafter.

Research is under way on the upgrading of conventional structures by use of improved conventional or new materials; this includes the development of new design materials. Field surveys have been conducted to study the nature of existing pavements that have performed essentially as zero-maintenance pavements. These diverse studies have produced valuable information for use on this and other zero-maintenance research projects.

An FHWA research project, Material Property Requirements for Zero-Maintenance Pavements, has as its goal the identification of material properties that will provide optimal performance in flexible, rigid, or composite premium or zero-maintenance pavements. The purpose of the portion of the study summarized in this paper was to identify various pavement distresses, to select those distresses that occur in premium pavements, and to identify the related material properties. This effort was subdivided into the following four tasks:

1. To develop a complete list of distresses for each pavement type, engineering properties related to the distress types, and factors that affect the engineering properties of the materials;
2. To assess the relative importance of distress types in terms of frequency of occurrence and to evaluate the effect on meeting the requirements of zero-maintenance pavements;
3. To assess the relative importance of material properties in each of the important distresses; and
4. To summarize the distresses and related material properties that have sufficient impact on pavement performance and maintenance requirements to warrant further consideration.

DEFINITIONS

The terms used to describe categories of distress, specific forms of distress, distress mechanisms, distress manifestations, response mechanisms, responses, material properties, and other descriptors must be clearly and concisely defined. Development of these definitions is necessary to ensure consistent use and to minimize the opportunity for personal interpretation. Most existing definitions were developed for the specific needs of other projects and were based on the level of understanding at that time (1-4). In view of recent advances in understanding of the physical pavement structure, the various loads, and the environment, some of these definitions needed updating; therefore, definitions were reviewed and evaluated for adequacy and consistency. Each of the definitions given by Hudson and others (3) was reviewed, and only those changes were made that appeared to be necessary to maintain the specificity of the definitions and to define needed terms.

1. A pavement structure is an organized combination of materials constructed in layers over a natural soil.
2. Material properties are those definitive descriptive measures of the quality of the material (5).
3. Distress is a condition of the pavement structure that reduces serviceability or leads to a reduction in serviceability.
4. Distress manifestations are the visible consequences of various distress mechanisms, which usually lead to a reduction in serviceability (3).
5. A distress mechanism is the physical or chemical process involved in or responsible for distress in pavements.
6. Structural failure is a fracture or distortion that may or may not cause an immediate reduction in serviceability but will lead to a future loss of serviceability.
7. Fracture is the state of a pavement material that is breaking.
8. Distortion is a permanent change in the shape of the pavement or pavement component.
9. Disintegration is the state of a pavement that is decomposing or abrading into its constitutive elements (3).
10. Reflection cracks are cracks that occur in the surface course of a pavement and that coincide with and are caused by the relative movement of cracks or joints in underlying layers.
11. Low-temperature cracks are generally transverse cracks that are caused when tensile stresses induced by frictional resistance of the underlying layer to thermal contraction of the surface layer exceed the tensile strength of the surface material.
12. Raveling is the progressive disintegration of an asphalt concrete layer from the surface downward by the dislodgment of aggregate particles. This can be caused by insufficient binder in the mix, hardening of the as-

phalt binder, wet or dirty aggregate, or aggregate with a smooth surface texture.

13. Ruts are longitudinal depressions that form in the wheel paths of flexible or composite pavements and result from compaction or lateral migration of one or more of the pavement-layer materials under the action of traffic and environment.

14. Shrinkage cracks are generally transverse cracks that are caused when tensile stresses induced by frictional resistance of the underlying layer to drying contraction of the surface layer exceed the tensile strength of the surface material. These cracks generally occur in portland cement concrete (PCC) and other cement-treated materials.

15. Spalling is cracking, breaking, or chipping of a rigid pavement along joints, edges, or cracks in which small portions of the slab are dislodged.

16. Faulting is a difference in the elevation of two adjacent rigid slabs at the joint or crack interface as a result of consolidation or swelling of underlying material, inadequate load transfer, or pumping.

17. D-cracking is a series of fine, crescent-shaped hairline cracks in a rigid slab surface, usually paralleling a joint or major crack.

18. Steel rupture is the occurrence of a tensile fracture failure in the reinforcing steel when excessive stress is transferred to the steel on fracture of adjacent concrete.

19. Punchouts are blocks of rigid pavement that are cracked around their periphery and displaced downward relative to the rest of the slab. Punchouts usually occur between closely spaced transverse cracks that are subsequently connected by longitudinal cracks.

20. Polished aggregates are surface aggregate particles that have smooth, rounded surfaces with fine microtexture, either in their original condition or after abrasive wear by traffic.

21. Fatigue cracks are cracks in a pavement layer caused by the combination of repetitive strains and apparent reduction of tensile strength caused by fatiguing of the layer material. The repetitive strains that cause fatigue are usually the result of passing wheel loads but may include thermally induced strains or other types of strains.

PAVEMENT DISTRESS

In this project, distress is defined as the condition of a pavement structure that reduces serviceability or leads to reduction of serviceability. Occurrence of distress may also require maintenance to restore serviceability. Distresses that do not directly result in significant losses of serviceability or lead to other distresses were of minor interest in this study.

The identification of distresses that affect the performance of the five types of pavement structures included in this project was the result of a combination of literature review and the experience of staff and consultants. The primary source of information was published field surveys, such as those by Darter and Barenberg (6), which identify the types of distress observed and, generally, the frequency of occurrence.

RELATED MATERIAL PROPERTIES

The identification of the material properties that have a significant effect on specific distresses was also the result of a combination of literature review and the experience of staff and consultants. Information is already available in the form of sensitivity analyses, such as that reported by Rauhut and others (7), and regression equations for various types of pavements. These studies are especially useful when the statistical significance of the various material properties is included.

RESEARCH APPROACH

The basic approach used to identify the various pavement distresses and the engineering material properties that affect these distresses involved an evolutionary process of review and refinement. The first cycle involved identifying and categorizing various distresses based on the experience of the research team. At the same time, the material properties that affect the specific distresses were identified. By using the resulting information as a base, a second cycle of review, expansion, and refinement was conducted. Previous identifications of distress from the literature and inputs from this research were introduced at this stage to ensure that all pertinent types of distress and related material properties had been considered (3, 6). The study was also expanded at this stage to identify the environmental, mix-design, construction, and traffic factors that influence the material properties.

During the second study cycle, each of the previously proposed distresses was carefully considered to determine whether it was a distress or a secondary effect. In addition, more definitive relations between distress and related material properties were developed, and a preliminary assessment of the relative importance of the various distresses and their related material properties was made. Finally, the results of this study were carefully reviewed to ensure that all pertinent distresses were considered and that the list of related material properties was complete.

RESULTS

The first two study cycles produced a complete set of distresses for each pavement type, a complete set of material properties that affect the specific distresses, and a reasonably complete set of independent mixture and construction factors—i.e., type of aggregate, cement factor, and mixing temperature—that affect these material properties. The final cycle involved establishing the relative importance of the distresses and their related material properties. These decisions were based on (a) the results of field surveys and the combined experience of the project staff and consultants, which were used to establish the distresses that warranted consideration [the work of Darter and Barenberg (6) and McCullough and others (8) provided the primary sources of field survey information] and (b) the results of the field surveys, sensitivity analyses on both regression and theoretical models, and the combined experience of the project staff and consultants, which were used to rank the material properties in order of their importance to specific distresses.

In developing these rankings, considerable use was made of the results reported by Darter and Barenberg (6) and McCullough and others (8). In both of these studies, significant efforts were expended to collect condition data for U.S. pavements. As a part of these condition surveys, summaries of the severity and frequency of occurrence of distress were prepared. Results from discussions with 13 state highway agencies in the United States were used in developing the rankings used by Darter and Barenberg (6). These discussions provided a basis for transforming the information from the condition survey into the severity categories used.

An example of the type of summary information prepared by Darter and Barenberg for flexible pavements

is given in Table 1 (6). Similar data are reported here for composite pavement, jointed concrete pavement (JCP), jointed reinforced concrete pavement (JRCP), and continuously reinforced concrete pavement (CRCP). The information in each table represents the type of moderate to severe distress observed in pavements that exhibited lives consistent with that desired for zero-maintenance pavements.

It should be noted that these distress rankings are for pavements that survived for 20 years and may not be applicable to pavements in general. The survival of a particular pavement may have resulted from favorable environmental, traffic, and construction factors rather than optimal material properties.

In this paper, some of the identifications for and rankings of distresses differ from those reported by Darter and Barenberg. The reasons for these differences are the following:

1. The distresses noted by Darter and Barenberg (6) were not identified within constraints such as those imposed by the definitions presented earlier, so Darter and Barenberg included as distresses two items that do not qualify within these constraints: weathering asphalt and polished aggregate.
2. Other distresses noted by Darter and Barenberg fit the definition of distresses but are not subject to material optimization within the context of this research effort. These distresses include joint filler extrusion or stripping, shoulder distress, interconnecting cracking, paved shoulder distress, and joint filler stripping.
3. Some distresses were identified more by their distress manifestations than by the cause of distress. For instance, distress in composite pavement included transverse, longitudinal, edge, and random cracking, whereas the terminology in this paper would include all surface cracking in composite pavements under reflection cracking and fatigue cracking. Similarly, corner cracking, longitudinal cracking, and diagonal cracking for JRCP are combined in this report as fatigue cracking.

Thus, the identifications of distresses and their importance rankings were developed by using those prepared by Darter and Barenberg (6) as a beginning point and then modifying them to represent the combined experience and opinion of the research team.

Moderate to severe distresses that occurred frequently were retained for additional study. Other minor distresses—i.e., distresses that do not occur if design is adequate or do not require significant maintenance—were eliminated, although some are briefly discussed. Fatigue cracking is typical of the distresses considered to be significant, whereas shoving and raveling of a flexible surface were omitted from further study because they can be and have been controlled by adequate mixture design.

Table 1. Summary of types of distress found in flexible pavements and rated moderate to severe.

Type of Distress	Number of Distresses	
	Found	Maintained[a]
Longitudinal cracking (lane joint in nearly all cases)	11	5
Transverse cracking (including reflective)	10	7
Alligator (fatigue) cracking	9	5
Polished aggregate	8	0
Rutting	6	1
Weathering asphalt	4	0
Depressions	3	0
Alligator or transverse cracking[b]	14	9
Alligator, transverse, or longitudinal cracking or rutting[b]	17	10

[a]Maintenance performed only for distress indicated.
[b]Whichever type was rated highest for each pavement.

Distresses

Distress is the condition of a pavement structure that reduces serviceability or leads to a reduction in serviceability. The three basic categories of distress, defined in the list above, are fracture, distortion, and disintegration. Several manifestations of distress within each of these categories have been observed in the field. Table 2 gives the major distresses in each category. On the basis of the definition of distress, a number of effects that have often been labeled distresses were eliminated. It is recognized that, although these affect the development of distress, they are not themselves distresses. Examples of such effects are curling and pumping.

The number of distresses was also reduced by combining into one distress those subgroups that have been used to account for small variations in the observed distress manifestations—e.g., types of cracking such as corner, diagonal, longitudinal, second-stage, third-stage, progressive, and random, all of which have been used in the past to account for slight variations in the observed crack pattern.

Another group of distresses eliminated from further consideration is those distresses that basically occur in secondary highways and would not be expected to occur in premium pavements, such as shoving, slippage, and corrugations. These distresses must be kept in mind, however, to ensure that distresses that can be avoided

Table 2. Pavement distress by distress category and pavement type.

Type of Pavement	Fracture	Distortion	Disintegration
Flexible	Fatigue cracking Thermal cracking Slippage cracking[a]	Differential frost heave Differential compaction-swelling Shoving[a] Rutting Corrugations[a]	Stripping Raveling Reduced skid resistance
Rigid	Fatigue cracking Shrinkage cracking Thermal cracking Blowups Spalling	Faulting Differential frost heave Differential compaction-swelling	D-cracking Scaling Reduced skid resistance
Composite	Fatigue cracking Thermal cracking Slippage cracking[a] Reflection cracking	Differential frost heave Differential compaction-swelling Shoving[a] Rutting Corrugations[a]	Stripping Raveling Reduced skid resistance

[a]Not important in premium pavements that use current design and construction techniques but should be considered to ensure that the condition does not develop.

by proper design and construction do not result when changes in material, mixture, and structural design are made to eliminate other distresses.

There is considerable recent evidence that stripping is an important distress in flexible pavements. However, the process of stripping is a very complicated physical-chemical interaction between the asphalt and the aggregate, and the effects of material properties on stripping are not well defined. Since the objective of this project is to optimize material properties and since stripping was not a major distress in nationwide surveys of flexible pavements (6), stripping was not considered further.

Table 3. Material properties considered to affect distresses in premium pavements.

Material Property	Type of Pavement Affected		
	Rigid	Flexible	Composite
Constants of the fatigue equation	X	X	X
Tensile strength	X	X	X
Shrinkage characteristics	X		X
Coefficient of thermal expansion	X	X	X
Aggregate characteristics	X	X	X
Compaction-volume change characteristics	X	X	X
Erodibility of subbase and subgrade materials	X		
Frost susceptibility of subgrade soil	X	X	X
Mixture stiffness[a]	X	X	X
Permanent deformation characteristics		X	X
Bond (adhesion)	X	X	X

[a] Includes stability, creep compliance, and elastic properties.

Material Properties

Engineering material properties are defined as those properties that can be used with a constitutive equation to predict the physical behavior of a material in a particular environment. For example, Hooke's Law can be used to describe the state of stress or strain of a linear, elastic material. By using Hooke's Law, other physical laws, and decision or design criteria, one can assess the suitability of a material with a certain modulus of elasticity (from Hooke's Law) for a particular application. Since modulus of elasticity is useful in evaluating the application of the material, it is categorized as an engineering property but is also a property of the material. Material properties, then, are those engineering properties that are used to represent the materials in mathematical models and equations or in decision criteria. These, in turn, are used to evaluate the behavior and the suitability of materials for particular application.

The material properties initially identified as having important effects on distresses in premium pavements are given in Table 3. Each of the distresses included was considered by the project team to affect the occurrence and magnitude of a distress. For clarity and ease of presentation, the distresses are also given separately in Tables 4, 5, and 6 for each pavement type even though several of the distresses occur in more than one pavement type.

In Tables 4-6, the independent material properties that affect a particular distress are coded by letter to indicate the type of material and the layer to which each property applies. For example, in Table 4, low-

Table 4. Relation between material properties and distresses by type of material and layer affected: premium flexible pavements.

Material Property	Cracking		Rutting	Compaction-Swelling[a]	Raveling	Stripping	Reduced Skid Resistance
	Fatigue	Low-Temperature					
Stiffness[b]	a, b, c, d, e	a, b	a, b, c, d, e		a	a, b	
Coefficient of thermal expansion		a, b					
Tensile strength		a, b					
Permanent deformation characteristics			a, b				
Aggregate characteristics						a, b	a
Compaction-volume change characteristics				e			
Frost susceptibility				e			
Bond (adhesion)						a	a, b
Fatigue constants	a, b						

Note: a = asphalt concrete surface, b = asphalt-treated material, c = lime-treated material, d = untreated granular material, and e = subgrade soil.

[a] Large, relative vertical differential displacements. [b] Includes stability, creep compliance, and elastic properties (E, ν).

Table 5. Relation between material properties and distresses by type of material and layer affected: rigid pavements.

Material Property	Cracking			Blowups	D-Cracking	Polishing	Spalling	Faulting	Compaction-Swelling
	Fatigue	Drying Shrinkage	Low-Temperature						
Mixture stiffness[a]	a, b, c, d, e, f		a, b	a					
Fatigue constants	a								
Tensile strength	a	a	a						
Coefficient of thermal expansion			a	a			a		
Tensile strength of paste					a	a			
Permeability of paste					a	a			
Pore and air-void characteristic of paste					a				
Aggregate characteristics					a	a			
Compaction-volume change characteristics									f
Erodibility								b, c, d, e, f	
Bond (adhesion)								b, c, d, f	
Frost susceptibility									f
Shrinkage characteristics		a							

Note: a = PCC surface, b = asphalt-treated materials, c = cement-treated materials, d = lime-treated materials, e = untreated granular material, and f = subgrade soil.

[a] Includes stability, creep compliance, and elastic properties (E, ν).

Table 6. Relation between material properties and distresses by type of material and layer affected: premium composite pavements.

Material Property	Cracking			Rutting	Compaction-Swelling[b]	Raveling	Stripping	Reduced Skid Resistance
	Fatigue	Low-Temperature	Reflection[a]					
Mixture stiffness[c]	b, c, d, e, f, g		a, c, d, e, f, g	a, c, d, e, f, g		b	b, c	
Fatigue constants	b, c, d		a			b	b, c	
Tensile strength		b, c	a					
Shrinkage characteristics			a					
Coefficient of thermal expansion		b, c, d	a					
Aggregate characteristics			a					b
Compaction-volume change characteristics					f, g			
Permanent deformation characteristics[c]				b, c				
Frost susceptibility					g	g	g	
Bond (adhesion)						b	b, c	

Note: a = asphalt concrete surface, b = PCC, c = asphalt-treated material, d = cement-treated material, e = lime-treated material, f = untreated granular material, and g = subgrade soil.

[a] Reflection cracking can be caused by any cracking of the PCC layer. See the PCC pavement distress summary for a breakdown of the various forms of cracking.
[b] Compaction-swelling refers to any large, relative vertical differential displacements.
[c] Includes stability, creep compliance, and elastic properties (E, ν).

Table 7. Priority ranking of significant distresses selected for future study.

Priority Ranking	Flexible Pavements	Rigid Pavements			Composite Pavements
		JCP	JRCP	CRCP	
1	Fatigue cracking	Fatigue cracking	Low-temperature and shrinkage cracking	Crack spalling	Reflection cracking
2	Rutting	Joint faulting	Fatigue cracking	Fatigue cracking	Fatigue cracking
3	Low-temperature cracking	D-cracking	Crack faulting	Low-temperature cracking	Rutting
4	Reduced skid resistance	Joint spalling	Joint spalling	Shrinkage cracking	Reduced skid resistance
5			D-cracking	Punchouts	
6				Steel rupture	

temperature cracking is affected by (a) the mixture stiffnesses of the surface and asphalt-treated base, (b) the coefficient of thermal expansion of the surface and asphalt-treated base, and (c) the tensile strength of the asphalt concrete surface and asphalt-treated base.

Dependent material properties have generally not been included in the lists of properties prepared in this study. Although dependent material properties can affect the magnitude of the independent property, all too often the relation is a statistical correlation rather than one of cause and effect. Since the dependent material properties are related to the independent properties and often are more easily or conveniently measured, they can be used in place of the independent material property in engineering analyses. For example, density, aggregate gradation and type, temperature susceptibility of the asphalt cement, air-void characteristics, and several other factors are related to the fatigue characteristics of an asphalt concrete mixture. In this study, fatigue characteristics are included in the optimization studies and not the other (dependent) properties. Since the independent properties are to be optimized, it is necessary to optimize the property that produces the effect rather than a second property with which the first may be correlated.

The importance of this approach is illustrated by the number of engineers who believe that increased density is always desirable. An attempt to maximize density does not mean necessarily that distress will be minimized or that other material properties will be maximized. In fact, in many cases material properties will not be maximized nor distress minimized. For example, fatigue life is not maximized at maximum density. In addition to not maximizing fatigue life, increasing density past optimum can lead to other distresses such as bleeding.

Both stiffness and air voids were considered to influence the fatigue properties of asphalt mixtures even though both are dependent on the same factors as are the fatigue properties. In addition, stiffness can account for the effect of a number of independent factors and has been used extensively, and air voids produce flaws that affect crack propagation.

Factors That Affect Material Properties

Factors that are believed to affect the magnitude of the various material properties were also identified and are given elsewhere (9, Appendix A). This information provided valuable insight in the evaluation of the relative significance of material properties for this project. All factors that have an effect on the various material properties were listed for each property and categorized to indicate whether the factor related to environment, mixture design and materials, construction, traffic, or time.

Distress Ranking

From the previous tables of various distresses, it was necessary to select those distresses that are of primary concern in producing premium pavements and that must be considered in the analysis or design of the pavement structures to minimize their occurrence and associated effects. Distresses not included in this list have been eliminated through improvements in existing design procedures, proper selection of materials, or proper construction practices, including quality control.

The results from condition surveys reported by Darter and Barenberg (6) and McCullough and others (8) were extensively used along with the experience of project engineers and consultants to rank order the pavement

Table 8. Priority ranking for material properties that affect major distresses found in premium flexible pavements.

Material Property	Layer	Fatigue Cracking	Rutting	Low-Temperature Cracking	Reduced Skid Resistance
Fatigue constants	Surface	1			
	Base	6			
Tensile strength	Surface			3	
Coefficient of thermal expansion	Surface			1	
Aggregate characteristics	Surface	-[a]	-[a]		1
	Base	-[a]	-[a]		
	Subbase	-[a]	-[a]		
Mixture stiffness[b]	Surface	2	1		
	Base	3	5		
	Subbase	4	7		
	Subgrade	5	3		
Permanent deformation characteristics	Surface		2		
	Base		6		
	Subbase		8		
	Subgrade		4		

Note: Rankings are based on the effect of a property on distress and not the ability to control that property in design.

[a]The effect of the variable is included with other properties.
[b]Includes stability, creep compliance, and elastic properties of any pavement layer.

Table 9. Priority ranking for material properties that affect major distresses found in premium composite pavements.

Material Property	Layer	Reflection Cracking	Fatigue Cracking	Rutting	Reduced Skid Resistance
Mixture stiffness[a]	Surface	1	4	2	
	Base[b]	3	1	3	
Fatigue constants	Surface		3		
	Base[b]		2		
Tensile strength	Surface	4			
	Base[b]				
Coefficient of thermal expansion	Surface	5			
	Base[b]	2			
Aggregate characteristics	Surface				1
Permanent deformation characteristics	Surface			1	

Note: Rankings are based on the effect of a property condition and not the ability to control that property in design.

[a]Includes stability, creep compliance, and elastic properties of any pavement layer.
[b]Existing PCC pavement in some situations.

Table 10. Priority ranking for material properties that affect major distresses found in premium rigid pavements.

Material Property	Layer	Joint and Crack		Cracking			Punchouts	Steel Rupture
		Faulting	Spalling	Fatigue	D	Low-Temperature and Shrinkage		
Stiffness[a]	Surface		3	2			2	2
	Subbase			3				
Fatigue constants	Surface			1				
Coefficient of thermal expansion	Surface		1			2	1	1
Permeability of paste	Surface				2			
Pore and air-void characteristics of paste	Surface				2			
Aggregate characteristics	Surface				1			
Erodibility	Surface							
	Subbase	1						
	Subgrade	2						
Tensile strength								
Concrete	Surface	3	2	4	4	1	3	3
Steel	Surface							4
Shrinkage coefficient	Surface					3		

Note: Rankings are based on the effect of a property on distress and not the ability to control that property in design.

[a]Includes stability, creep compliance, and elastic properties of any pavement layer.

distresses given in Table 2. The resulting priority ranking of pavement distresses is given in Table 7. The results of the priority ranking of distress will be used in further research to more clearly define the material properties that most affect the occurrence and extent of distress. The models used to predict the occurrence of these distresses have typically included variables such as material properties, traffic, and environmental effects. A second priority ranking was performed to allow for the inclusion of the most significant material properties in the evaluation of the available models. These priority rankings (by layer) of material properties that affect distress in premium pavements are given in Tables 8, 9, and 10. In developing the priority rankings for material properties within a particular distress, the rankings were based on total effect and no consideration was given to whether the material property could be controlled or manipulated during design.

SUMMARY

The pavement distresses that occur most frequently and have the greatest effect have been noted and ranked in order of their effect on realizing the objective of zero-maintenance pavements for each type of pavement. The material properties that affect each of the distresses

have also been noted and ranked. To determine optimal values of each of these material properties, the effect of change in these properties on structural response must be evaluated and compared with the requirements for zero-maintenance pavements. It should be noted, however, that some important distresses cannot be evaluated by using available analytical models and must be investigated in special studies. Papers by Rauhut and others (9 and a paper elsewhere in this Record) include detailed discussions of analytical models that predict distress as a function of material properties, load, and environmental factors.

ACKNOWLEDGMENT

The work presented in this paper was accomplished by a team that included Thomas W. Kennedy, J. Brent Rauhut, Freddy L. Roberts, Harvey J. Treybig, W. Ronald Hudson, B. Frank McCullough, Fred N. Finn, James Ma, and Lee Jane Ream. Appreciation is extended to Carl L. Monismith for his ideas on models and for his review and discussion of distresses and material properties.

Support for the project was provided by the Office of Research and Development of the Federal Highway Administration. We are grateful for the technical coordination provided by Ken Clear and William Kenis and also for the time and effort they expended in participating in technical discussions and meetings with project staff.

REFERENCES

1. F. N. Hveem. Types and Causes of Failure in Highway Pavements. HRB, Bull. 187, 1958.
2. E. J. Barenberg, C. L. Bartholomew, and M. Herrin. Pavement Distress Identification and Repair. Construction Engineering Research Laboratory, U.S. Department of the Army, Tech. Rept. P-6, March 1973.
3. W. R. Hudson, F. N. Finn, B. F. McCullough, K. Nair, and B. A. Vallerga. Systems Approach to Pavement Design, System Formulation, Performance Definition, and Material Characterization. NCHRP Project 1-10, Interim Rept., March 1968.
4. W. R. Hudson and F. N. Finn. A General Framework for Pavement Rehabilitation. Federal Highway Administration, U.S. Department of Transportation, Rept. FHWA-RD-74-60, June 1974.
5. G. Murphy. Properties of Engineering Materials. International Textbook Co., New York, 1957.
6. M. I. Darter and E. J. Barenberg. Zero-Maintenance Pavements Requirements and Capabilities of Conventional Pavement Systems. Federal Highway Administration, U.S. Department of Transportation, Interim Rept. FHWA-RD-76-105, April 1976.
7. J. B. Rauhut, J. C. O'Quinn, and W. R. Hudson. Sensitivity Analysis of FHWA Structural Model VESYS II. Federal Highway Administration, U.S. Department of Transportation, Rept. FHWA-RD-76-24, March 1976.
8. B. F. McCullough, A. Abou-Ayyash, W. R. Hudson, and J. P. Randall. Design of Continuously Reinforced Concrete Pavements for Highways. NCHRP Project 1-15, 1975.
9. J. B. Rauhut, F. L. Roberts, and T. W. Kennedy. Models and Significant Material Properties for Predicting Distresses in Zero-Maintenance Pavements. Federal Highway Administration, U.S. Department of Transportation, Rept. FHWA-RD-78-84, June 1978.

Publication of this paper sponsored by Committee on Theory of Pavement Design.

Evaluation of Permanent Deformation in Asphalt Concrete Pavements

Kamran Majidzadeh and Safwan Khedr, Ohio State University, Columbus
Mohamed El-Mojarrush, Roads and Railways Department, Tripoli, Libya

Results of an evaluation of permanent deformation, or rutting, in asphalt concrete pavements subject to traffic load and environmental conditions are presented. Because previous studies have shown rutting to be a major mode of distress in various pavement systems, rutting criteria should be considered in any rational method of pavement design. For practical applications, it is often necessary to estimate the rutting expected in a pavement for a certain period or set of conditions. To accomplish this, a model of rutting estimation is necessary. An approach to rutting estimation applied successfully to subgrade soils in research at Ohio State University was used to study the variation of rutting parameters with asphalt content, temperature, and loading conditions for two mixtures that met Ohio specifications for surface-course mixtures. The data and results were obtained from uniaxial dynamic tests performed on laboratory-prepared samples and from previous research conducted at Ohio State University. The findings of the study, and comparisons with results of previous similar studies, indicate that a direct general relation exists between rutting parameters, dynamic moduli, and applied stress. The rutting parameter m was found to be almost constant within the range of study, which confirms previous results on subgrade soils that showed m to be an almost universal constant independent of soil type, stress, dynamic modulus, or saturated environmental conditions. A method for estimating permanent deformation in asphaltic concrete layers is proposed on the basis of the relation found in this study, in which the dynamic modulus was found to characterize such mix properties as density, asphalt content, gradation, air voids, and temperature with respect to rutting criteria. A general relation was also found between the rutting parameter A and the dimensionless ratio of dynamic modulus to applied stress. This relation satisfactorily describes the test results regardless of other influential factors such as type of material.

A recent survey among various state highway departments by the American Association of State Highway and Transportation Officials (AASHTO) has shown the importance of excessive permanent deformation, or rutting, as a common cause of failure in flexible pavements. Table 1 gives a summary of the most prevalent types of pavement distress reported by state highway

Table 1. Most prevalent types of pavement distress as reported by state agencies.

Type of Distress	States Reporting Distress as Most Prevalent on							
	Interstate Highways		Primary Highways		Secondary Highways		Farm-Market Highways	
	Number	Percent	Number	Percent	Number	Percent	Number	Percent
Cracking								
Longitudinal	5	10.0	7	15.9	3	6.4	0	0.0
Alligator	1	2.0	2	4.5	5	10.6	7	25.0
Multiple	7	14.0	9	20.5	14	29.9	2	7.1
Transverse	7	14.0	7	15.9	4	8.5	2	7.1
Raveling	1	2.0	2	4.5	3	6.4	3	10.7
Rutting	14	28.0	13	29.5	6	12.8	5	17.8
Flushing	2	4.0	1	2.3	1	2.1	0	0.0
Roughness	1	2.0	1	2.3	5	10.6	0	0.0
Patching	10	20.0	1	2.3	3	6.4	5	17.9
Base failure	0	0.0	0	0.0	2	4.2	2	7.2
Corrugations	0	0.0	0	0.0	0	0.0	1	3.6
Shrinkage	2	4.0	1	2.3	1	2.1	1	3.6
Total	50	100.0	45	100.0	47	100.0	28	100.0

agencies. Under nonfailure conditions, permanent deformation reduces road serviceability and driving comfort. The hydroplaning and icing that result from accumulated water in rutting paths reduce highway safety. Therefore, any rational design scheme should include rutting as an important limiting criteria.

Several research programs at the Ohio State University have focused on establishing a comprehensive model for the estimation of permanent deformation. Majidzadeh and others have presented a mechanistic model that describes rutting phenomena in subgrade soils (1, 2) and in asphaltic concrete layers (3, 4). Research is also being conducted on unstabilized granular bases. This paper deals with the problem in asphaltic concrete.

Numerous design methods with limiting subgrade strain criteria have been proposed to control rutting in the subgrade. Discussions of various approaches to rutting prediction can be found elsewhere (1-6) and need not be repeated here. Pavements designed on the basis of limiting subgrade strain criteria have sufficient thickness to protect the subgrade soil from shear failure, but the method does not ensure that permanent deformation in the upper pavement layers will not occur. The AASHO Road Test has shown that the asphaltic concrete layer contributes anywhere from 5 to 50 percent of total pavement rutting, depending on pavement composition and season of investigation.

To investigate rutting in asphaltic concrete layers, three basic steps should be considered:

1. Determine the traffic and environmental conditions that may occur in the field.
2. Find a reliable technique of stress-strain analysis to adequately describe the distribution of stress in the pavement system.
3. Investigate material characteristics under such traffic loading and the probable intensity, function, and frequency of applied stress, and consider the role of environmental changes, which in this case are primarily those of temperature.

Step 3 is the prime concern in this study of nonfailure pavement conditions.

Laboratory simulation of field conditions is difficult but can be achieved by conducting dynamic tests under different stress levels and temperature changes. This approach, which has proved successful in several studies at the Ohio State University (1-6), was used in this study. A half-sinusoidal compressive dynamic load was applied by using 0.125-s pulses separated by 0.375-s rest periods. A hydroelectronic Material Testing System (MTS) was used to conduct the test program. Only uniaxial tests were used because previous studies on subgrade soils (6-8) and on asphaltic concrete (4) have shown that small magnitudes of confining pressure [σ_3 up to 34 kPa (5 lbf/in^2)] have no significant effect on the resilient behavior of the sample, which matches closely the behavior under three-dimensional dynamic loading with σ_3 vertical and σ_3 horizontal applied stresses.

On the basis of a linear elastic stress analysis using the Chevron program (3) and reported actual stress measurements (9), the range of applied deviatoric stresses was selected at 206.7, 275.6, 344.5, and 402.4 kPa (30, 40, 50, and 60 lbf/in^2) to simulate field conditions. A static load, approximately 4 percent of the dynamic load amplitude, was first applied to ensure complete contact between loading cell and sample to avoid impact action during dynamic testing.

Testing also has a significant effect on permanent deformation in asphalt concrete. For any given condition, the rate of deformation increases with temperature. At temperatures below a certain limit, however, the accumulation of permanent deformation is negligible. It has been reported (10) that the average temperature at which rutting occurs is 22°C (72°F). Accordingly, temperatures of 27°C, 38°C, and 49°C (80°F, 100°F, and 120°F) at each stress level and asphalt content were selected for this study to approximate temperature conditions in the field.

Each sample was subjected to at least 2000 load repetitions at certain stress levels and temperatures. Permanent deformations were measured by using Daytronic linear variable differential transformers mounted on the loading piston. Elastic deformations were recorded by two MTS extensometers (see Figure 1).

MIX CHARACTERISTICS AND SAMPLE PREPARATION

Two similar limestone aggregates (referred to as series 1 and 2) were used to prepare mixes that met gradation and other specification requirements of the Ohio Department of Transportation for surface-course mixtures, as given below (1 mm = 0.039 in):

U.S. Sieve Size (mm)	Percentage Passing by Weight	
	Specification	Mix Composition
12.7	100	100
9.5	90-100	94
4.75	45-75	55
2.36	26-58	40
0.6	8-32	15
0.3	3-22	8

Figure 1. Sample setup for testing.

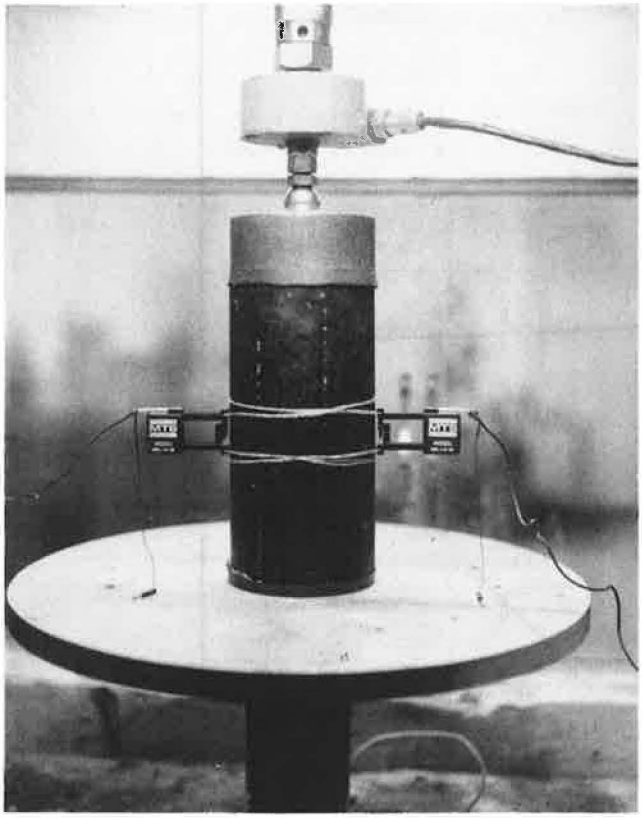

U.S. Sieve Size (mm)	Percentage Passing by Weight	
	Specification	Mix Composition
0.15	1-4	5
0.075	0-8	3

The bitumen used in preparing the mixes was 85/100 penetration AC-20. The specification limits for asphalt content were 4.5-0.5 percent. For the series 1 aggregate, only the optimum asphalt content of 6.5 percent was used; for the series 2 aggregate, three asphalt contents were used: 5.5, 6.5, and 7.5 percent.

Samples 10 cm (4 in) in diameter and 20 cm (8 in) in height were compacted statically by using a compaction pressure of 76.8 MPa (11 000 lbf/in^2), and representative samples were checked for uniformity. The general trend was for the sample to be denser at the bottom and at the middle third to have a density equal to the average overall sample density. The greatest difference in density was 80.1 kg/m^3 (5 lb/ft^3) between sample top and middle third. Sample density varied from 2336.7 kg/m^3 (145.41 lb/ft^3) at 5.5 percent asphalt content to a maximum of 2369.2 kg/m^3 (147.89 lb/ft^3) at 7.5 percent asphalt content. Air voids ranged from 4.32 to 5.11 percent at 5.5 percent asphalt content, from 2.71 to 3.27 percent at 6.5 percent asphalt content, and from 0.58 to 0.76 percent at 7.5 percent asphalt content.

ANALYSIS OF RESULTS

Dynamic Modulus |E*|

In recent research, the dynamic modulus is considered a major characteristic of highway pavement materials that reflects pavement performance under traffic load-

Figure 2. E* versus temperature at various stress levels.

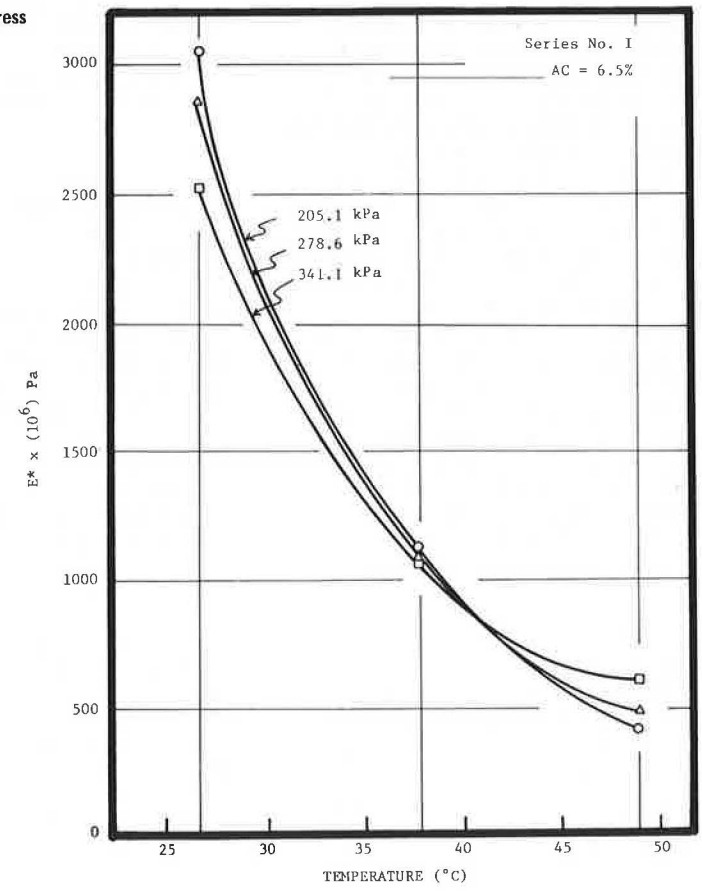

Figure 3. E* versus σ_{apl} at various temperatures.

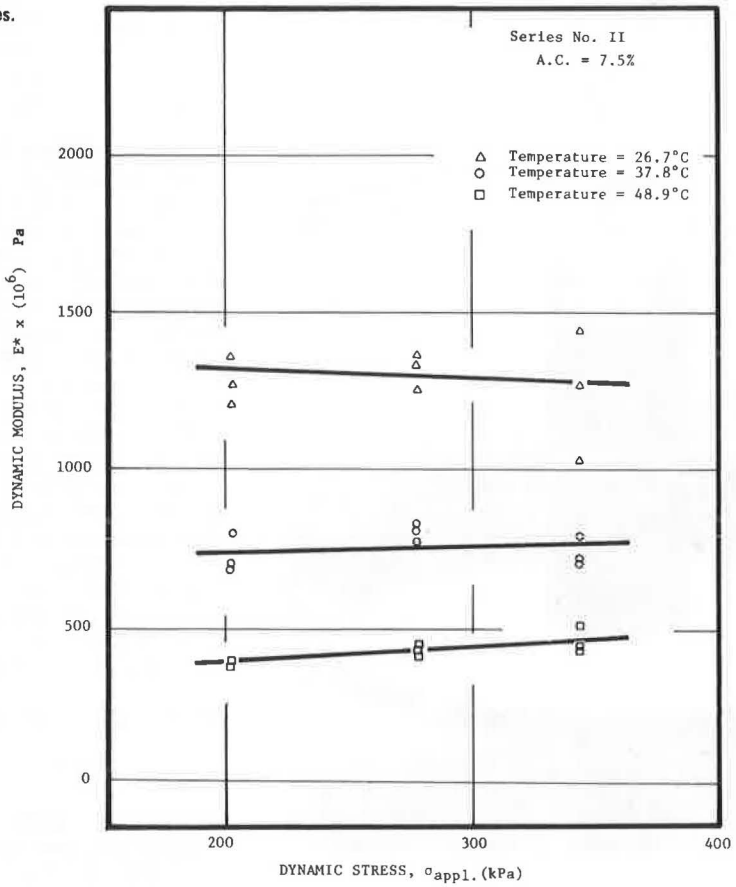

ing. It is defined as the ratio between applied dynamic stress and corresponding elastic strain. A previous study (5) has shown that E* tends to decrease with the number of stress cycles N if the applied stress is higher than the endurance limit (defined as that stress level under which the sample can withstand an infinite number of cycles without failure). E* tends to increase with N when applied stress σ_{apl} is less than the endurance limit. However, in both cases E* will be almost constant after the first 1500 cycles over a wide range of stresses and temperatures (except in cases of failure, which are not the concern of this study). Therefore, E* was calculated for each sample after 2000 cycles.

Variation in temperature was found to be the factor that had the greatest effect on dynamic modulus. Figure 2 shows a typical variation of E* with temperature. An increase from 27°C to 49°C (80°F to 120°F) results in a reduction in moduli values by a factor of four to five. Applied deviatoric stress, in the ranges used, had insignificant effects on the dynamic modulus (see Figure 3). Asphalt content had a noticeable effect at lower temperatures but little effect at higher temperatures (see Figure 4).

Permanent Deformation

Figure 5 shows the typical relation between permanent strain accumulation ϵ_p/N and N on a log-log graph. This relation could be satisfactorily represented by a straight line for a nonfailure, steady-state condition, which is the normal field condition of interest in this paper.

For a failure condition, the rate of ϵ_p/N increases with N, leading to complete failure. This is the case for sample 11 in Figure 5. The concept of threshold stress, proposed by Francken (11), is that stress level under which the steady-state condition is satisfied. It depends on mixture characteristics, temperature, and stress conditions.

Such a nonfailure condition could then be represented by the following formula:

$$\epsilon_p/N = AN^{-m} \quad (1)$$

where A and m are parameters that are dependent on mix composition, applied stress intensity and frequency, and temperature.

There were 110 samples tested for the study that did not experience progressive failure conditions and were found to satisfy the proposed equation. Ten samples followed the formula until a certain stage, after which progressive failure was observed. Similar equations have been proved true by El-Mojarrush (3) and Francken (11).

The evaluation of m and A should completely describe rutting phenomena in asphalt concrete so that we can establish a model for estimating permanent deformation in such material.

Parameter m

Parameter m was calculated for each sample as the absolute value of the slope of the straight-line relation of log (ϵ_p/N) to log N. The values of m showed no significant variation over the testing domain of various stress levels, temperatures, asphalt contents, and the two types of aggregates used. Figure 6 shows the values of m for all testing to range from 0.73 to 0.87.

Test data were divided into groups according to asphalt content, stress level, testing temperature, and/or series of aggregate. One-way analysis of

variance with multiple comparisons was conducted on the means of the m values of these groups (3). Three comparative techniques were used: Tukey B, Tukey HSD, and Scheffé (12). For a 95 percent confidence level, no significant difference was found among these groups. The general mean value of m is 0.78 with a standard deviation of 0.04. This trend is in excellent agreement with previous studies on subgrade soils (1, 2, 6, 7) in which m was found to be constant regardless of material type, mixture composition, stress, dynamic modulus, or saturated environmental conditions.

Parameter A

Parameter A is the permanent strain after the first cycle $[(\epsilon_p/N)_{N=1}]$. It was measured as the interception

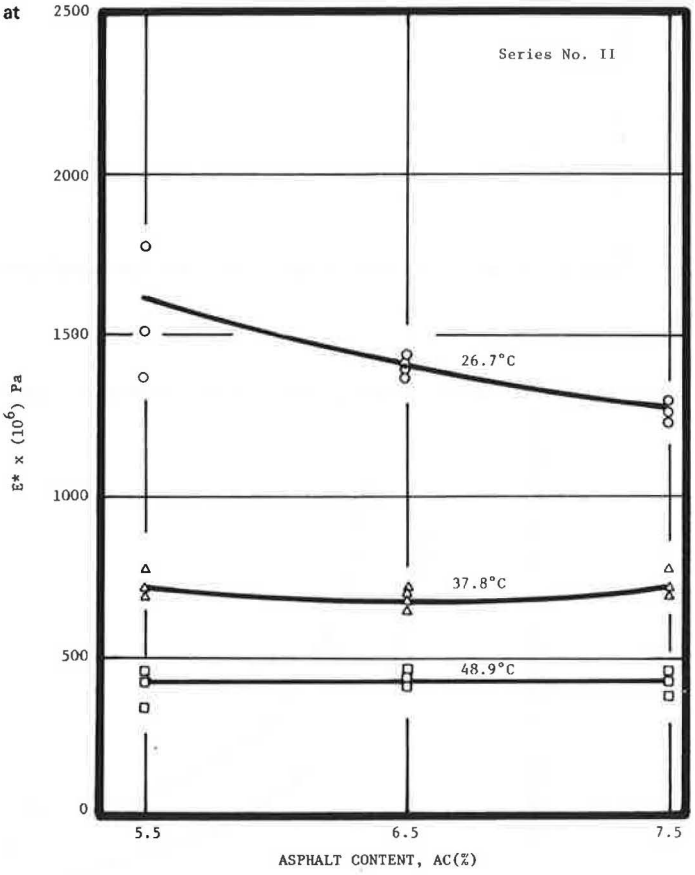

Figure 4. E* versus asphalt content at various temperatures.

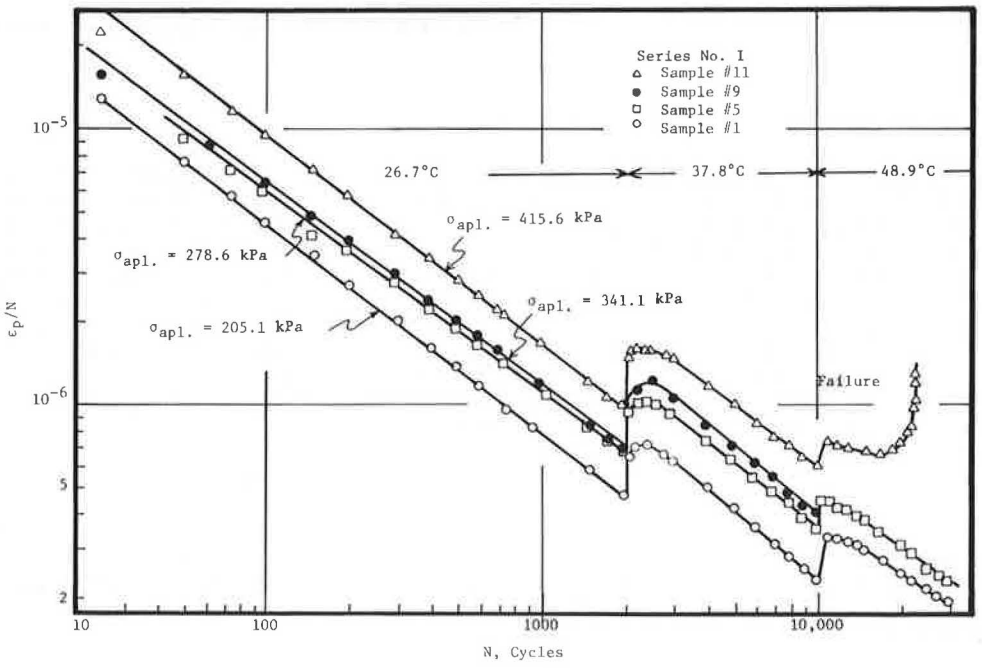

Figure 5. Typical relation between ϵ_p/N and N (continuous test).

Figure 6. E* versus m for types 1 and 2 aggregate.

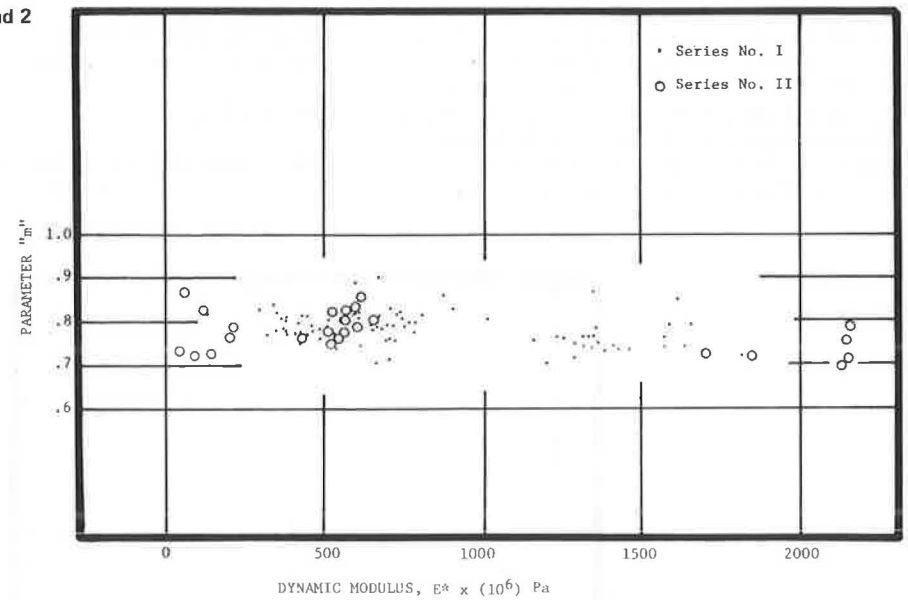

Figure 7. E* versus A for various stress levels (series 2).

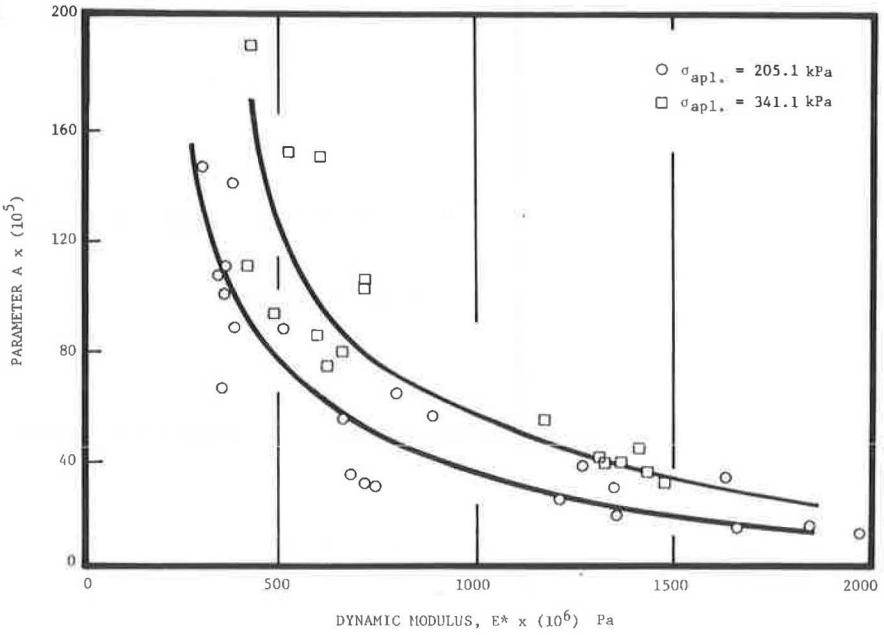

of the straight line of log (ϵ_p/N) versus log N with the axis of N = 1. In general, A increases with applied dynamic stress and testing temperature.

Recognizing the fact that E* is a basic material mechanical characteristic, we plotted the values of A versus the corresponding values of E* for each stress level. Figure 7 shows typical curves for one case. From these curves, it can be deduced that a power relation may exist between A and E* (see Figure 8). The relation could be represented by a straight line with an adequate correlation coefficient. Mathematically, this relation is

$$A = K(|E^*|)^{-S} \quad (2)$$

where K and S are constants that are dependent on applied dynamic stress. A similar relation has been proposed by Majidzadeh and others (1) for fine-grained subgrade soils.

Furthermore, Figures 9-11 show the relation between log A and log (E^*/σ_{apl}) for data obtained from samples using series 1 and 2 aggregate, respectively, for all the various conditions of stress levels, asphalt contents, and temperatures. It can be seen that a straight line can represent the relation with a high correlation coefficient. Figure 12 shows the same relation—and the same trend in the relation—for all samples tested in this study. Accordingly, the parameter is correlated with the dimensionless ratio E^*/σ_{apl} by the following formula:

$$A = J(E^*\sigma_{apl})^{-S} \quad (3)$$

where J and S are constants believed to be universal for asphalt concrete. However, studies of other mixtures are required to investigate this point.

It is clear that, in experimentally establishing the

Figure 8. General relation between E* and A for series 2 (all asphalt contents).

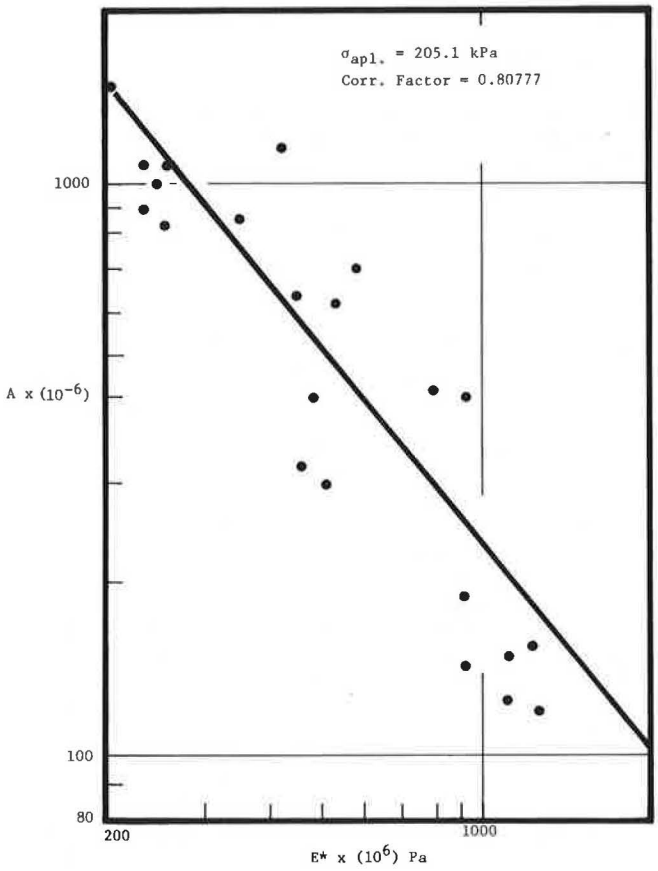

Figure 9. E^*/σ_{apl} versus A for series 1 (initial tests).

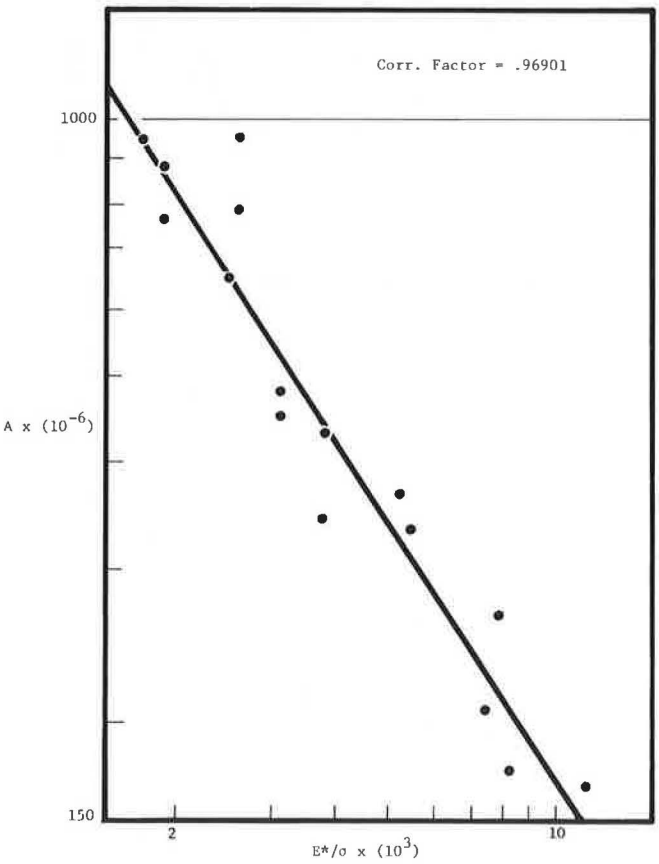

Figure 10. E^*/σ_{apl} versus A for series 1 (continuous tests).

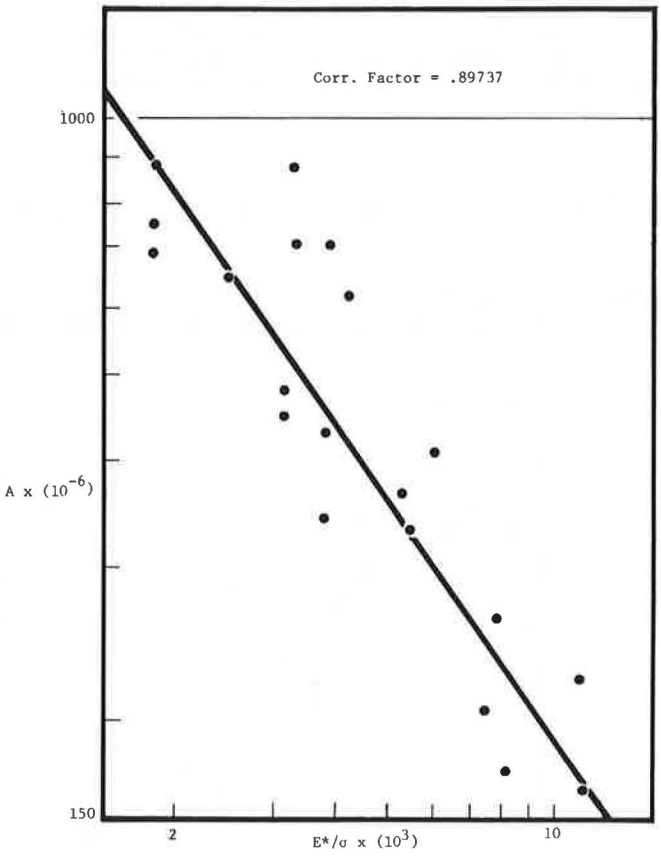

Figure 11. E^*/σ_{apl} versus A for series 2 (all asphalt contents).

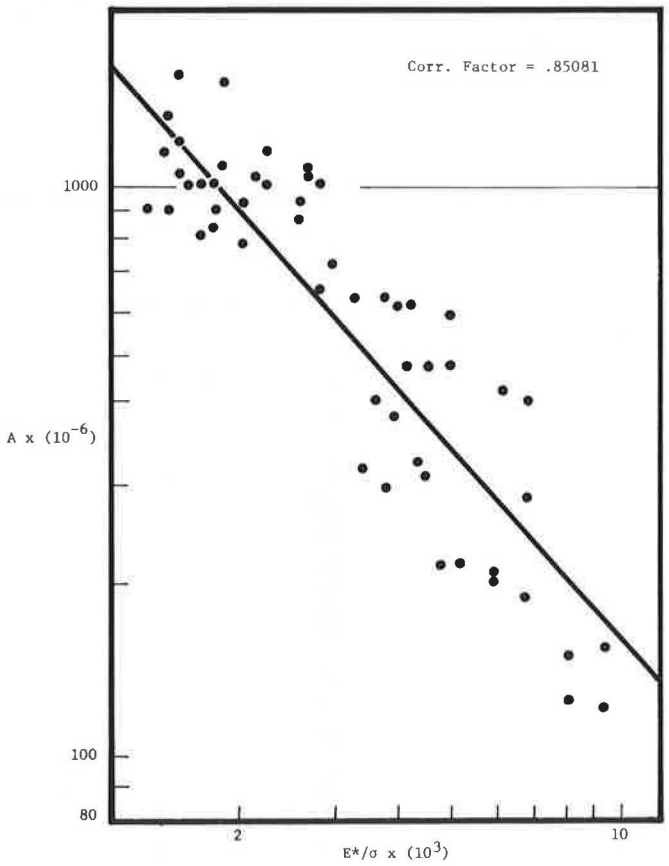

constants J and S for any mix, A could be determined in correspondence with measured values of E* and applied dynamic stress. This means that Equations 1 and 3 describe the phenomena of permanent deformation in asphaltic concrete for any specific condition as follows:

$$\epsilon_p/N = J(E^*/\sigma_{apl})^S N^{-m} \quad (4)$$

Equation 4 has contributed to a substantial reduction of the experimental work that should be performed to evaluate rutting in asphaltic concrete under different conditions.

Figure 12. E^*/σ_{apl} versus A for all samples tested.

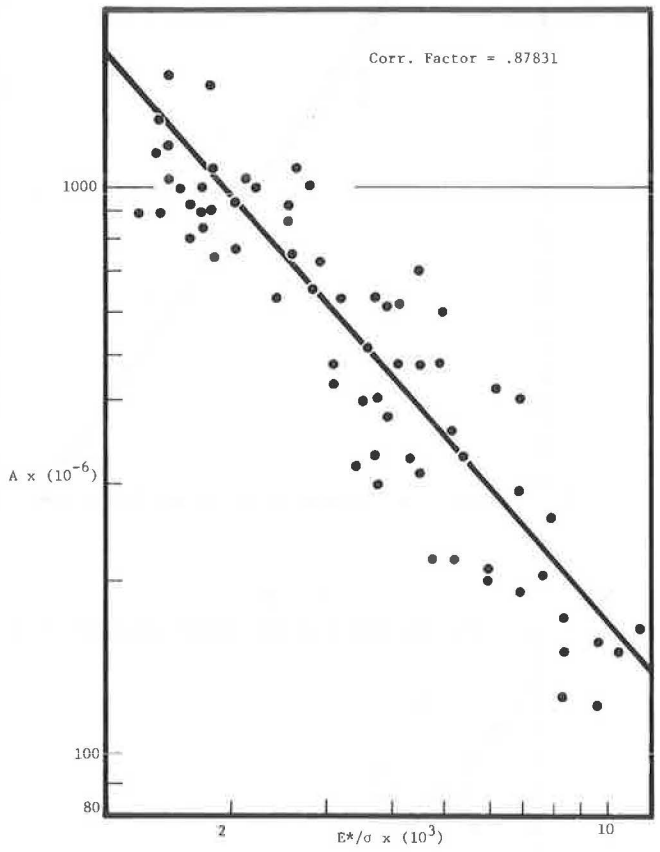

Temperature Variation

As mentioned above, Equation 4 describes rutting in an individual environmental and stress condition. But what about the prediction of rutting under a series of different conditions? The main influencing factor in this case is variation in temperature.

The 30 samples prepared by using series 1 aggregate were subjected to continuous testing under a series of temperature changes. Each sample was tested under constant dynamic and static stress levels while the temperature was changed, after a specific number of loading cycles, from 27°C to 38°C to 49°C (80°F to 100° F to 120°F) or from 38°C to 49°C (100°F to 120°F). Figures 13 and 14 show typical results of these tests.

Some samples experienced failure when tested continuously at a high stress level and 49°C temperature. Those samples were not included in the analysis (see sample 7 in Figure 13). In the nonfailure cases, when the temperature was increased at a certain point the samples showed a sudden increase in rate of deformation and followed a different dynamic creep curve (Figure 13). This is also shown by the vertical jump in the rate of deformation of the curves for ϵ_p/N versus N at the points of temperature changes (see Figure 14). After the first few hundred cycles at the new higher temperature, the creep curve becomes more steady and follows Equation 1 with a higher value of A. Apparently, these few hundred cycles are necessary to rearrange the sample structure in its strongest form to compensate for the new temperature level. It also goes through a diverse stage in which E* decreases in value.

Parameters m and A were analyzed for these continuity tests by following the same pattern used for initial testing. First, m in Equation 1 falls in the same range as that discussed at the beginning of this paper. A was calculated by using the accumulative values of permanent deformation over the whole testing sequence before each temperature state. Equation 3 was also found to hold for these conditions with a correlation coefficient of 0.897.

Figure 13. Typical dynamic creep curves.

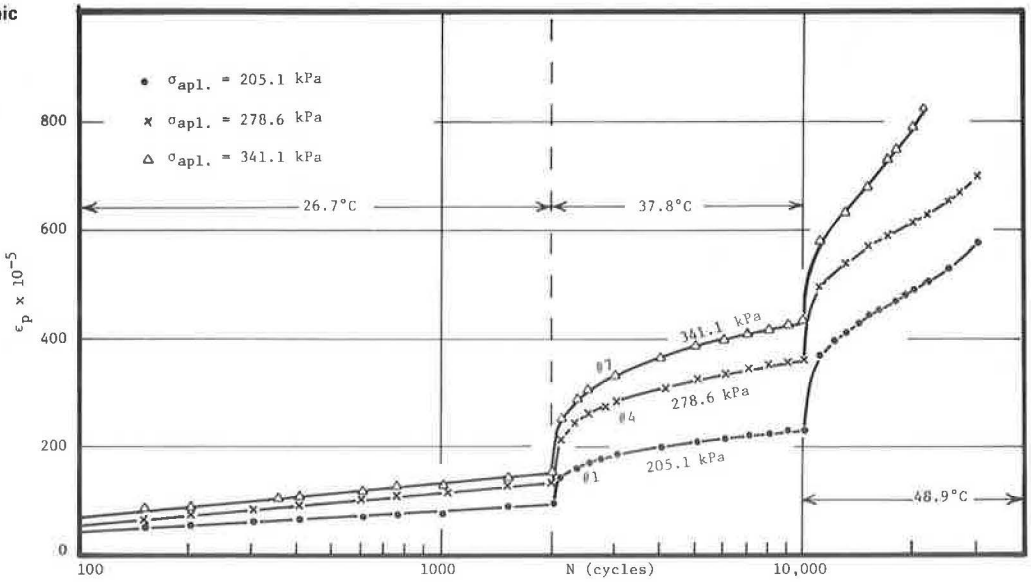

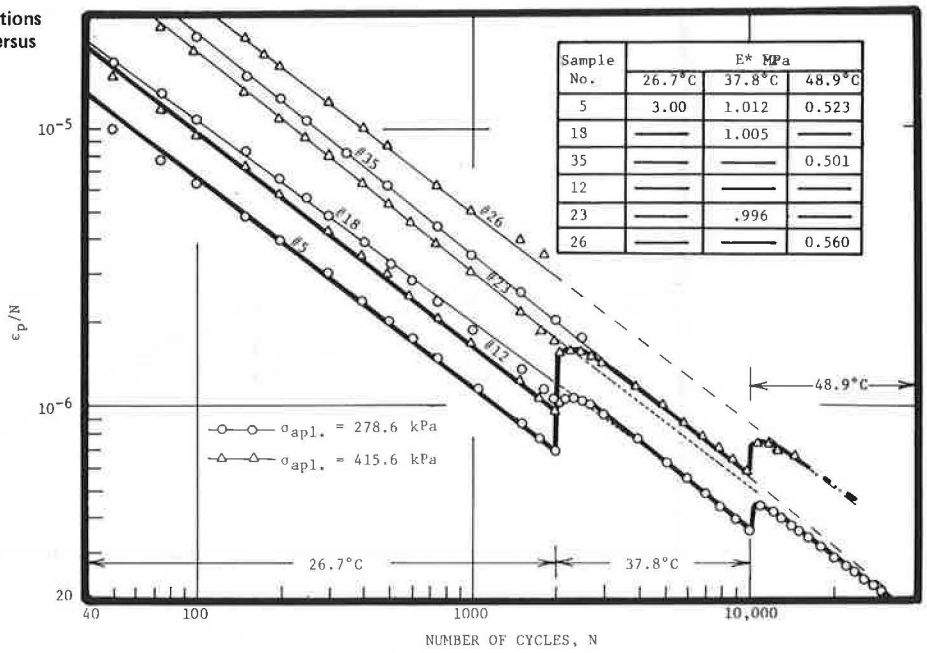

Figure 14. Effect of variations in temperature on ϵ_p/N versus N.

Identical samples, which had been tested initially at 38°C or 49°C (100°F or 120°F), were introduced for comparison. The idea was to compare the dynamic creep curves of the samples tested, either initially or in a continuity test, under the same stress level and temperature and, if possible, the same E*. To perform such a comparison, the results of such samples were plotted on log (ϵ_p/N) versus log N graphs (Figure 14). The dynamic modulus was considered a basic mechanical property according to which samples were judged and determined to be identical.

In Figure 14, sample 5 is compared with sample 18 at 38°C and with sample 35 at 49°C. At 38°C, both lines that represent the data of samples 5 and 18 are close. At 49°C, sample 5 has a higher dynamic modulus than sample 35, and sample 5 thus shows a higher resistance to rutting. That is expected even if both samples have been tested for rutting under the same conditions. The same analysis can be applied to samples 12, 23, and 26 in Figure 14.

In other words, Figure 14 shows that, if a sample that was previously tested at a lower temperature is retested at a higher temperature, the resulting dynamic creep curve could be represented by that of an identical sample initially tested under the same condition, provided the stress level is kept constant in all cases. Although this conclusion was not completely satisfied in all cases, the relation was generally acceptable. The observations are encouraging for further investigation into this approach.

MODEL FOR RUTTING PREDICTION

The findings of this study can be put to use in the following procedures for rutting evaluation:

1. Divide the time period over which rutting is to be evaluated into seasons. Exclude those seasons in which the temperature is lower than 22°C (72°F) (10). Find the traffic and the average corresponding temperature for each season. Investigate variation in temperature along the asphalt depth.
2. Conduct an analysis of stress distribution in the pavement under the equivalent traffic load by using an appropriate technique (several techniques are proposed by the literature, i.e., linear or nonlinear elastic, elastoplastic, and viscoelastic).
3. Divide the asphaltic concrete layer(s) within the pavement system into imaginary sublayers. The number of these sublayers depends on total thickness and stress distribution.
4. Perform dynamic tests on representative samples. Apply dynamic stress levels in the ranges obtained in step 2, and use testing temperatures found in step 1. Measure elastic and plastic deformations. The measured values of E* should be fed back into step 1 to check the assumed values.
5. From step 4, find the constants J and S of Equation 4 to establish A versus E* and σ_{apl}.
6. Calculate the permanent strain for each sublayer (ϵ_{pr}) as in the following example: Assume four consecutive environmental changes to be considered. E_i*, A_i, N_i, and M_i are the corresponding variables at the i th condition (see Figure 15). At the end of the first stage (condition a) and according to Equation 1, the value of log (ϵ_p/N) can be written as

$$\log(\epsilon_p/N)_1 = \log A_1 - m_1 \log N_1 \quad (5)$$

During the second stage (condition b), the pavement undergoes an increase in temperature. Assume incremental change in environmental conditions, i.e., a sudden change in the pavement characteristics caused by this temperature change at ($n_1 + 1$) cycles. $E_2^* < E_1^*$; consequently $A_2 > A_1$, and permanent deformation will increase at a higher rate. Assume that log (ϵ_p/N) will correspondingly increase suddenly at ($N_1 + 1$) cycles by the value (log A_2 - log A_1) (Figure 15). Then, at the end of this stage log (ϵ_p/N) is

$$\log(\epsilon_p/N)_2 = \log(\epsilon_p/N)_1 + \log A_2 - \log A_1 - m_2(\log N_2 - \log N_1) \quad (6)$$

In the third stage (condition c), the temperature gets higher; $E_3^* < E_2^*$ and $A_3 > A_2$. Under the same assumption as that given for condition b above, ϵ_p/N at the end of this stage is

$$\log(\epsilon_p/N)_3 = \log(\epsilon_p/N)_2 + \log A_3 - \log A_2 - m_3(\log N_3 - \log N_2) \quad (7)$$

Figure 15. Prediction of accumulation of permanent deformation.

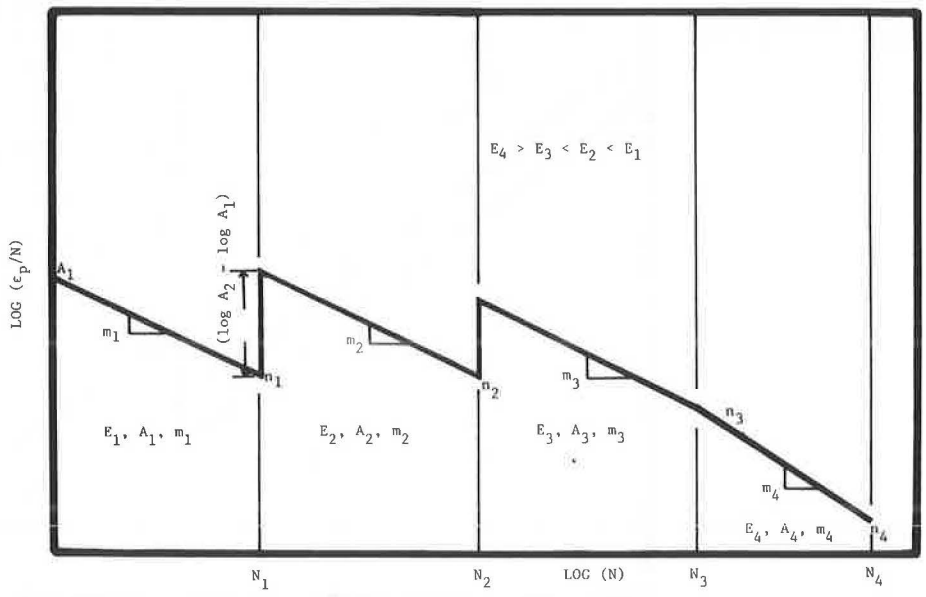

Finally, the improving stage occurs where the temperature is lower than that of condition c. The pavement passes through a hardening phase where $E_4^* > E_3^*$. Since permanent deformation is irrecoverable, no jump is expected in log (ϵ_p/N) at N_3 cycles. Hence, the expression for log (ϵ_p/N) at the end of this stage is

$$\log (\epsilon_p/N)_4 = \log (\epsilon_p/N)_3 - m_4 (\log N_4 - \log N_3) \quad (8)$$

Substituting Equations 5, 6, and 7 into Equation 8, we get

$$\log (\epsilon_p/N_4) = \log [A_3 N_1^{-(m_1-m_2)} N_2^{-(m_2-m_3)} N_3^{-(m_3-m_4)} N_4^{-m_4}]$$

or

$$(\epsilon_p/N)_4 = A_3 N_4^{-m_4} \prod_{i=1}^{3} N_i^{-(m_i-m_{i+1})} \quad (9)$$

If m is constant, Equation 9 takes the following form:

$$(\epsilon_p/N)_4 = A_3 N_4^{-m} \quad (10)$$

In general, if we have j environmental changes and if A_{max} is the maximum value of A for the weakest condition of the pavement during these j changes, at the end of the jth stage, ϵ_p/N is expressed as

$$(\epsilon_p/N)_j = A_{max} N_j^{-m_j} \prod_{i=1}^{j-1} N_i^{-(m_i+m_{i+1})} \quad (11)$$

For $m_1 = m_2 = \ldots = m_i = m$, Equation 11 can be written as

$$(\epsilon_p/N)_j = A_{max} N_j^{-m} \quad (12)$$

Obtaining ϵ_p for each sublayer for different seasons by using step 5, the total contribution of the asphalt concrete layer(s) to total pavement rutting is

$$\gamma_p \text{ total} = \sum_{i=1}^{n} \epsilon_{pi} h_i \quad (13)$$

where

n = number of sublayers,
ϵ_{pi} = permanent strain of the ith sublayer, and
h_i = thickness of the ith sublayer.

CONCLUSIONS

Based on the results on this study, a complete methodology for rutting evaluation has been proposed. The following conclusions can be drawn:

1. Equation 1 represents the dynamic creep curves for asphalt concrete.
2. Parameter m in Equation 1 is constant in the range of study.
3. The dynamic modulus characterizes the material properties; i.e., it reflects the effects of asphalt content, density, mix gradation, air voids, and temperature as far as permanent deformation criteria are concerned.
4. A general relation was found between A and the dimensionless ratio E^*/σ_{apl} (Equation 4). This relation was found to describe test results regardless of other influencing factors, including type of material. This may lead to the projection of the constants J and S in Equation 4 to be universal for asphalt concrete mixes.

REFERENCES

1. K. Majidzadeh, S. Khedr, and H. Guirguis. Laboratory Verification of a Mechanistic Subgrade Rutting Model. TRB, Transportation Research Record 616, 1976, pp. 34-37.
2. K. Majidzadeh, F. Bayomy, and S. Khedr. Rutting Evaluation of Subgrade Soils in Ohio. TRB, Transportation Research Record 671, 1978, pp. 75-84.
3. M. El-Mojarrush. Permanent Deformation in Asphalt Concrete Mixes Under Variable Stress and Environmental Conditions. Ohio State Univ., Columbus, M.S. thesis, 1978.
4. K. Majidzadeh, N. Safwat, M. El-Mojarrush, and R. N. El-Mitiny. Optimization of Design of Asphaltic Mixtures. Engineering Experiment Station, Ohio State Univ., Columbus, Project EES 560, Final Rept. (in preparation).
5. K. Majidzadeh, C. L. Saraf, G. Ilves, and F. Makdiski-Ilyas. A Laboratory and Field Durability

Study of Asphaltic Mixtures. Engineering Experiment Station, Ohio State Univ., Columbus, Project EES 356, Final Rept., 1974.
6. K. Majidzadeh, S. Khedr, and F. Bayomy. A Statewide Study of Subgrade Soil Support Conditions. Engineering Experiment Station, Ohio State Univ., Columbus, Project EES 518, Final Rept. (in preparation).
7. K. Majidzadeh and H. Guirguis. Field Study of Subgrade Compaction. Engineering Experiment Station, Ohio State Univ., Columbus, Project EES 406, Final Rept., 1974.
8. M. Thompson and A. Robnett. Resilient Properties of Subgrade Soils. Univ. of Illinois, Urbana-Champaign, Project IHR-603, Final Rept., 1976.
9. S. Brown, B. Brodrick, and C. Bell. Permanent Deformation of Flexible Pavements. Univ. of Nottingham, Nottingham, England, Res. Project Dm 161102B2B, Final Tech. Rept., 1977.
10. Austin Research Engineers, Inc. Asphalt Concrete Overlays of Flexible Pavements. Federal Highway Administration, U.S. Department of Transportation, Final Rept., 1975.
11. L. Francken. Permanent Deformation Law of Bituminous Road Mixes in Repeated Triaxial Compression. Presented at 4th International Conference on Structural Design of Asphalt Pavements, Ann Arbor, MI, Vol. 1, 1977.
12. Statistical Package for the Social Sciences (SPSS). National Opinion Research Center, Chicago, 1970.

Publication of this paper sponsored by Committee on Strength and Deformation Characteristics of Pavement Sections.

Subjective and Mechanical Estimations of Pavement Serviceability for Rural-Urban Road Networks

Matt A. Karan, Pavement Management Systems Limited, Paris, Ontario
D. H. Kobi, Federal Technical Surveys Limited, Paris, Ontario
Clare B. Bauman, Regional Municipality of Waterloo, Waterloo, Ontario
Ralph C. G. Haas, Department of Civil Engineering, University of Waterloo, Waterloo, Ontario

To manage paved road networks efficiently, highway agencies require comprehensive, periodic inventory or pavement evaluation data. These data should be reliable, quickly and easily acquired, and manageable. The results of a study that involved subjective and mechanical measurements of both the roughness and structural adequacy of a combined rural-urban road network are presented. A new high-speed, computerized unit was used to make the mechanical measurements of roughness, and panel ratings were used for the subjective measurements. Structural adequacy was both rated by a panel and mechanically measured with a Dynaflect. Very good correlations were obtained between panel ratings and measured roughness for both urban and rural sections. The relations obtained and the resource and time requirements involved demonstrate that, by using such methods, highway agencies can quickly and efficiently inventory the serviceability of paved road networks. Ratings of structural adequacy did not correlate with measured deflection. The results suggest that, whereas surface distress or condition can be measured by panel ratings, structural adequacy can only be measured by mechanical means.

All highway agencies conduct inventory measurements and needs studies of some sort on their road networks based on various measures of functional, structural, and serviceability adequacy. Candidate projects are identified from these studies, and priorities are determined for investments in both new construction and rehabilitation to the limit of the available budget. Figure 1 shows the major elements of such a system of inventory needs priority within the framework of an overall system of road management.

Periodic inventory or evaluation measurements provide the basis for the identification of needs and all subsequent management activities. In other words, this is the basic management information.

Much of the inventory information currently collected by highway agencies is a combination of subjective and objective measurements. Ideally, such information would be subject to the following criteria:

1. It would be capable of being collected quickly, easily, and efficiently; be as objectively based as possible; be reliable and repeatable; and relate directly to the structural, functional, and serviceability indicators;
2. It would cover or represent the entire network and include sufficient frequency on the more deteriorated sections so that needs could be identified soon enough in advance to allow for proper programming; and
3. The information would itself be manageable.

In the light of these considerations, the Waterloo region of Ontario initiated a pavement evaluation study in 1978 as a part of their 1979 needs study update (1, 2). This regional municipality is about half urban and half rural and has about 1935 km of arterial roads and streets. A key requirement for the needs study update was the correlation of certain subjective pavement ratings with actual physical field measurements. The purpose of this paper is to describe the following specific results of the study:

1. The use of a new high-speed unit for obtaining roughness and other road data on an automated, mass-inventory basis;
2. The correlation of measured roughness with

Figure 1. General structure of road management system.

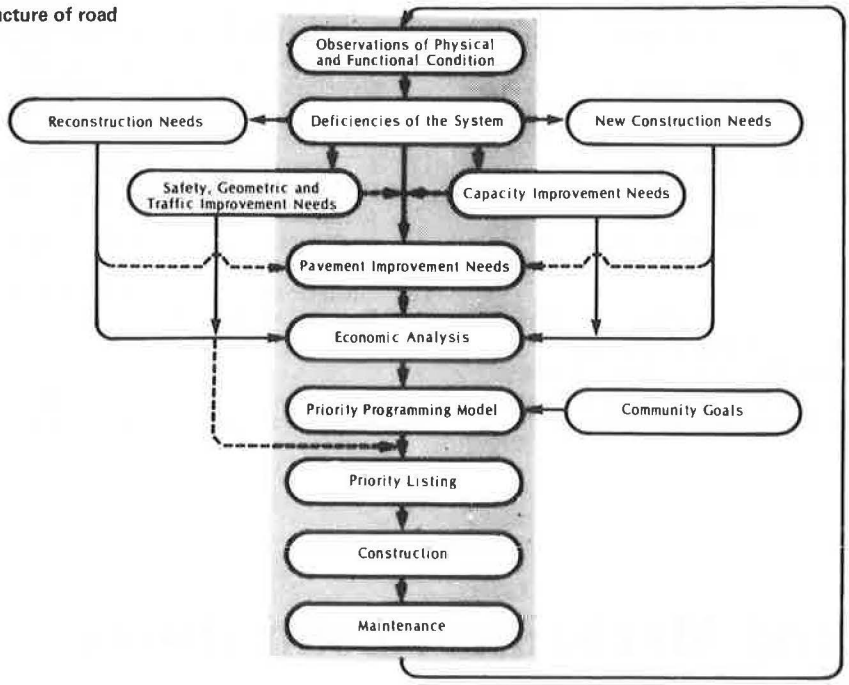

Figure 2. Automatic Road Analyzer unit.

panel ratings of riding comfort in a designed experiment that recognizes the requirements and resources of the agency involved and rural versus urban conditions; and

3. The correlation of measured surface deflection with subjectively based ratings of structural adequacy.

SELECTION OF STUDY SITES

Both urban and rural road sections were considered to be needed because of differences in such factors as speed, operating condition, and environment. It has been shown that the opinions of road users about the quality of a road vary depending on the condition (i.e., urban or rural) in which they are traveling (3).

In selecting the location of the sections, which consisted of 28 rural and 27 urban, an attempt was made to obtain as many sections as possible for each range of riding comfort index (RCI) values. [RCI is the Canadian measure of present serviceability, on a scale of 0 to 10, adopted by the Roads and Transportation Association of Canada (4).] RCI was measured in 10 groups: 0.0-0.9, 1.0-1.9, and so on to 9.0-10.0. Although the majority of values would naturally fall in the middle range, sections with very low and very high RCIs were also needed to establish a complete range of conditions for regression analysis.

All rural sections selected were on two-lane paved regional roads. Half of the urban sections selected were on four-lane regional streets, and the rest were on two-lane streets.

An attempt was made to select the rural sections so that they were well spread out across the region. Urban sections were selected from all three of the major cities in the region—Kitchener, Waterloo, and Cambridge.

All rural sections were approximately 1200 m long. Urban sections, however, were relatively shorter (300 m long) because of traffic lights, stop signs, and other such constraints.

FIELD MEASUREMENTS

Roughness

Longitudinal roughness on the study sections was measured by a recently developed unit, the Automatic Road Analyzer (ARAN), which is housed in a Ford van and measures roughness by use of an accelerometer. The data are recorded in digital form on magnetic tape. Other parameters that can be measured and similarly recorded in digital form include crossfall and grade angle, right and left rut depths (a process that is still being developed), skid resistance, and 12 coded categories of pavement distress that are entered on a keyboard. The ARAN unit, shown in Figure 2, has an on-board "intelligent" computer terminal with keyboard plus an acoustic coupler transmission system. It also has hard-copy recording and on-board editing capabilities for which specially developed software is used. Extensive repeatability measurements at various speeds and roughness levels have been made on the ARAN unit in cooperation with the Ontario Ministry of Transportation and Communications (MTC) (5). These measurements indicate that the unit provides a high degree of repeatability and can be used over a wide speed range (i.e., "float" in traffic).

Table 1. Field data for rural and urban sections.

Section	Average RCI		Average Roughness Value		Structural Index		Deflection (mm)	
	Rural	Urban	Rural	Urban	Rural	Urban	Rural	Urban
1	4.1	5.3	645.99	496.58	2	15	0.028	0.028
2	7.9	5.0	113.13	553.29	20	14	0.026	0.029
3	1.4	5.1	1168.94	406.26	-	5	0.029	0.021
4	4.5	3.3	361.00	660.02	6	-	0.018	0.028
5	8.2	8.2	115.58	199.14	20	20	0.025	0.022
6	4.8	4.6	252.88	387.80	3	15	0.035	0.024
7	4.5	5.8	235.77	200.41	3	16	0.026	
8	7.9	6.4	82.97	210.09	20	9	0.022	0.02
9	6.1	7.3	182.03	150.27	5	20	0.029	0.028
10	8.3	5.1	77.00	470.14	20	-	0.028	0.028
11	5.6	4.5	227.57	588.39	0	-	0.042	0.04
12	2.6	7.7	417.82	170.23	0	19	0.042	0.015
13	8.0	8.3	87.29	198.67	19	20	0.019	0.019
14	4.3	4.8	363.00	431.61	6	16	0.035	0.027
15	7.8	7.7	96.20	208.91	17	19	0.016	0.029
16	8.0	5.0	86.89	398.12	20	-	0.020	0.039
17	9.0	3.4	67.28	687.27	20	1	0.025	0.033
18	7.5	3.7	101.41	568.68	19	5	0.020	0.04
19	6.6	7.3	378.76	174.64	8	18	0.019	0.03
20	6.7	7.3	157.73	191.01	10	20	0.029	0.023
21	2.8	6.1	658.25	374.01	15	17	0.018	0.033
22	7.0	4.6	169.60	519.97	19	5	0.026	0.03
23	6.4	7.0	123.04	217.10	-	19	0.023	
24	3.4	5.7	613.69	286.72	18	12	0.029	0.022
25	4.5	7.7	326.08	186.08	12	20	0.032	
26	6.7	4.8	133.89	408.55	15	17	0.028	
27	4.9	4.0	224.68	571.01	3		0.022	
28	7.8		71.15		20		0.018	

Note: 1 mm = 0.039 in.

A software package has also been developed to calculate and enter into a data bank any summary statistics, such as mean roughness for a section or mean plus standard deviation, desired by direct computer analysis of the magnetic tapes. This means that mass-inventory, raw data can be efficiently used and "managed," with no manual recording, keypunching, etc.

In this study, roughness was measured on each rural section at 50-m intervals and at 80-km/h operating speed. Urban sections were measured at 50 km/h because of speed-limit restrictions. An average roughness for each section was then calculated from the raw data. Table 1 gives the average roughness values for each rural and urban section used in the study.

Deflection

In the next step, surface deflection was measured on the same sections. An average of four Dynaflect tests were taken on rural sections. The average maximum deflection on each section was calculated and converted to maximum spring deflections by using a spring-fall ratio of 1.2. Two tests were taken on each urban section, and average spring maximum deflections were calculated for purposes of correlation. Table 1 gives the average spring deflections for rural and urban sections, respectively.

Riding Comfort

In the second part of the field study, panel ratings were used to determine the RCIs of the previously selected rural and urban sections. A panel was formed for rating purposes under guidelines described by Nakamura and Michael (6). Nakamura and Michael have shown that a panel consisting of highway engineers does not rate pavements any more consistently than a similar panel consisting of members from various professions. They have also developed a table for selecting a panel size to achieve a certain degree of accuracy.

A panel of eight was used in the study with the assumption that the average of their ratings would be 0.6 units away from the true rating 19 out of 20 times, as suggested by Nakamura and Michael (6). The panel included five men and three women; their occupations were secretary (one), housewife (one), teacher (one), technician (two), farmer (one), and engineer (two).

Panel members were "trained" before the rating sessions. The purpose of the study was explained, and the pavement serviceability concept (RCI) and its use to the pavement engineer were discussed. The rules of the rating sessions and factors to be considered in the rating process were explained. After the instruction session, the panel members were taken to the field and asked to rate four urban and four rural sections. Their ratings were then discussed with them to make sure that they had understood the rules.

The instructions to be followed by each rater during the rating sessions were prepared under the guidelines of a Texas study (7). Raters were located in the test vehicle (a 1978 Chrysler Lebaron) in a random order. There were four raters in each vehicle; all, including the driver, rated each of the 28 rural and 27 urban sections. Ratings were completed in four days.

Six rural and six urban sections were rated again by each rater. Because of time limitations, these replications were done one day before the actual rating sessions. The sections selected for replication were chosen at random.

Structural Adequacy

In the second phase of the rating sessions, a panel of three was used to rate the structural adequacy of the 28 rural and 27 urban sections used in the study. This panel was composed of professionals in the field: the director of roads and traffic for the region, a representative from MTC, and an experienced engineer from a consulting firm.

Ratings were performed according to the procedures set by MTC, which are described in detail elsewhere (1). Ratings were completed in one day. Table 1 gives the results in terms of a "structural index" for all sections used in the study.

ANALYSIS OF DATA

Riding Comfort

The panel ratings were first analyzed to see if any systematic error occurred in the rating procedures. The leniency error (8), which can be defined as the deviation of each rater's average rating for all sections from the overall mean rating, was calculated for each rater. The analysis indicated that the magnitude of leniency error in the data was insignificant.

Similarly, further analyses showed halo and central tendency effects (8) to be insignificant. It was therefore decided that the raters' performance was reasonable and no correction in the raw data was necessary.

The raw data were then analyzed to see if the ratings were affected by (a) location in the automobile and (b) differences between drivers and passengers. Analysis of variance (ANOVA) techniques were used for this purpose. None of the effects was found to be significant. It was possible, therefore, to use the average panel rating on each section as a reasonable approximation of its true rating.

The replicated ratings were also analyzed to check raters' ability to repeat an observation of the same pavement section. The results of the ANOVA indicated that there is a significant variation between raters and sections. In other words, ratings vary significantly from one section to another. This, of course, is quite normal since the same response cannot be expected from all raters on all sections.

The replication factor was not found to be significant for rural sections, but it was significant for urban sections. From a statistical point of view, this means that raters are capable of repeating their ratings on rural but not on urban sections. This cannot be generalized, however, because the urban replication session was done immediately after the rater training sessions and before the actual rating sessions. The main reason for the significant replication effect on urban sections was probably the raters' lack of sufficient experience. The extremely good results obtained from the subsequent rating sessions clearly support this argument.

In summary, the riding comfort data were first analyzed to see if any systematic error occurred in the rating process. It was found that the magnitude of the systematic errors in the data was negligible and did not affect the overall outcome of the process. The data were then analyzed to see if the ratings were affected by location in the automobile and differences between drivers and passengers. None of these effects was found to be significant. Analysis of the replication data produced reasonable results. It was therefore concluded that the average of eight raters on each section could be used to represent the true ratings of the sections. These average values are given in Table 1.

Approximating Riding Comfort Data

The average RCI data on each section were then related to the roughness of the pavement as measured by the ARAN unit. Several regression models were tested to approximate RCI by roughness. The following regression equations were selected as best representing these relations. For rural sections,

$$RCI = 18.8744 - 5.6398 \log_{10} X \quad (1)$$

For urban sections,

$$RCI = 22.8457 - 6.7686 \log_{10} X \quad (2)$$

where X = pavement roughness divided by 10, as measured by the ARAN unit.

Figures 3 and 4 show the data used in the analysis and the resulting regression equations for rural and urban sections, respectively. Statistical characteristics of the relations, as shown in Figures 3 and 4, are quite acceptable.

Rural sections 12 and 19 were excluded from the analysis because of the nonuniform nature of their roughness. Section 12, for example, was generally rough but contained a very smooth subsection that affected the ratings. Urban section 7 was excluded because, as a result of a mix-up in the rating process, raters did not rate the same section that was measured by the ARAN unit.

Equations 1 and 2 are generally similar. This, of course, is quite acceptable because the RCI concept is basically the same for both rural roads and urban streets. The minor changes in the slopes of the curves are attributable to changes in speed, driving conditions, and environment.

In the practical use of Equations 1 and 2, therefore, one can measure the roughness of a pavement section and then estimate the road user's subjective opinion (i.e., the RCI) from the equations. Once they are developed, such equations should be fairly "stable" for an area or region for several years and require no new or check panel ratings.

The rural and urban data were also analyzed together because of the similarity of Equations 1 and 2 and the fact that speed appeared to be the only major difference in the relations of Figures 3 and 4. The following equation was derived:

$$RCI = 22.8147 - 5.9607 (\log_{10} X) - 0.0402 (S) \quad (3)$$

where S = speed in kilometers per hour. The statistics for this equation are $S_e = 0.54$, $R^2 = 0.91$, $t_1 = 22.51$, $t_2 = 7.38$, and $F_{2,49} = 255.59$. These statistics indicate that Equation 3 could be used with sufficient accuracy for both rural and urban sections instead of Equations 1 and 2.

It also appears that the curves of Figures 3 and 4 would merge at the extremes; in other words, the effect of speed is more significant in the medium roughness range. This is quite logical because a very smooth pavement should give a good ride no matter what the speed and a very rough pavement is rough at all speeds.

Approximating Structural Adequacy Ratings

Correlating a subjectively based structural adequacy rating with surface deflection was one of the objectives of the study. But, as Figure 5 shows, it was not possible to develop an acceptable relation between these two factors. Figure 5 clearly indicates that there is no relation between ratings of structural adequacy and surface deflection. This, of course, supports the argument that the structural adequacy of a road or street cannot be accurately rated by visual means. It also indicates that the raters do not actually rate the load-supporting ability of the pavement but other factors such as appearance, distress, or ride quality.

Future rating sessions and measurements of condition in terms of percentage of damaged area are

Figure 3. RCI versus roughness for rural roads.

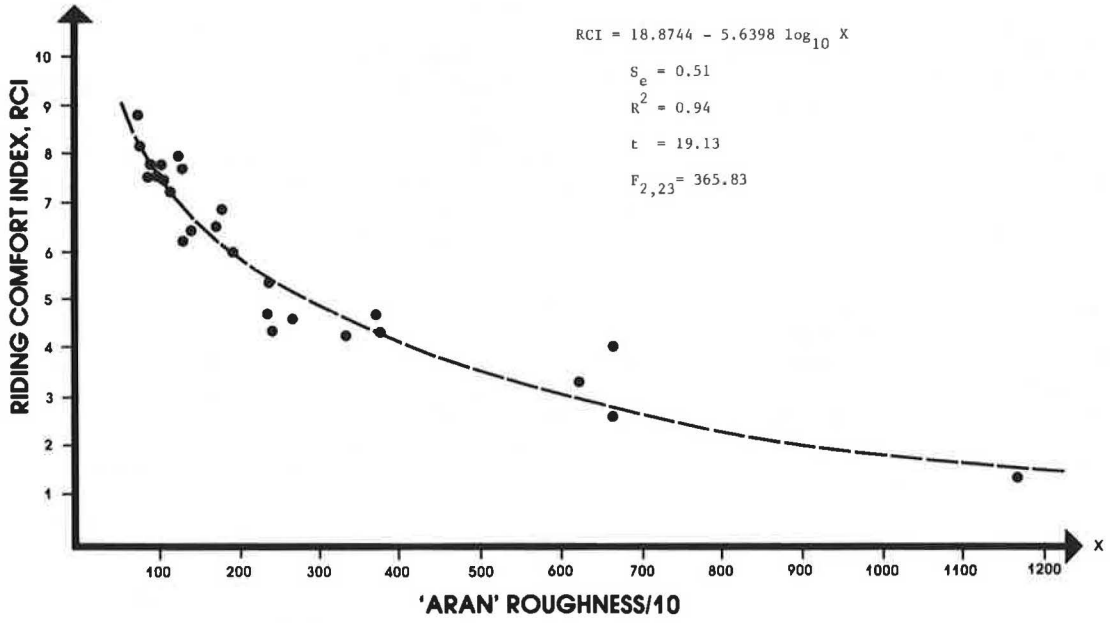

Figure 4. RCI versus roughness for urban roads.

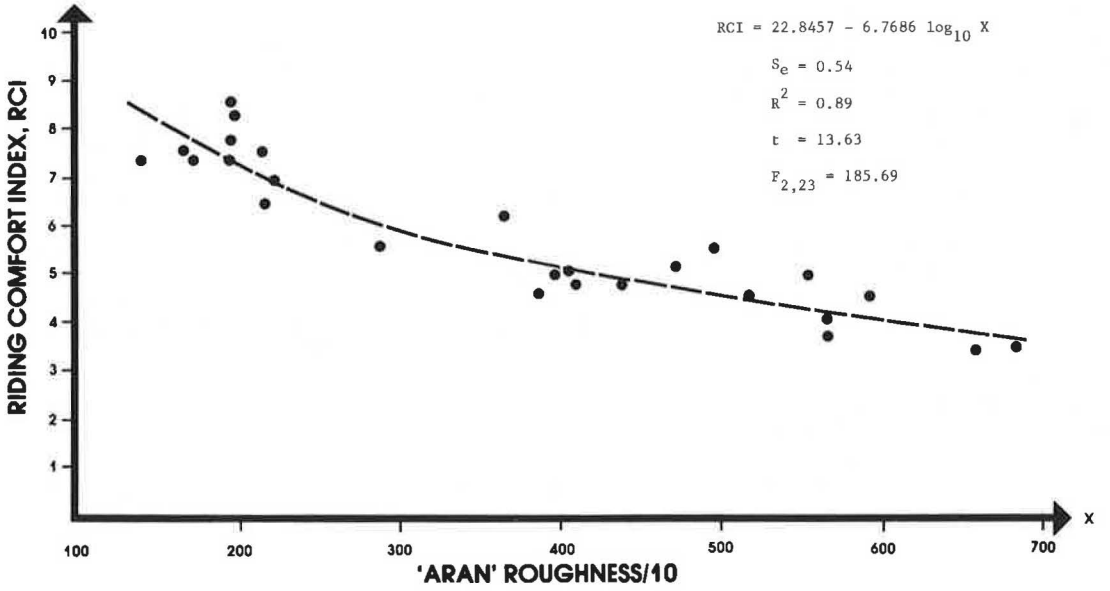

Figure 5. Structural adequacy versus deflection.

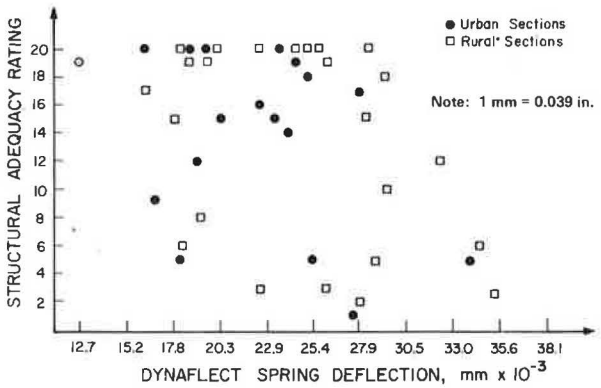

planned, and it is hoped that they will assist in solving this problem [Karan (3) has shown in a previous study that panel ratings of pavement condition or surface distress can be well correlated with condition survey measurements].

It is quite obvious, however, that ratings of structural adequacy do not give any indication of the structural strength of a pavement. The probable reason for this is that surface distress, which has actually been rated in this process, does not always correlate with the structural capacity of the overall pavement system. For example, a relatively thick pavement with extensive surface distress may have a better structural support than a thinner, new pavement with very little or no surface distress. In addition, the time delay between loss of structural adequacy and surface distress has an effect. A crack, for example,

may reduce the rating because it increases the amount of the distressed area, but it usually takes some time to affect the structural capacity of the road surface.

It is, of course, difficult (if not impossible) to take these factors into account in the visual rating process. Thus, it seems more logical to use mechanical techniques to determine the structural capacity of a pavement and condition survey techniques to measure the degree of surface distress.

OPERATING SPEED VERSUS ROUGHNESS

Karan and others (9) have shown that vehicle speeds are significantly affected by pavement roughness. Tests performed on two-lane highways in southern Ontario have clearly indicated this effect. The following equation has been presented for estimating average highway speed:

$$Y = 30.7368 + 1.0375 X_1 - 11.2421 X_2 + 0.0062 X_3^2 \quad (4)$$

where

Y = average highway speed (km/h),
X_1 = RCI,
X_2 = volume/capacity (V/C) ratio, and
X_3 = speed limit (km/h).

It should be emphasized that this equation is only for rural highways. Apparently, there are no data or studies available on the effects of pavement roughness on vehicle speeds on urban streets. However, at lower speeds this effect should be quite insignificant, and on an urban street vehicles can always maintain the speed limit regardless of roughness. Speed limit can therefore be used as the average street speed in the urban situation.

For rural roads, the relation given by Equation 4 can be used for estimating average highway speed.

CONCLUSIONS

Panel ratings of riding comfort and pavement structural adequacy, deflection measurements, and mechanical roughness measurements with a new high-speed, automated unit were made on 28 rural and 27 urban road sections in Ontario. The major conclusions of the study can be summarized as follows:

1. Very good correlations were obtained between panel ratings of riding comfort and mechanically measured roughness for both urban and rural sections.
2. Panel ratings of structural adequacy did not correlate with measured deflection, probably because the panel was actually rating surface distress.
3. The results demonstrate the practicability and usefulness to highway agencies of quickly and efficiently inventorying the serviceability of their paved road networks by developing relations between mechanically measured roughness and panel ratings of riding comfort.

REFERENCES

1. Inventory Manual: Municipal Roads and Structures. Ontario Ministry of Transportation and Communications, July 1975.
2. Methods Manual: Municipal Road Systems Needs Measurements. Ontario Ministry of Transportation and Communications, July 1975.
3. M. A. Karan. Municipal Pavement Management System. Univ. of Waterloo, Waterloo, Ontario, May 1977.
4. Pavement Management Guide. Roads and Transportation Assn. of Canada, Ottawa, 1977.
5. C. Young. An Analysis of Repeatability of the ARAN Unit. Department of Statistics, Univ. of Waterloo, Waterloo, Ontario, draft rept., Dec. 1977.
6. V. F. Nakamura and H. L. Michael. Serviceability Ratings of Highway Pavements. HRB, Highway Research Record 40, 1963, pp. 21-36.
7. F. L. Roberts and W. R. Hudson. Pavement Serviceability Equations Using the Surface Dynamics Profilometer. Center for Highway Research, Univ. of Texas at Austin, Res. Rept. 73-3, April 1970.
8. J. P. Guilford. Psychometric Methods. McGraw-Hill, New York, 1954.
9. M. A. Karan and others. The Effects of Pavement Roughness on Vehicle Speeds. TRB, Transportation Research Record 602, 1977, pp. 122-127.

Publication of this paper sponsored by Committee on Pavement Condition Evaluation.

Quantifying Pavement Serviceability as It Is Judged by Highway Users

Robert J. Weaver, New York State Department of Transportation, Albany

A method for applying scientific psychophysical principles to quantification of the attribute of pavement serviceability is presented. The method has been used in New York to develop, and to serve as the calibrating-recalibrating standard for, the Pavement Serviceability System, which completed a fourth consecutive network survey in the fall of 1978.

In 1963, shortly after the AASHO Road Test, the rationale that had been used there to rate pavement serviceability was critically examined by Hutchinson (1). The concept of serviceability and performance defined for the AASHO Road Test (2) is, of course, beyond challenge; the greatest contribution of that study was to show that serviceability and performance had to be quantified, and a rating system was devised to do it. Hutchinson's critique asserted that, for proper measurement of the attribute of serviceability, the panel-rating procedures used should have incorporated well-established principles and methods of psychophysics and applied psychology. Hutchinson discussed the variation between those principles and what was done, with concern for the potentially serious impacts on the validity of the conclusions about pavement serviceability drawn from Road Test data. He concluded that subjective estimation procedures, typified by Road Test panel ratings, were inappropriate for the task and, further, that they tended to measure pavement distortion and deterioration rather than riding quality, which is the essence of serviceability. He pointed out, however, that much experimental work was necessary to disclose the severity of these impacts and to develop a practical methodology for the measurement of serviceability. Moreover, conduct of that work involved yet another problem—the lack of a precise, measurable physical correlate that varies nearly one-to-one with serviceability. Hutchinson very accurately sized up the task, mapped the direction, and stated the dilemma that has inhibited progress for many years: The first (the method) cannot be found with assurance until one has the second (the statistic), and the second cannot be found with assurance until one has the first.

In 1969, pressure was building among officials of the New York State Department of Transportation (DOT) to find objective, reproducible means of measuring pavement condition and deterioration and to implement the AASHO Road Test serviceability-performance concept in some manner. The objectives were concerned first with pavement design but then grew to include project selection and programming as well. Two years spent in testing all conceivable approaches to measuring serviceability versus physical characteristics did not produce working correlations that were capable of sustained statewide or long-term serviceability measurement as a decision-making data source. Trends were present, but there was intolerable point scatter. Regression only masked the imprecision. The results tended to prove that either (a) people make astonishingly poor "measuring instruments" or (b) highway users are not served by highway pavements in any simple or uniform way according to the definition of serviceability. There was a third possibility—that, as Hutchinson suggested, the panel-rating procedure used over the years was not an effective means of finding out how people are affected by pavement conditions. This is now known to be the case.

The scope of this paper is limited to determining the characteristics of serviceability of pavement test sections as an independent variable. The experimental work required is a panel-rating procedure that somewhat resembles present serviceability rating (PSR) procedures, the principal differences being the larger number of raters required and their instructions. The method of analysis, although considerably more complex than that for PSRs, has vast compensatory benefits. Its principal benefits are that it provides (a) a serviceability scale of great significance to highway users and agencies and (b) the ability to measure serviceability directly with greater accuracy and reproducibility than can be achieved by using the objective measurements generally held to be the physical correlates of serviceability. The method outlined here is the foundation and primary calibration standard for New York's Pavement Serviceability System, which completed its fourth consecutive annual network survey in 1978.

SERVICEABILITY

Serviceability has been defined by Carey and Irick as "the ability of a pavement to serve the highway user" (2). In 1972, Carey expressed concern that "the technology of profile measurement frequently seems to reflect a lack of concern for the basic issue" (3). Hutchinson states, "the serviceability and failure of an engineering design can only be defined relative to the purpose for which a design has been provided " (1).

The purpose of pavements is to provide adequate traveling surfaces for highway users; this, then, must be the object of measuring serviceability as a characteristic of pavements. As Carey and Irick defined serviceability, it was to be a measure of the one aspect that had no prior measure—the effect of present pavement deterioration on the immediate level of service the pavement provides to the highway user. Their concept held that this variable had to be measured because the changing value of serviceability with time is the only means of properly quantifying performance. Moreover, it was held that serviceability was a subjective variable that had to be measured by the human instrument.

It is a simple fact that any physical measurement of profile distress generally increases as visual deterioration of the pavement proceeds and that serviceability decreases on a roughly parallel course. Measurements are not needed to prove the obvious but rather to distinguish exact relations that are not obvious. As Carey (3) states, performance rests on serviceability, serviceability depends on surface profiles, and this is the basis for pavement evaluation. Thus, pavement evaluation begins with independent measurement of serviceability, and that is possible only by applying psychophysical principles to discover how pavement condition affects pavement users.

PSYCHOPHYSICS

Psychophysics is the science of uncovering fundamental quantitative relations between human responses and

applied physical stimuli. The techniques are quite powerful and widely used in experimental psychology, marketing research, and product development. How pavement condition affects the general highway user is exactly the kind of situation in which psychophysics has application.

In summary, we have learned that, although human sensory systems reacting to such stimuli as sound, taste, smell, feeling, and vibration are indeed marvelous "instruments", the ratings obtained from the person about what he or she felt, heard, saw, or tasted make very poor readouts. To give a rating, we must construct it in our conscious minds. While we are doing so, our concentration varies, we have trouble remembering what was sensed, distractions intervene, and random thoughts intrude. It is typical for ratings by any panel of raters to range over half to three-fifths of a rating scale. This is not something peculiar to PSR results; it is the way all human beings function in rating any physical experience. Psychophysical techniques provide many ways of stripping away this superficial variability to get at the true response of all people for all magnitudes of a stimulus.

Many engineers are familiar with how an electronic signal can be buried in random noise during transmission but then extracted from the noise unchanged after being recorded. The techniques of signal analysis used to extract the signal from the random electrical noise make a fine analogy to psychophysical analyses as they are used to extract the true human response from what can be thought of as random "rater noise". In both cases, a record is needed of all possible values of (signal + noise) before analysis is possible. Taking the mean of (signal + noise) at any time and place can give one only a mean of the signal and noise combined, at that time and place. That is what a PSR represents. Consequently, if one wishes to measure serviceability, there are two stringent experimental requirements, neither of which is met in conventional PSR practice:

1. A wide range of test sections, encompassing the full range of serviceability to be experienced, to differentiate small differences adequately as well as to define a complete value scale of serviceability; and
2. Approximately 60-80 persons functioning as raters for adequate definition of the rater-noise factor across the entire experiment.

Figure 1. Serviceability model.

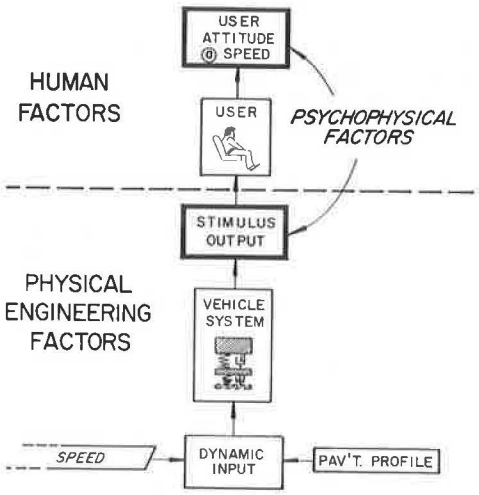

The true serviceability value of a given test section cannot be found from human ratings in any other way.

PSYCHOPHYSICS APPLIED TO SERVICEABILITY

Road Test Ratings

At the AASHO Road Test, variability, or noise, in human ratings was treated as abnormal. Because the whole experiment depended on measuring serviceability, a crash effort went into making PSRs reproducible through training, discussions, and continued trials. Those who participated soon learned to converge to a "right" rating arrived at by consensus. This unfortunate development ran exactly counter to psychophysical principles and introduced an irreversible bias that seemed to Hutchinson the most serious deficiency in the conclusions. Under such conditions, the individual rater is almost completely distracted from stimulus response, drawing into his or her evaluation any and all attributes of the pavement and even guessing what other raters are going to do. In psychophysical terms, these types of bias are, respectively, (a) autokinetic or central tendency and (b) the halo effect. The PSRs of the AASHO Road Test were made more numerically reproducible but were biased even farther away from serviceability.

Serviceability Model

For either psychophysical scaling of serviceability or evaluating which physical measurements of pavements relate to serviceability, one needs a comprehensive model. The model developed shows how the important human and physical factors interact (see Figure 1).

The stimulus output from the vehicle is the interface between these two groups of factors. Travel over a test section provides a definite and reproducible stimulus to the rater or user that varies with travel speed. When road users slow down because of bad pavement conditions, they are unconsciously using the speed relation to raise serviceability to a more tolerable level. In the new methodology, rater instruction provides a clear concept of serviceability as a "travel experience, on this pavement at this speed". A fixed travel speed must be established for all raters for each test section in an experiment. The stimulus is a complex function of travel speed and vehicle characteristics. One might conclude that the obvious differences in the ride provided by various types of vehicles and the resulting sensitivity to vehicle characteristics produce prohibitive complications. In the absolute sense—input-output transfer functions—this is the case. However, this is where human psychology enters in. Both raters and users judge the speed-profile input from a single vehicle—the one in which they are riding. After a period of acclimation to a strange vehicle, raters' discrimination of pavement serviceability is easily separated in their own minds from that portion of the ride experience affected by vehicle type and quality.

The model shown in Figure 1 depicts human perception of pavement serviceability as a vibratory experience in which travel speed is a major variable. A given profile will thus be perceived differently in terms of serviceability as travel speed varies. This speed does not enter into the analysis of ratings but is important in determining physical correlates of serviceability.

Physical Correlates of Serviceability

The model is equally useful in evaluating physical measurements that are likely to vary closely with service-

ability. Although that subject is beyond the scope of this paper, a few comments are necessary.

Historically, PSR-based serviceability has focused on measures of pavement distress rather than on how that distress affects the serviceability provided by the pavement at various travel speeds. Consequently, when the output of response-type devices has been found to be sensitive to speed or vehicle characteristics, there has been no way to treat those facts except as shortcomings of the device or problems that required standardization. The serviceability model shows rather clearly that any technique of profile characterization that is not vehicle mounted and speed sensitive is bound to correlate very poorly with the highway user's perception of pavement quality and hence with psychophysically scaled serviceability.

BASIC DIFFERENCES IN RATING METHODS

The new rating methods were evolved deliberately to follow the original AASHO Road Test scheme as closely as possible. For instance, raters use a 0-5 scale with five main categories and express their judgment by a mark on this scale. The mark is then scaled as a number and referred to as the individual serviceability rating (ISR). In the psychophysical application, however, each ISR is only a tool that is used to determine how all raters rated the serviceability of each section in relation to that of all other sections. PSR, on the other hand, takes each ISR as an absolute number without regard to any question of relativity among raters or sections. In fact, in one of the classical psychophysical methods—paired comparisons—each rater merely determines which of a pair of items is better or worse. Each rater, however, must make $n(n - 1)/2$ pair comparisons for each of n stimuli included in the experiment, which results in an astronomical number of total judgments.

Pavements cannot, of course, be presented in pairs for simultaneous comparison. But if they could be, the final scale value of each section determined by this procedure would be identical to the scale value determined by using the successive categories. In psychophysics, this has been established to be the case whenever a reproducible physical stimulus is involved. The difference between these two psychophysical methods for 88 test sections and 79 raters is merely one of experimental efficiency and analytical simplicity—6952 judgments versus 302 412. Thus, although the numerical rating was made to look like an AASHO Road Test ISR, it was not obtained in the same way, and the two are interpreted entirely differently to arrive at the serviceability of a test section.

RATING EXPERIMENTS

The overall rating experiment must completely embrace all the major variables of pavement profile condition, travel speed, and pavement type (rigid, flexible, and flexible-over-rigid overlays). Properly correlating these variables with collateral physical measurements requires a minimum of about 90 test sections. No fewer than 60 raters should be considered, and the more the better up to about 100. Crisp, efficient execution of such a large experiment requires a great deal of careful preparation and attention to detail. Detailed methods and procedures are available elsewhere (4) to amplify this outline of major considerations.

Selection of Test Sections

Important psychological factors in rating experiments are as follows:

1. The standard maximum length of test sections is 0.8 km (0.5 mile); the minimum length is 396 m (1300 ft).
2. Homogeneity in the nature of the stimulus over the section is desirable.
3. Rapid transition from one section to the next is required; circuit layout should average 10 or more sections/h/team.
4. Atypical surroundings that could distract the rater should be avoided.

Selection of Raters

Raters should be selected for their ability to make sincere, independent judgments and to follow simple instructions. Nondrivers and engineers who are accustomed to studying pavement distress as a means of judging serviceability should not be selected.

Rater Instruction and Scale Anchoring

The objectives of rater instruction are to explain the attribute of serviceability that is to be rated and the scale for doing so, to discuss the process of rating, and to clear up other details. No attempt should be made to train raters to the point of actually rating specific test sections, and raters should understand that their ratings will not be compared directly with those of any other rater. All instruction lectures should start by clearing up the normal concerns of most persons about the schedule, such as stops, lunch, and return time, and anything else even remotely likely to be of concern. Since many teams of raters are necessary, the entire lecture should be given uniformly to all raters from a prepared text. Raters must be told that all ratings are confidential and that they are not permitted to discuss ratings or pavements or even to comment on a past rating experience among themselves during their tour.

"Anchoring" the rating scale is an important part of instruction. For every relation between human response and a physical stimulus, magnitudes of the stimulus exist beyond which a change in stimulus has no proportional change in response. These two points on the stimulus scale are the liminal points, or "limens", of the relation and, of course, the ends of the rating scale. It is to these two limens that scale anchoring is directed, and this is done by describing a liminal serviceability experience to the raters to correspond to the end labels, as follows:

1. Perfect—"At the travel speed, this experience is so good that you doubt whether you could detect any improvement even if the pavement were made smoother."
2. Impassable—"At the travel speed, this experience is so bad that you feared you or the vehicle would not make it in one piece to the end of the test section."

Without this anchoring, defined relative to the limens of the serviceability attribute, the labels alone remain vague, floating references for each rater's interpretation.

Raters must believe their judgments to be exact. The instructions must ask for exactness. To arrive at an exact judgment, raters generally take three iterative mental steps. They contemplate the two scale ends and the indifference point (midscale), which readily places their judgment to within a one-third portion of

the scale. Then they consider the category descriptions—good, fair, and so on—and this places their judgment to within a one-fifth or smaller portion of the scale. Raters usually need help in making the third and final iteration. Left alone, they will obtain help unconsciously by letting their attention drift toward other attributes (distractions). To keep raters concentrating on serviceability, the instructions should provide them with a mirror image of serviceability—the nature and intensity of their feelings about the need for rehabilitation. They should be invited to consider how far from indifferent they rate the highway agency's performance in providing adequate traveling surfaces, as if the test section were a standard.

The rating form used, which is shown in Figure 2, is similar to a PSR form, but the question of "acceptability" that is asked separately on conventional PSR forms is noticeably absent. This is a logical second question for raters in rating the attribute of pavement distress and distortion, but serviceability, properly measured, is acceptability.

Teams and Vehicles

Rating vehicles must be driven by a nonrating staff member who knows the exact itinerary and test speeds and can supervise the rating procedure. A team of three raters is assigned as a group. To avoid possible distractions, males and females are not teamed together. The team and seating position remain fixed on all rating days. On different days, a different vehicle and driver are assigned to each team, but no such changes are permissible in a single day. There are no special requirements for vehicles other than good mechanical condition and reasonable comfort.

Figure 2. Rating form.

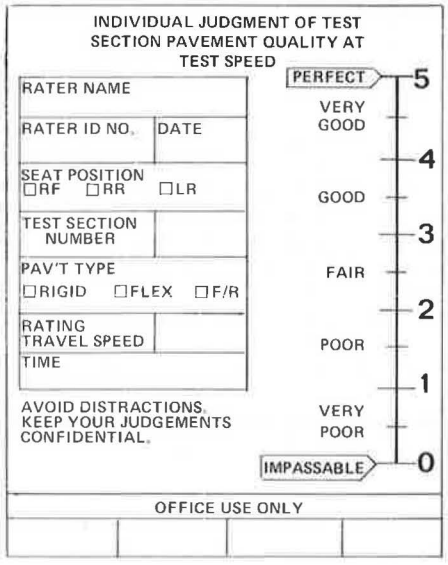

Figure 3. Flowchart of computer program basis for Z(x) matrix.

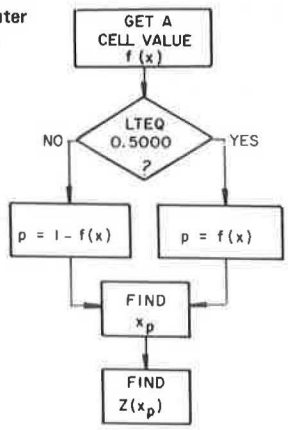

PSYCHOPHYSICAL ANALYSIS OF RATING RESULTS

The analysis for serviceability scale values (SSVs), the final result, starts by taking all raters and pavements in a single matrix. Given 90 test sections and 80 raters, the resulting 7200 ratings are placed in a 90x80 matrix and then transformed into a 90x10 matrix for 10 class intervals on each test section. The 7200 ratings are thus reduced to 900 observations of class-interval frequency and cumulative frequency. Individual raters or ratings are no longer of interest. The only other figure carried forward from the rating experiment is the total number of raters. The calculations involve conversions into five more successive 90x10 matrices and finally to five 20-element tables before the SSV is found for each test section.

The analytical procedure is a straightforward but lengthy process. It cannot be described by an equation, but it has been reduced to a purely step-by-step clerical task, as follows:

1. Assemble a two-dimensional matrix (matrix 1) of individual ratings by test section number and rater number. Scale the rater's marks to the nearest 0.01 division and enter.
2. Select class intervals to be used in converting the original matrix to a matrix of test section versus frequency in class interval. Use the smallest class interval possible, but they must generally (not necessarily completely) be large enough to avoid zero-frequency intervals embedded between those with substantial frequency counts. The size of class interval permitted becomes smaller as the number of raters becomes larger. Prepare this matrix (matrix 2). A class interval of 0.50 is adequate for 60-80 raters (divide the rating scale into 10 intervals).
3. Fill the blank matrix 2 with a fraction in which the numerator is taken as the frequency of rating in each class interval and the denominator as the cumulative frequency up to and including that class interval (reckoned from the low to the high end of the rating scale).
4. Prepare a new matrix (matrix 3) of test section versus class interval. Fill the cells of this matrix by dividing the cumulative frequency (the denominator in the matrix 2 values) by the total number of raters. The result is a decimal value of cumulative proportions.
5. Prepare a new matrix (matrix 4) of test section versus class interval. Convert the cumulative proportions in each cell of matrix 3 to the normal probability function Z(x) for each cell of this matrix. This requires a statistical table that gives Z(x) in terms of P(x) and Q(x) (5) or a computational algorithm such as that described below (see Figure 3): To find x_p, the following rational approximation for $Q(x_p) = p$ is used. The maximum error is $|\epsilon(p)| < 4.5 \times 10^{-4}$, which is quite adequate for the purpose. The calculation involves the following steps:

Find $t = \sqrt{\ln (1/p^2)}$.
Find $x_p = t - [c_0 + c_1 t + c_2 t^2)/(1 + d_1 t + d_2 t^2 + d_3 t^3)]$, with

the following values for constants: $c_0 = 2.515517$, $c_1 = 0.802853$, $c_2 = 0.010328$, $d_1 = 1.432788$, $d_2 = 0.189269$, and $d_3 = 0.001308$.

Take the result x_p and find $Z(x_p) = (1/\sqrt{2\pi})\, e^{-x^2/2}$, where $e = 2.718282$.

Test values for the check of the module are given below:

f(x)	t	x_p	$Z(x_p)$
0.2000	1.794 12	0.841 45	0.279 96
0.4500	1.263 73	0.125 38	0.395 80
0.5500	1.263 73	0.125 38	0.395 80
0.8400	1.914 46	0.994 42	0.243 31

6. Prepare a new matrix of test section versus class interval (matrix 5). The cell value for this matrix is determined by the Z(x) value in the corresponding cell of the completed matrix 4, which is subtracted from the cell value immediately to the left in that matrix. The result, including the algebraic sign, is entered in the new matrix.
7. Prepare a new matrix of test section versus class interval (matrix 6) to be the matrix of frequency proportion. Use the numerator in matrix 2, divide it by the total number of raters, and enter the result in this new matrix.
8. Prepare a new matrix of test section versus class interval (matrix 7). Obtain cell values by dividing the cell values of matrix 5 by the corresponding cell values in matrix 6.
9. Prepare a table (referred to here as Table A) with class-interval columns and two rows. Label the rows A and B. The value for each element is obtained from matrix 7: for row A, the sum of all elements that have nonzero values in cells immediately to their right, and for row B, the sum of all elements that have nonzero values in cells immediately to their left. (In computing this element, keep count of the number of values used for each entry for use in step 11.)
10. Prepare a new table (Table B) by class-interval columns with a single row of elements. The elements to be computed for this table are the resultant values (with sign) of adjoining intervals in Table A that have nonzero entries in both rows A and B (see Figure 4).
11. Prepare a new table (Table C) that is similar to Table B. This is the mean of differences between intervals. Divide the value in Table B by the number of cell values used to obtain the value in line B in Table A.
12. Prepare a new table (Table D) that is similar to Tables A and B. This will be used to compute cumulative interval values. Proceeding from the lowest interval, the value to be entered in each cell is the summation of the cell value in Table C with all cell values to the left.
13. Prepare a new table (Table E) that is similar to Tables A, B, C, and D. The entries into this table are obtained from Table D. Take the value in Table D for the interval that contains the original midpoint of the rating scale, subtract that value from each interval value in Table D, and enter the result (with sign) in Table E. This is the final result of the analysis. This table of values and the matrix of frequency proportion (matrix 6) are the tools to use in computing the scale value of each test section in the experiment.

The scale value of a test section is computed as the sum of products of each cell in matrix 6 multiplied by the corresponding value in Table E. The serviceability of each test section is computed in this way. These scale values have zero as a point of indifference, which is the most important feature of the scale. Positive values indicate increasingly positive highway user attitudes toward pavement serviceability at the rating speed. Negative values conversely indicate increasingly negative attitudes.

The positive-zero-negative scale values can be used as is for a serviceability scale or transformed to any other linear scale. For instance, 0 to 100 scale ends, 0.00 to 5.00, -250 to +250, and so on. The technique easily reproduces a 500-unit scale but not a 1000-unit scale.

The object of this procedure is to analyze frequency distributions, frequency proportions, and probability functions to establish the scale of user response and finally to determine where each test section belongs on it. The ISRs and mean ISRs shown in the remaining figures in this paper (Figures 5-10) were computed from the original ratings especially to show comparisons with SSVs. We chose to transform the positive-negative scaling back into a 0.00-5.00 scale to emulate the AASHO Road Test (this has been the practice in New York). On the transformed scale, the indifference point is at 2.40; experience has shown that such a transformation is best performed by adding 2.40 to all values on the psychophysical positive-zero-negative scale.

RESULTS

The validity of the new rating methods is best examined independently from all physical factors to show how ISRs, test sections, SSVs, and time relate. The evidence was acquired by computing mean ISRs on test sections of full-scale experiments. The main data set was taken from a May 1977 experiment to recalibrate New York's Pavement Serviceability System. This experiment contained 6952 judgments (ISRs) by 79 raters on 88 test sections.

The results shown in Figures 5-10 are in no way comparable to PSR although individual raters' ratings and mean ratings of panels of various sizes are shown in addition to the single output of the new method—the underlying true serviceability scale value found for each test section included in a proper experiment.

An ISR from this experiment is not the same as the judgment of a single rater making a PSR because PSR rater instructions psychologically incapacitate the rater for judging serviceability. The PSR rater believed he was rating a pavement and either gravitated toward or was pushed into a subjective evaluation of a different

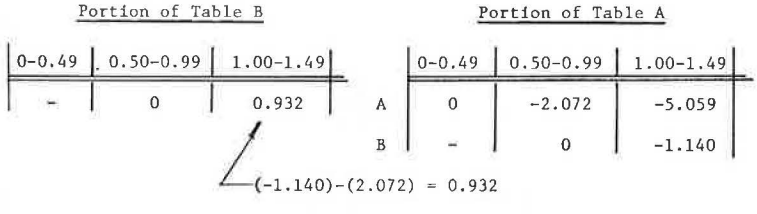

Figure 4. Formulation of Table B in analytical procedure.

Figure 5. Mean ISR versus SSV for 79-member panel.

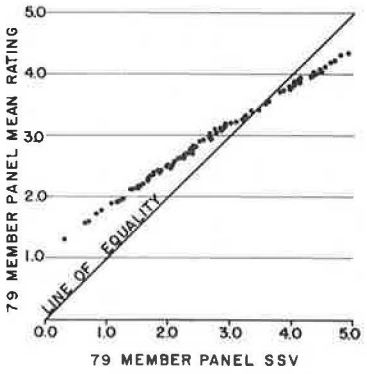

Figure 6. Mean ISR versus SSV from 1972 experiment.

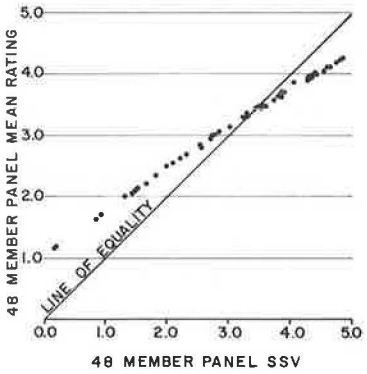

Figure 7. Functioning of typical rater as one of 79-member panel.

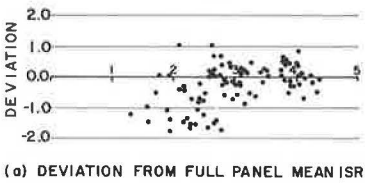

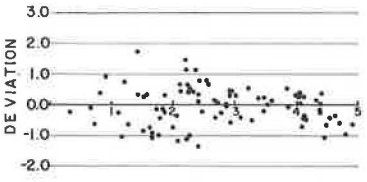

Figure 8. Functioning of single "expert" rater as one of 79-member panel showing bias toward rating the visual condition of the pavement.

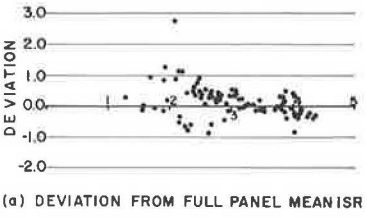

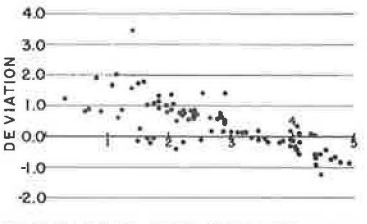

characteristic of a pavement—i.e., surface distress and distortion. Further, he knew his ratings would be compared and he could be "odd man out", so he avoided extreme ratings. His rating scale of 0-5 or 0-10 did not have its ends anchored, i.e., defined relative to either the attribute of serviceability or surface distress. Speed was not a controlled variable on a test section

Figure 9. Small-panel versus full-panel mean ISR of test section.

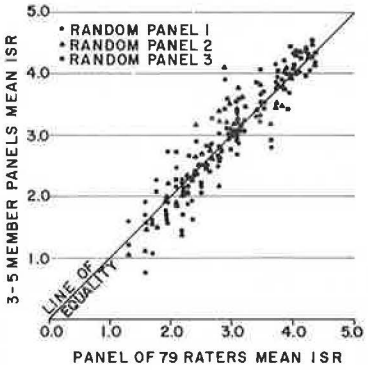

Figure 10. Effect of team size on mean ISR versus SSV of test sections.

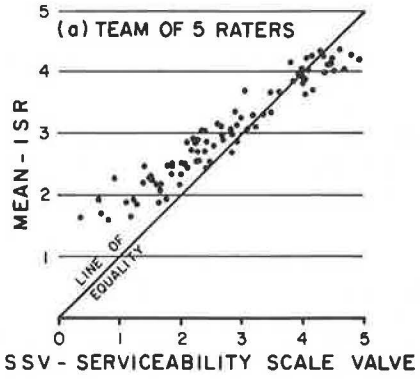

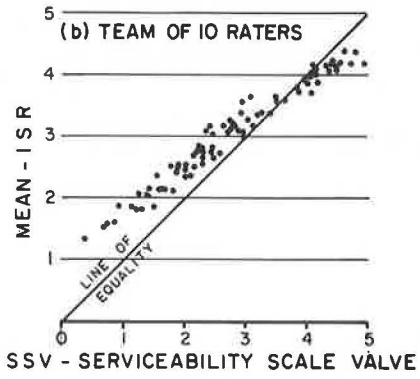

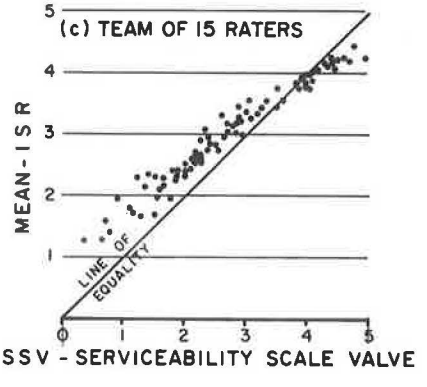

for all raters. These are a few of the differences that have led to the strange variability encountered in PSR work. They are also reasons why one cannot retrofit the new analysis method to old PSR data. Those data are psychologically and psychophysically invalidated.

Mean ISR Versus SSV for Each Test Section

Data from the May 1977 psychophysical experiment can show how mean ISR relates to serviceability and provide some insight into the characteristics of ISRs as rater noise. Figure 5 shows that, given enough rater noise (as in this experiment), the mean ISR converges to a curve that has a clear relation with the value scale of serviceability. The mean ISR is only the mean of the signal plus rater noise on a test section, and the SSV is the signal. An SSV of 2.40 is the indifference point. The highway user becomes angry at an SSV under 1.00. If the user were to maintain speed at an SSV of zero, his or her vehicle would probably become an accident statistic because zero indicates impassable at the travel speed. One can see here how misleading the mean ISR is because of rater noise operating to obscure the true human response signal. One can also see that there is a clear—almost perfect—relation. The equation used is that of a second-order polynomial, as follows:

$$SSV = c + b\bar{x} + c\bar{x}^2 \quad (1)$$

where $\bar{x}$ = the mean ISR of a large panel of n raters. The correlation statistics for the 1977 experiment are given below:

Statistic	1977
Number of test sections	88
Number of raters	79
c-intercept	−1.3369
b	
Coefficient	1.1974
Standard error	0.0364
a	
Coefficient	0.0523
Standard error	0.0060
F-value	52 946

It can be seen that the mean ISR and the corresponding SSV are far from numerically equal. One reason is that the rating procedure has a scale with fixed ends but the underlying human-value scale has no preestablished ends. When one senses an experience, one's psychological response will be found in the "white noise" that surrounds the underlying (and as yet unknown) scale value found by the analysis. The essence of psychophysical analyses is that the noise has a Gaussian distribution around the underlying scale value, not the mean rating scale value. The constraint introduced by the fixed-end rating scale (where the subject communicates his or her rating) is that obviously only a midscale experience has even the opportunity to display a Gaussian distribution. The end points act as sources of rater bias, causing a distortion in the distribution as the serviceability of a test section approaches the end points. As Figure 5 shows, even with the relatively bias-free nature of the ISRs in this experiment, no section mean can clear the bounds of the 1.5-4.4 range typical of PSR.

Reproducibility

The ultimate test of reproducibility would appear to be that the exact relation (Figure 5) be invariant across separate experiments: a different set of test sections, a different group of raters, and preferably a different point in time. For such a test, data from the earliest psychophysical experiment, which was conducted in July 1972, were analyzed for the relation between mean ISR and SSV. Although that particular experiment used only 41 raters and 48 test sections, the same relation resulted (see Figure 6). The regression results for the 1972 experiment are given below:

Statistic	1972
Number of test sections	48
Number of raters	41
c-intercept	−1.1297
b	
Coefficient	1.0822
Standard error	0.0430
a	
Coefficient	0.0755
Standard error	0.0075
F-value	27 509

Both regressions show the relation to be that of a second-order polynomial. The following equation was computed from the full set of 1977 data:

$$SSV = -1.3369 + 1.1974\bar{x} + 0.0523\bar{x}^2 \quad (2)$$

where $\bar{x}$ is the mean ISR of a sufficiently large number of raters.

The primary usefulness of the equation appears to be as a means of direct comparison of the results of psychophysical experiments used to calibrate systems at different places and times. The equation can also be used as an analytical shortcut should one for some reason require a serviceability measurement at a predetermined travel speed on a few pavements. Such use would still require, however, that a large enough number of persons (60-80) be used for a mean ISR and that rater selection, instruction, and other details be adhered to without exception.

Rater Randomness

In Figure 7(a), the data of a typical rater show interesting trends relative to both mean ISR and SSV. The rater shows typical randomness with respect to the panel mean and a slight tendency to rate more negatively. When the final SSV is determined, however, the same rater's randomness is around the SSV [Figure 7(b)].

It was intended that the panel would not include any "experts" who would be biased by cracks and the appearance of the pavement. Fortunately for this study, however, one professional—a materials engineer who had had experience in conventional pavement evaluation—did join the panel as a last-minute substitute, undetected. His ratings, which are shown in Figure 8, indicate a bias not seen in the ratings of other raters. The trends are those to be expected from one who, consciously or unconsciously, considers cracks and visual condition. His skew from zero SSV shows that an excellent pavement with cracks is downgraded, and any bad pavement is often severely overrated because it appears better than it feels. If this rater had been blindfolded, he undoubtedly would have functioned like the remaining 78.

It would be interesting to compare SSVs from a panel of 79 experts with those for this panel since this type of bias is one of the disturbing consequences of AASHO Road Test PSRs detected by Hutchinson. But one can only speculate, for there is no way to retrofit the AASHO Road Test PSRs. Nevertheless, it is clear

that the attribute of pavements called "cracks" is not the attribute defined as serviceability any more than are lane width, skid resistance, roughness, curvature, cross-slope, and sight distance.

Mean of ISRs with Small Panels

It has been shown how enough raters will cause the mean rating to converge to a fixed number on each test section. It is illuminating to show how well small panels can reproduce the mean of a 79-member panel on each test section. Random numbers were used to select three 5-member teams from the panel of 79, and the mean of ISRs on each test section was computed. The results are shown in Figure 9. The central tendency toward the equality line is clear, but the full-panel mean for any test section could not possibly be identified from any combination of data from these 15 raters.

To examine this question further, the three panels are used to make 5-, 10-, and 15-member panels. These mean ISRs versus the SSV determined from the full panel of 79 are shown in Figure 10. It can be seen that each addition of 5 new members draws the results slightly closer to a linear relation identical to those shown in Figures 5 and 6. At the same time, it is also clear that substantial convergence will not occur until a very large number of raters are included.

CONCLUSIONS

The serviceability of a pavement profile as perceived by the highway user can be precisely measured. This involves finding basic human responses to the range of physical stimuli generated by travel speed and pavement conditions. The principles of psychophysics have provided a solution to the measurement problem. Panel ratings have long been regarded as the most nebulous, controversial, and irreproducible means of evaluating pavement serviceability. However, when they are properly devised, conducted, and analyzed, panel ratings can measure serviceability with more precision and reproducibility than the common devices used to measure the pavement profile.

The method presented in this paper produces test-section SSVs that are shown to be independent of time, place, and differences in rating panels. This method differs in many ways from the classical AASHO Road Test PSR procedures. Unfortunately, the nature of PSR methods precludes any retrofit of AASHO Road Test data.

Requirements for application of the new methodology are as follows:

1. The raters should be 60-80 ordinary highway users, each rating all test sections.
2. Rater instruction, which differs considerably from the PSR type of instruction, must firmly anchor the end points of the rating scale and fully describe the attribute of serviceability.
3. Travel speed is a vital serviceability variable. Each test section must maintain a defined travel speed for all raters, thus constituting not merely a profile but a "travel experience" whose serviceability is rated. The SSV that is computed is thus the serviceability of a test-section profile at its rating speed.
4. The method of analysis encompasses the entire set of judgments and test sections from its outset.
5. Combinations of test section and speed must provide a full range of serviceability experiences as well as profile conditions.

This method was developed to obtain a precise measure of serviceability on test sections at any time or place. It is then possible to calibrate (or recalibrate) vehicle-mounted profile-measuring systems whose output is to be correlated with scalar serviceability at the posted travel speed. Obviously, this method is also of great value in determining the merits of various profile-measuring systems.

The interplay of profile, speed, and serviceability variables has also been found to be sensitive to three different types of pavement: rigid, flexible, and flexible-over-rigid overlay. For these reasons, approximately 90 test sections (six serviceability levels × three pavement types × five speeds) are required in a single experimental plan. Independently of the ratings, the profile-measuring systems obtain outputs at all five speeds on all test sections (only the ratings are dealt with in this paper).

Application of this methodology admittedly involves a great deal of work, but it has the advantage of turning the serviceability-performance concept from a somewhat abstract idea into a powerful reality with precise results. A standard of serviceability exists that can be mobilized as needed by the psychophysical method presented here. The results measure serviceability exactly as it was originally defined—how the pavement serves the highway user.

ACKNOWLEDGMENT

Without the encouragement of W. R. Hudson of the University of Texas at Austin to reexamine available psychophysical data and find a way to present this subject to others, this paper would not have been prepared. I am also indebted to Robert O. Clark, Jr., and William F. Rever, whose dedicated and painstaking efforts over the years were the critical difference between ideas and their fruition, not only on this subject but also in many other developments that have led to the successful operation of New York's Pavement Serviceability System.

REFERENCES

1. B. G. Hutchinson. Principles of Subjective Rating Scale Construction. HRB, Highway Research Record 46, 1963, pp. 60-70.
2. W. N. Carey, Jr., and P. E. Irick. The Pavement Serviceability-Performance Concept. HRB, Bull. 250, 1960, pp. 40-58.
3. W. N. Carey, Jr. Uses of Surface Profile Measurements. HRB, Special Rept. 133, 1973, pp. 5-7.
4. R. J. Weaver and R. O. Clark, Jr. Psychophysical Scaling of Pavement Serviceability. Soil Mechanics Bureau, New York State Department of Transportation, Albany, Manual SEM-9, May 1977.
5. Handbook of Mathematical Functions. National Bureau of Standards, U.S. Department of Commerce, Applied Mathematics Series 55, 1970, p. 975.

Publication of this paper sponsored by Committee on Pavement Condition Evaluation.

Measuring Pavement Performance by Using Statistical Sampling Techniques

Joe P. Mahoney*, Department of Civil Engineering, University of Washington, Seattle

A stratified two-stage sampling survey is described that was selected for use in Texas to obtain cost-effective objective information on road-network performance. The sample was obtained by first randomly selecting counties within each highway district and then randomly selecting 3.2-km (2-mile) highway segments within each county. Approximately 1 percent of total statewide centerline kilometers were sampled by using the technique. Various kinds of data were obtained for each of the sampled highway segments; serviceability index and pavement rating score (visual condition) are used as examples to demonstrate the kinds of inferences that can be made. The type and size of sampling survey that should be used are examined. To make these determinations, one highway district was used in conjunction with a simulation procedure. The results of the simulation study and two separate optimization procedures revealed that two-stage sample sizes, generally about 2 percent of total centerline kilometers, provided good estimates for determining roughness, visual condition, deflection, and skid resistance.

To allocate highway rehabilitation and maintenance funds fairly and consistently, a highway administrator needs information about the actual condition of the road network. He or she can get this information in a variety of ways, some of which are more costly than others. This paper presents a methodology that was applied to pavements in Texas for selecting an optimally cost-effective sample size for collecting information on pavement condition and performance evaluation.

There are two broad categories of pavement evaluation information: subjective and objective. Routine or regular visual inspections of roadways are in the subjective category; objective measurements are made with the aid of mechanical devices and include several methods. In addition, combinations of subjective and objective information are often made.

One of the objective methods is the use of mass-inventory surveys (1). These surveys are used to obtain extensive data on all highways in a given area—state, district, county, and so on. The primary advantage of this type of survey is that all segments of the highway system are carefully surveyed so that all the weaknesses in a given highway are indicated. Presumably, the highway with the greater number of weaknesses would receive corrective maintenance sooner than other pavements that serve the same function. This survey method also allows general inferences to be made about the complete highway system. The most obvious problem with this type of survey is the cost associated with the collection and reduction of data and the interpretation of the results.

A method used to obtain both subjective and objective data is the "partial" survey. A partial survey occurs where some type of preliminary, routine visual examination of the highway system is made. The visual examination is used to identify highway segments that require additional, more detailed information. For example, a highway segment is identified as being severely cracked. Some type of deflection survey is then made to determine the load-carrying capability of the pavement. This survey can then be used to assist in making the proper maintenance decision. One advantage of partial surveys is that they are generally low in cost. The disadvantage is that the data obtained do not allow general inferences to be made about the total highway network (state or district).

This leads to the third type of survey—the sampling survey. This method of obtaining objective data on a highway system has a number of characteristics that can be of value to highway departments.

CHARACTERISTICS AND TYPES OF SAMPLE SURVEYS

The purpose of a sampling survey is to make inferences about the sampled "population" (2). The population in this case is the state-maintained highway network.

In any sampling process, two factors affect the usefulness of the data contained in the sample: the size of the sample and the variability of the data within the sample. The goal of most sampling surveys is to keep the sample size as small as possible while keeping the variability of the data below some maximum acceptable limit. To accomplish this goal, careful consideration should be given to the survey design.

Such surveys are generally inexpensive in comparison with other data collection procedures but can still represent a significant investment. Enough emphasis cannot be placed on the design of a sampling survey to minimize costs while maximizing the information gained from the survey. Some of the survey methods available (2-4) are (a) simple random sampling, (b) stratified random sampling, (c) one-stage cluster sampling, (d) multistage cluster sampling (multistage sampling), and (e) systematic sampling.

A brief description and an example of each of these sampling methods follows:

1. In simple random sampling, every sample has an equal probability of being chosen from a population. For example, if all highways in a given geographic area were divided into equal lengths (segments), each highway segment would have an equal chance of being chosen for the required sample size.
2. In stratified random sampling, a population is divided into strata and then random samples are obtained within the described strata. For example, if a given state were divided into a number of highway department districts and data estimates were required for each district, each district could be considered a stratum and individual highway segments randomly selected within each district.
3. In one-stage cluster sampling, elements within a population are first grouped together and then randomly sampled. For example, if data estimates are required for a state, counties can be randomly selected throughout the state. All highway segments in each selected county are sampled. The pavement segments surveyed are considered to be clustered within the selected counties.
4. Multistage cluster sampling (or multistage sampling) is similar to one-stage cluster sampling but takes the process further. Multistage clustering allows for larger areas to be clustered together and then randomly sampled. The elements within these clusters are also randomly sampled. As in one-stage cluster sampling, counties within a district can be randomly selected and then pavement segments within those counties can be randomly selected. Sampling all data within the pavement segment constitutes a two-stage

cluster sample. If only the data within the pavement segment are sampled, this is referred to simply as a two-stage sample. In a three-stage sample, highway department districts within a state, then counties within those districts, then pavement sections within those counties would all be randomly selected.

5. In systematic sampling, every Kth element of a set of data is sampled. For example, if data estimates are required for a state that is assumed to have 100 counties, then every 10th county from a listing of all counties is selected for a total of 10 counties. All highway segments in each selected county would be sampled in the data collection effort.

Combinations of these five methods can also be created—for example, a stratified two-stage cluster sample.

A properly designed highway sampling survey can provide

1. Inexpensive indication of the condition and performance of statewide, district, or county pavements;
2. Year-to-year differences in pavement condition and performance;
3. A valuable research tool for various statistical pavement experiments;
4. Expansion or reduction to accommodate changing needs; and
5. More detailed objective data since the amount of pavement surveyed is much smaller than that surveyed by mass-inventory methods.

TEXAS SAMPLE SURVEY

A sampling survey has been and is continuing to be done in Texas under the sponsorship of the Texas State Department of Highways and Public Transportation (TSDHPT) and the Federal Highway Administration (FHWA) through the Texas Transportation Institute.

A statistically random selection of 3.2-km (2-mile) long Interstate, U.S. and state, and farm-to-market (FM) highway segments was made during 1973. A stratified two-stage sample was used. The stratification involved dividing the highway network into the 25 TSDHPT districts. This was done because separate data estimates were required for each district since each is considered to have its own unique characteristics (e.g., soils or traffic). The two-stage sample was obtained by first randomly sampling counties in each district and then randomly sampling the 3.2-km-long highway segments in each county. This was done for the three types of state-maintained highways by considering each type to be a separate population. Currently, the percentages of centerline kilometers sampled for the three types of highways are as follows: Interstate, 1.8 percent; U.S.-state, 1.0 percent; and farm-to-market, 0.6 percent. These percentages reflect the importance attributed to each kind of highway and are the result of the sampling method used. A total of 250 highway segments were initially selected by using this process.

Several kinds of data have been collected on the highway segments selected. Most of the data are updated annually by using the same highway segments each year. The following kinds of data are collected:

1. Construction information, including layer thickness and width and available material properties as well as the dates and types of all major maintenance that currently represents the highway segment cross section;
2. Traffic histories, including average daily traffic and 80-kN [18 000-lb (18-kip)] equivalent axle loads applied with time;
3. Climatic data, including monthly rainfall and temperatures, freeze-thaw cycles, and Thornthwaite indices;
4. Roughness, in the form of serviceability indices obtained by using the Mays road meter (5);
5. Visual condition, in the form of distress manifestations obtained primarily by a visual process (6);
6. Deflection measurements obtained by using the Dynaflect;
7. Rut-depth measurements; and
8. Skid number (SN) at a speed of 64.4 km/h (40 mph).

Examples of estimates that can be produced from such data are given in Tables 1 and 2. These two tables indicate statewide and district estimated serviceability index (SI) means and standard errors for data obtained in 1974 and 1976, respectively, for Interstate, U.S.-state, and FM highways. The standard errors can be used to estimate the precision of the survey. Estimated means and standard errors for visual condition and deflection data can also be presented in this way.

Table 1, which gives data obtained in 1974, indicates for the statewide condition that Interstate highways have an average SI of about 4.0, which represents a relatively smooth condition. U.S.-state highways have a mean value of about 3.6 and FM highways a value of about 2.9. The data summarized in Table 1 were obtained at about the same time as one district in Texas conducted a mass-inventory survey. This is discussed in more detail later in this paper.

Table 2 gives the estimated mean values of SI data obtained in 1976. Note that both means and standard errors have decreased with respect to the 1974 data by approximately 0.1 unit for two of the three highway types.

The following questions arise:

1. How "good" are the various estimates based on the current highway segment sample with respect to other (larger and smaller) sample sizes?
2. What is the least costly sample size to achieve adequate estimates?
3. Will some other sampling procedure yield better precision?

An approach toward answering these questions is presented below.

SIMULATION STUDY TO EVALUATE SAMPLING PROCEDURE

To begin to answer the questions posed above, a simulation study was done for one of the 25 Texas highway districts to determine the precision of various highway segment sample sizes. This approach was used because direct experimentation on the highway network was too expensive and direct computation of consistently accurate two-stage sampling errors for various sample sizes was not possible.

The highway district studied was district 21, which is located in the southernmost part of the state. For 1974 and 1975, virtually a complete mass inventory of four major kinds of data was performed on all highway types. Since this district has only 53 km (33 miles) of Interstate highways, Interstate highways were not considered in the simulation study.

The kinds of data used are as follows:

1. Serviceability index, which was obtained every 0.32 km (0.20 mile) by use of the Mays road meter;
2. Pavement rating score (PRS), which ranged be-

Table 1. Estimated 1974 district and statewide SI means and standard errors for randomly located highway segments by type of highway.

District	Interstate		U.S.-State		FM	
	Mean	Standard Error	Mean	Standard Error	Mean	Standard Error
1	3.4	-	3.6	0.1	2.5	0.2
2	3.1	-	3.7	0.1	2.4	0.2
3	-	-	3.5	0.3	3.2	0.2
4	4.4	0.1	3.8	0.3	3.2	0.2
5	-	-	3.2	0.1	3.2	0.2
6	4.3	-	4.3	0.2	3.6	0.3
7	-	-	3.9	0.2	3.2	0.1
8	4.6	-	2.9	0.2	3.0	0.3
9	4.7	-	3.7	0.4	2.8	0.3
10	-	-	2.9	0.2	2.7	0.3
11	-	-	3.3	0.2	2.0	0.2
12	4.2	-	4.2	0.1	3.4	0.3
13	-	-	3.8	0.2	2.4	0.4
14	-	-	3.9	0.1	2.8	0.2
15	3.4	0.3	3.2	0.2	2.9	0.2
16	3.8	-	3.5	0.1	3.1	0.2
17	-	-	3.2	0.1	2.5	0.3
18	3.4	-	3.9	0.1	2.9	0.3
19	-	-	3.5	0.1	3.1	0.2
20	4.6	-	3.6	0.1	3.3	0.1
21	-	-	3.6	0.1	2.8	0.4
22	-	-	3.3	0.2	3.4	0.1
23	4.3	-	4.0	0.3	2.6	0.1
24	4.4	-	3.5	0.3	2.5	0.4
25	-	-	2.9	0.6	3.0	0.3
Statewide	4.0	0.2	3.6	0.2	2.9	0.2

Table 2. Estimated 1976 district and statewide SI means and standard errors for randomly located highway segments by type of highway.

District	Interstate		U.S.-State		FM	
	Mean	Standard Error	Mean	Standard Error	Mean	Standard Error
1	3.4	-	3.7	0.2	2.2	0.4
2	3.7	-	3.7	0.2	2.1	0.1
3	-	-	3.3	0.4	3.0	0.4
4	4.3	0.3	4.0	0.4	3.0	0.4
5	-	-	2.9	0.3	3.3	0.3
6	4.4	-	4.5	0.3	3.7	0.3
7	-	-	3.9	0.2	3.3	0.2
8	4.6	-	2.7	0.3	2.5	0.5
9	4.5	-	3.5	0.4	2.5	0.3
10	-	-	2.7	0.2	2.4	0.4
11	-	-	3.0	0.4	1.3	0.2
12	4.3	-	4.2	0.1	3.7	0.2
13	-	-	4.0	0.3	2.2	0.6
14	-	-	3.7	0.1	2.8	0.2
15	3.4	0.3	3.4	0.3	2.9	0.3
16	3.5	-	3.4	0.2	2.9	0.3
17	-	-	3.2	0.1	2.0	0.3
18	3.4	-	4.0	0.1	2.8	0.3
19	-	-	3.7	0.1	2.6	0.4
20	4.7	-	3.4	0.1	3.3	0.2
21	-	-	3.7	0.1	3.1	0.6
22	-	-	3.8	0.1	3.9	0.2
23	4.5	-	4.0	0.3	2.2	0.2
24	4.4	-	3.2	0.4	2.4	0.6
25	-	-	2.6	0.7	3.1	0.5
Statewide	4.0	0.2	3.5	0.3	2.8	0.4

Figure 1. District 21 1974 mass-inventory SI data for U.S.-state highways.

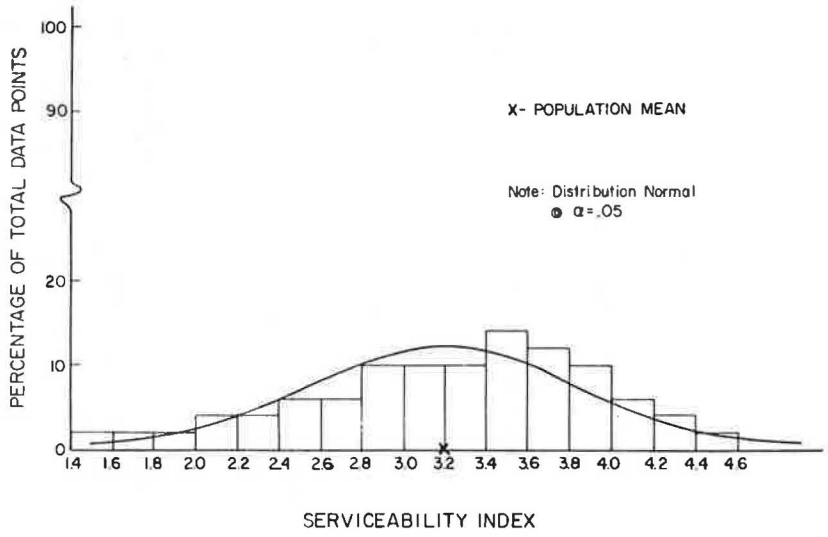

tween 100 (no distress) and 0 (a large amount of distress);

3. Skid number at 64.4 km/h (40 mph); and
4. Surface curvature index (SCI), which was obtained by use of the Dynaflect.

From this mass inventory of data, Figure 1 shows a typical plot of SI data for U.S.-state highways distributed by use of a histogram. The normality of these data was checked by using the chi-square test. The null hypothesis tested was that the distribution conforms to a normal distribution. The generated normal curve is shown superimposed on Figure 1. At a level of significance of 0.05 (i.e., a probability of 0.05 of rejecting a true hypothesis), the data test approximately normal. Similar plots made for pavement condition, skid, and deflection data also indicated that such distributions were normally or nearly normally distributed.

Since a mass inventory was available for district 21 for both 1974 and 1975, a comparison was made of the summary statistics for each year. This information is given in Table 3 and shows total kilometers and population means and standard deviations for each data type. The numbers of kilometers given vary between the two years. This occurs primarily for SCI data because the Dynaflect survey was not completed until 1975 and only partial data were available in 1974. It should also be pointed out that there was some overlap of data between the two years for SI and SN data, which reduces potential year-to-year differences. This is not true for PRS since independent surveys of these data were conducted during each of the two years.

The differences between the estimated SI means given for district 21 in Table 1 and the population means given in Table 3 are of interest. The estimates given in Table 1 for U.S.-state and FM highways were obtained from the statewide sample survey for which sampling of highway segments was done in district 21 as well as in the other 24 districts. The population means given in

Table 3. District 21 mass inventory: statistical summary.

Highway Type	Year	Data Type	Number of Kilometers	Mean	Standard Deviation
Interstate	1974	SI	61	3.3	0.6
		SCI	0	-	-
		SN	53	0.35	0.06
		PRS	61	83	8
	1975	SI	60	3.6	0.5
		SCI	61	0.2	0.1
		SN	63	0.38	0.06
		PRS	59	91	6
U.S.-state	1974	SI	1760	3.2	0.7
		SCI	600	0.7	0.5
		SN	1630	0.32	0.10
		PRS	1723	82	13
	1975	SI	1722	3.3	0.7
		SCI	1129	0.6	0.4
		SN	1807	0.34	0.10
		PRS	1745	78	14
FM	1974	SI	2214	2.6	0.7
		SCI	720	0.8	0.4
		SN	1983	0.34	0.09
		PRS	2314	78	16
	1975	SI	2361	2.6	0.8
		SCI	1892	0.8	0.4
		SN	2473	0.35	0.09
		PRS	2374	75	16

Note: 1 km = 0.62 mile.

Table 4. District 21 mass inventory: statistical summary for Zapata County.

Highway Type	Year	Data Type	Number of Kilometers	Mean	Standard Deviation
Interstate	1974	SI	0	-	-
		SCI	0	-	-
		SN	0	-	-
		PRS	0	-	-
	1975	SI	0	-	-
		SCI	0	-	-
		SN	0	-	-
		PRS	0	-	-
U.S.-state	1974	SI	127	3.1	0.5
		SCI	88	0.7	0.3
		SN	123	0.32	0.05
		PRS	124	94	4
	1975	SI	129	3.1	0.6
		SCI	89	0.7	0.3
		SN	133	0.34	0.06
		PRS	128	89	6
FM	1974	SI	38	2.3	0.7
		SCI	32	1.2	0.4
		SN	37	0.39	0.10
		PRS	43	89	8
	1975	SI	53	2.3	0.7
		SCI	44	1.0	0.5
		SN	63	0.38	0.08
		PRS	53	75	25

Note: 1 km = 0.62 mile.

Table 3 were obtained from a complete districtwide mass inventory for each highway type. The differences are 0.4 SI unit for U.S.-state highways and 0.2 SI unit for FM highways (1974 comparison). These variations between the means are believed to result primarily from differences between the Mays road meters used to conduct the surveys and from sampling error. This is discussed in more detail in a later section of this paper.

The treatment used for the entire district 21 was also applied to each county in the district. For example, the summary statistics for Zapata County are given in Table 4 for both 1974 and 1975. Of special significance in this table is that PRS decreased significantly from 1974 to 1975, especially for FM highways. As the PRS means decreased, the standard deviations increased for this county. The source of these year-to-year differences is not known. They could be the result of an increase in pavement deterioration, rating error, or a combination of the two.

After the mass-inventory data had been organized into a computer-accessible form, they were reorganized into a format similar to that of data for the statewide random segments. To accomplish this task, a FORTRAN computer program was written that divided all highways in the district into 3.2-km (2-mile) segments. The program also organized the data contained in each of these 3.2-km segments into the form of a summary that consisted of the number of data points, means, and standard deviations for each of the data types. This information was computed and stored for future processing.

An additional computer program was prepared to access these segments, draw samples, and make estimates of the population mean and standard error for various sample sizes. The computer program performed essentially the same task on all the 3.2-km highway segments as was performed manually to select the statewide sample. This selection process was computerized because hundreds of samples would be selected and statistically summarized.

To select a given sample size, total highway kilometers were multiplied by the sample-size percentage desired. This gave the approximate number of kilometers to be sampled. The number of kilometers thus obtained was divided by 3.2 km to obtain the number of required highway segments. Next, the program randomly selected a county from the total number of counties in the district. Highway segments were then randomly selected within the selected county for both U.S.-state and FM highways. The number of highway segments chosen for each highway type depended on county kilometers and the desired sample size. Additional counties and highway segments were selected until the required sample size for the entire district had been achieved.

To further explain this process, for each trial computer iteration the following numbers of 3.2-km (2-mile) U.S.-state and FM highway segments were selected for district 21 for the given sample sizes, which are based on the percentage of centerline kilometers:

Sample Size (%)	Number of Segments
0.5	6
1	12
2	24
3	35
5	59
10	117

The lower and upper bounds for sample sizes were 0.5 and 10 percent, respectively. A 0.5 percent sample size was felt to represent the smallest reasonable sample that should be considered. Conversely, a 10 percent sample size was felt to represent a more than adequate estimate of the population parameters.

Means and standard errors were computed for each of the sample sizes for both the 1974 and 1975 data. The overall district mean was computed by averaging the means obtained from each of the sample estimates calculated. The formula used to compute the stratified two-stage sample mean is

$$\hat{\bar{Y}} = \sum_{1}^{n} M_i \bar{y}_i \Big/ \sum_{1}^{n} M_i \qquad (1)$$

Table 5. District 21 means and standard errors for six sample sizes and 300 sample-selection iterations: 1975 data.

Sample Size (%)	Highway Type	SI		PRS		SCI		SN	
		Mean	SE	Mean	SE	Mean	SE	Mean	SE
0.5	U.S.-state	3.33	0.35	78.6	7.8	0.62	0.20	0.34	0.05
	FM	2.62	0.42	75.8	9.3	0.79	0.21	0.36	0.05
1	U.S.-state	3.31	0.28	78.9	5.7	0.61	0.14	0.34	0.04
	FM	2.61	0.27	75.5	5.6	0.80	0.14	0.36	0.04
2	U.S.-state	3.32	0.17	78.6	3.8	0.60	0.09	0.34	0.03
	FM	2.62	0.18	75.1	3.9	0.78	0.09	0.35	0.02
3	U.S.-state	3.30	0.15	78.2	3.5	0.61	0.08	0.34	0.02
	FM	2.66	0.13	75.0	3.2	0.79	0.07	0.35	0.02
5	U.S.-state	3.30	0.11	78.6	2.5	0.61	0.06	0.34	0.02
	FM	2.65	0.11	75.7	2.4	0.79	0.06	0.35	0.02
10	U.S.-state	3.31	0.08	78.4	1.7	0.60	0.04	0.34	0.01
	FM	2.64	0.07	75.2	1.6	0.79	0.04	0.35	0.01

Table 6. District 21 means and standard errors for three sample sizes and 300 sample-selection iterations: 1974 data.

Sample Size (%)	Highway Type	SI		PRS	
		Mean	SE	Mean	SE
0.5	U.S.-state	3.19	0.35	82.1	7.6
	FM	2.59	0.39	80.4	9.9
1	U.S.-state	3.21	0.27	82.5	5.4
	FM	2.59	0.26	79.9	6.0
3	U.S.-state	3.19	0.15	82.9	3.0
	FM	2.61	0.13	78.8	3.2

where

$\hat{\bar{\bar{Y}}}$ = estimate of district mean for a given sample size, highway type, and data type;
n = number of counties selected for a given sample size;
M_i = number of possible 3.2-km (2-mile) highway segments within a county; and
$\bar{y}_i$ = estimate of mean value for the i th county.

Equation 1 was used to compute a sample mean for each highway and data type considered. This was repeated for 300 sample-selection iterations. Each of the 300 district estimates so calculated was used in calculating the overall district mean.

The simulation standard error (SE) was computed based on the means obtained by using Equation 1. The formula used to accomplish this is

$$SE = \sum_{1}^{t} (\hat{\bar{\bar{Y}}} - \bar{\bar{Y}})^2 \Big/ (t - 1)^{1/2} \qquad (2)$$

where $\bar{\bar{Y}}$ is the average of all district estimates for a given sample size, highway type, and data type and t is the number of sample-selection iterations for a given sample size (300 in all cases). This formula is similar to that used for calculating the standard deviation of a set of data and is calculated differently from the standard error computation for a sample used in Tables 1 and 2.

The overall means and standard errors computed by Equations 1 and 2 are given in Tables 5 and 6. Table 5 gives the overall means and standard errors for six sample sizes for data obtained primarily during 1975, and Table 6 gives the same kind of data for 1974. The data processed for 1974 were not as extensive as those for 1975 because of the incompleteness of 1974 SN and SCI data. In addition, the 1974 data presentation is intended only as a check on the 1975 data. As should be expected, the data contained in both tables indicate that standard error decreases as sample size increases. If all possible highway segments were repeatedly sampled (100 percent sample sizes), the standard error would approach zero.

It is of interest to compare the above method of obtaining standard error with that used in simple random sampling, which would involve sampling the required highway segments by using a completely random pattern throughout a district. The standard error of various sizes of simple random samples can be computed as follows:

$$SE = \sigma_{\bar{y}} = (S/\sqrt{n}) \sqrt{1 - (n/N)} \qquad (3)$$

where

S = standard deviation of the population,
n = number of 3.2-km (2-mile) highway segments sampled for a given sample size,
N = total number of 3.2-km highway segments in the district, and
(n/N) = sampling fraction.

Standard errors for a simple random sampling technique were computed by using Equation 3 and the population standard deviations in Table 3 for the 1975 data. The values so calculated were compared with standard errors obtained from the simulation study for the two-stage sampling technique. Table 7 gives a comparison of both standard errors for different sample sizes and highway and data types.

The data given in Table 7 reveal that the standard errors obtained for the two-stage sampling technique are in most cases lower than those calculated by simple random sampling. Of 48 possible comparisons, the two-stage standard errors are lower in 34 cases, the same in 9 cases, and larger in 5 cases. The largest observed difference is 50 percent, in which case the standard error obtained by simple random sampling is the larger.

The primary goal of this study of sample size was to determine the optimum sample size for each combination of highway and data type. Figure 2 is a plot of sample size versus standard error divided by the mean times 100. The ordinate term, called the coefficient of sample variation, is analogous to a coefficient of variation and allows the standard errors for each data type to be compared. The figure shows that the variability of a given sample size decreases rapidly at first and then begins to stabilize at about 10 percent. For SI, PRS, and SN, the coefficient of sample variation at a 0.5 percent sample size ranges from 10 to 15

Table 7. District 21 standard errors for simple random and two-stage sampling techniques.

Sample Size (%)	Highway Type	Simple Random Sample				Two-Stage Sample			
		SI	PRS	SCI	SN	SI	PRS	SCI	SN
0.5	U.S.-state	0.49	9.9	0.28	0.07	0.35	7.8	0.20	0.05
	FM	0.40	3.0	0.20	0.04	0.42	9.3	0.21	0.05
1	U.S.-state	0.31	6.2	0.18	0.04	0.28	5.7	0.14	0.04
	FM	0.30	6.0	0.15	0.03	0.27	5.6	0.14	0.04
2	U.S.-state	0.22	4.4	0.13	0.03	0.17	3.8	0.09	0.03
	FM	0.21	4.2	0.11	0.03	0.18	3.9	0.09	0.03
3	U.S.-state	0.18	3.7	0.11	0.03	0.15	3.5	0.08	0.02
	FM	0.17	3.4	0.09	0.02	0.13	3.2	0.07	0.02
5	U.S.-state	0.14	2.8	0.08	0.02	0.11	2.5	0.06	0.02
	FM	0.13	2.6	0.06	0.02	0.11	2.4	0.06	0.02
10	U.S.-state	0.10	2.0	0.06	0.01	0.08	1.7	0.04	0.01
	FM	0.09	1.8	0.05	0.01	0.07	1.6	0.04	0.01

Figure 2. District 21 coefficient of sample variation versus sample size: 1975 data.

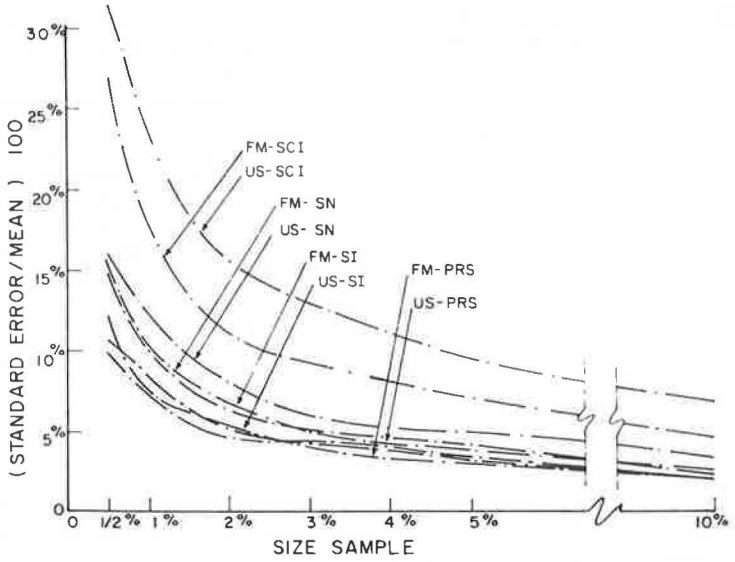

percent. At a 10 percent sample size, this coefficient ranges from about 3 to 5 percent. The exception is the coefficient for SCI, which ranges from about 27 to more than 30 percent at a 0.5 percent sample size and less than 10 percent at a 10 percent sample size.

Although the data shown in Figure 2 give a good indication of the precision gained with increasing sample size, a better gauge was sought to answer the question, How large is large enough? To answer this question, a procedure for minimization of variance was used for various levels of fixed survey costs. A simple utility method was also developed as an independent check of this procedure.

The procedure for minimization of variance is described in a number of sampling survey texts (4, 7). This technique minimizes the variance of the estimated mean for a fixed survey cost. The procedure is possible since both the number of sampled counties in a district and the number of 3.2-km (2-mile) highway segments sampled within a county are considered within the variance term. Lagrange multipliers are used to determine a minimum variance as a function of the number of highway segments within a county. The following equation results from this procedure:

$$m_{opt} = S_2 / \sqrt{S_1^2 - (S_2^2/M)} \sqrt{c_1/c_2} \quad (4)$$

where

m_{opt} = optimum number of 3.2-km (2-mile) highway segments per county;
S_1^2 = variance among county means in a district;
S_2^2 = variance among 3.2-km highway segments within counties;
M = total number of potential 3.2-km highway segments within a county;
c_1 = costs associated with sampling a county, including travel costs; and
c_2 = costs associated with obtaining a specific type of data within a 3.2-km highway segment.

The optimum number of counties can now be determined for a fixed survey cost by use of the following equation:

$$C = c_1 n + c_2 nm \quad (5)$$

where

C = total available budget for the survey,
n = number of counties to be sampled in a district, and
m = m_{opt}.

The appropriate variances and costs were determined from data available from the district 21 mass inventory and the prior statewide two-stage sample surveys. The optimum sample sizes for a district were determined for both U.S.-state and FM highways and the four data types. This process first involves using Equation 4 to determine the optimum number of highway segments to sample in each sampled county. The resulting optimum numbers of highway segments, given in Table 8, range from a minimum of two to a maxi-

Table 8. Procedure of variance minimization to determine optimum sample size.

Highway Type	Data Type	Ratio of Costs (c_1/c_2)	Highway Segments per County (m_{ppt})	Budget ($/district)	Counties per District (n)	Optimum Sample Size (%)
U.S.-state	SI	1.6	2	100	2	0.9
				200	5	2.2
				400	9	3.9
	SCI	1.0	3	250	2	1.3
				500	3	2.0
				1000	7	4.6
	SN	4.0	2	100	2	0.9
				200	3	1.3
				400	7	3.0
	PRS	1.6	2	150	2	0.9
				300	5	2.2
				600	9	3.9
FM	SI	1.6	2	100	2	0.6
				200	5	1.4
				400	9	2.6
	SCI	1.0	2	250	2	0.6
				500	5	1.4
				1000	9	2.6
	SN	4.0	2	100	2	0.6
				200	3	0.9
				400	7	2.0
	PRS	1.6	4	150	2	1.1
				300	3	1.7
				600	6	3.4

Table 9. Comparison of district 21 two-stage random sample and population means: 1974 data.

Original Sample Size (%)	Highway Type	Data Type	Original Sample Mean	Population Mean	Mean Plus One Standard Error	Mean Minus One Standard Error
0.9	U.S.-state	SI	3.6	3.2	3.5	2.9
		PRS	85	82	88	76
0.6	FM	SI	2.8	2.6	3.0	2.2
		PRS	76	78	87	69

mum of four. Then, if the fixed survey budgets are known, the appropriate number of counties per district can be calculated by using Equation 5.

Three budget levels were selected for each combination of highway and data type to represent the minimum (low), expected (medium), and maximum (high) budget levels that can be expected from TSDHPT funding. The budgets for each data type were the same regardless of highway type. This weights the U.S.-state highways since they have fewer kilometers in a district than farm-to-market highways. In light of these budgets, the range of counties per district to be sampled was calculated (Table 8). The overall optimum sample size for a district can now be calculated by multiplying the number of segments per county by the number of counties to be sampled within a district. This result is multiplied by the 3.2-km (2-mile) length of each segment and is then divided by the appropriate total highway district kilometers. Kilometers of U.S.-state and FM highways for district 21 were used to perform this final calculation.

The resulting sample sizes, given in Table 8, range from a low of 0.6 percent for the low budget to a high of 4.6 percent for the highest budget. More specifically, for U.S.-state highways and the four data types, the mean optimum sample size is 1 percent for the low budget, 1.9 percent for the medium budget, and 3.8 percent for the high budget. For FM highways, the optimum sample sizes for these three budgets are 0.7, 1.4, and 2.6 percent, respectively.

In addition to the procedure of variance minimization, a utility method was developed to provide an independent check on the optimum sample size. That procedure is not described in this paper since it has been reported elsewhere (8). It suffices that the results of the two optimization methods provide similar results for approximately equivalent budgets.

Finally, a comparison between the two-stage random sample means obtained for the highway segments originally selected in district 21 as part of the statewide sample, the district population means, and simulation standard errors is appropriate. Only the SI and PRS data types for each highway type are considered in this case (see Table 9).

The sample sizes given in Table 9 are for the original two-stage samples. For U.S.-state highways, the actual sample size was 0.9 percent; for FM highways, it was 0.6 percent. This consisted of four U.S.-state 3.2-km (2-mile) segments and four FM segments. The population means and the simulation standard errors are compared with the original sample means. It can be seen that all means except one compare favorably.

The population means plus or minus one standard error are also given in Table 9 for the actual sample sizes used. Approximately 68 percent of all possible sample means for the given sample sizes should fall within these ranges. For U.S.-state highways, this range is 0.6 SI units for the 0.9 percent sample, less than 0.4 for a 2 percent sample (not given in the table), and less than 0.2 for a 10 percent sample (not given in the table). By using a different highway and data type, PRS ranges for FM highways are 18 PRS units for a 0.6 percent sample, less than 8 for a 2 percent sample (not given in the table), and slightly more than 3 for a 10 percent sample (not given in the table). This again demonstrates how the range of the standard error decreases with increasing sample size.

SUMMARY AND CONCLUSIONS

The state of Texas has used a stratified two-stage random sample to obtain a limited amount of highway performance data throughout the state. Highway segments 3.2 km (2 miles) long were used, and approximately 1 percent of total statewide centerline kilometers was sampled. Information on construction, traffic, climate, roughness, visually determined condition, deflection, rut depth, and skid resistance was obtained for each of the sampled highway segments. District and statewide estimates of serviceability index for 1974 and 1976 were indicated.

To examine the method and size of sampling survey currently used in Texas, simulation techniques were used on a complete set (mass inventory) of data available for one highway district, district 21. The precision (as measured by standard error) of the two-stage sampling method was shown to be superior to that of simple random sampling. In addition, a procedure of variance minimization and a utility method both indicated that about a 2 percent sample of total centerline kilometers appears to best minimize sampling error. The analysis further shows that, for Texas conditions, approximately two highway segments for each highway type should be sampled in each sampled county. The above information was determined by using four types of data: serviceability index, pavement rating score, surface curvature index (deflection), and skid number. For two of these data types, the estimates provided by the portion of the original statewide sample in district 21 are generally in reasonable agreement with the population means obtained for that district even though the sample sizes used are about half the optimum size.

The information provided by the sample sizes currently used in Texas is most reliable for statewide data estimates and next most reliable for district estimates. Current instrument, personnel, and sampling errors make small year-to-year variations in district data difficult to detect, but reductions in all three error sources are continuing to be made.

Some highway-oriented government agencies may wish to conduct a sampling survey that conforms to a selected precision. Thus, a determination of optimum sample size may not be necessary for such agencies.

A sampling survey will not answer all of the important questions about the condition and performance of a highway network, but it can provide a significant amount of valuable, relatively inexpensive information. To that end, the information contained in this paper could be used by any state or other government agency in planning a sampling survey.

ACKNOWLEDGMENT

I wish to acknowledge the assistance and encouragement of Robert L. Lytton and Jon A. Epps of the Texas Transportation Institute and also the assistance of TSDHPT, the sponsorship of the Federal Highway Administration, and the help of Larry Ringer of the Institute of Statistics, Texas A&M University.

REFERENCES

1. R. L. Lytton, W. M. Moore, and J. P. Mahoney. Pavement Evaluation. Federal Highway Administration, U.S. Department of Transportation, Final Rept. FHWA-RD-75-78, Phase 1, March 1975.
2. W. G. Cochran. Sampling Techniques. Wiley, New York, 1963.
3. W. Medenhall, L. Ott, and R. L. Scheaffer. Elementary Survey Sampling. Duxbury Press, Belmont, CA, 1971.
4. T. Yamane. Elementary Sampling Theory. Prentice-Hall, Englewood Cliffs, NJ, 1967.
5. J. A. Epps, C. W. Shaw, G. G. Harvey, J. P. Mahoney, and W. W. Scott. Operational Characteristics of Mays Ride Meter. Texas Transportation Institute, Texas A&M Univ., College Station, Res. Rept. 151-3, Sept. 1974.
6. J. A. Epps, A. H. Meyer, I. E. Larrimore, and H. L. Jones. Roadway Maintenance Evaluation User's Manual. Texas Transportation Institute, Texas A&M Univ., College Station, Res. Rept. 151-2, Sept. 1974.
7. M. H. Hansen, W. N. Hurwitz, and W. G. Madow. Sample Survey Methods and Theory. Wiley, New York, Vols. 1 and 2, 1953.
8. J. P. Mahoney and R. L. Lytton. Measurements of Pavement Performance Using Statistical Sampling Techniques. Texas Transportation Institute, Texas A&M Univ., College Station, Res. Rept. 207-2, March 1978.

Publication of this paper sponsored by Committee on Pavement Condition Evaluation.

**J. P. Mahoney was with Texas A&M University when this research was performed.*

Laboratory Testing of a Full-Scale Pavement: The Danish Road-Testing Machine

Per Ullidtz and Christian Busch, Institute of Roads, Transport, and Town Planning, Technical University of Denmark, Lyngby

Full-scale pavements can be tested under controlled climatic conditions and with a controlled groundwater level by using the Danish road-testing machine. The response of the pavement in terms of stresses, strains, and deflections can be monitored during performance tests of a maximum ten-thousand 65-kN wheel loads/day. A qualitative evaluation of pavement response during the first two test series (0.5 million loads) has confirmed

that the machine is well suited to simulating heavy traffic loading. The response of the pavement was reasonably well predicted from linear elastic theory, considering the large scatter in the measured values and in the elastic parameters of the materials. No cracking was observed during the two performance tests although both Danish and Nottingham criteria predicted extensive cracking. Subgrade criteria (normal stress and strain) derived partly from the AASHO Road Test agreed fairly well with a decrease of the present serviceability index to about 2.5, but this deterioration was not associated with any appreciable permanent deformation of the subgrade. Finally, prediction of pavement performance in terms of rutting and present serviceability index was attempted by using a simulation program developed at the Technical University of Denmark. Reasonably good agreement was found for both of these performance criteria.

Mechanistic (or theoretical) design procedures are needed in order to design pavement structures if the materials, loads, or climatic conditions are different from those on which the empirical design methods are based. Because an increasing amount of road construction is taking place in the less developed countries and resources of traditional road-building materials are dwindling in many industrialized countries, the need for a mechanistic design procedure is growing. The ideal mechanistic design procedure should be capable of predicting the response as well as the performance of pavement structures from measured fundamental properties of the materials.

To check the validity of different design procedures—or to develop new procedures—a large number of road-testing machines (RTMs) have been developed. Most of these have been of the roundabout type, with limited facilities for controlling climatic conditions or the moisture condition of the subgrade. Recently, some linear tracked RTMs have been developed; of these, the Danish RTM is believed to be one of the most sophisticated (1).

The Danish RTM can be used for fatigue testing of full-scale pavement structures under controlled climatic conditions and with a controlled groundwater level. During fatigue testing, critical stresses and strains in the structure as well as deflections, temperatures, and pore-water pressure can be monitored.

Cross-sectional and longitudinal views of the Danish RTM are shown in Figures 1 and 2, respectively. The device consists of (a) a test pit with automatic water-level control, (b) a wheel-loading system, (c) a climate chamber, and (d) a system of transducers, amplifiers, and a data logger for measuring and recording stresses and strains.

The test section of the concrete pit is 9 m long, 2.5 m wide, and 2 m deep. Finite-element calculations have shown that there is no perceptible influence from the stiff boundaries on the critical stresses or strains at the centerline of the pit.

The wheel load is hydraulically applied and may consist of a single or a dual wheel. The maximum dual wheel load is 65 kN and the maximum velocity is approximately 25 km/h, which makes it possible to simulate heavy truck traffic. As many as 10 000 wheel loads can be applied in a 24-h day. This corresponds to approximately 60 000 passages of a standard 80-kN axle load. During fatigue testing, the lateral position of the wheel can be automatically changed to give a desired lateral wheel-load distribution.

The RTM is enclosed in a climate chamber that is 27.5 m in length, 4 m wide, and 3.8 m in height. Because of the large size of the chamber, ordinary construction equipment can be used. Heating and cooling aggregates make possible a temperature range of -10° C to +40° C.

The main difference between conditions in situ and in the RTM is the time scale during performance (fatigue) testing. If the loads of, say, a 10-year period are applied in only 1 year, long-term changes in the materials—e.g., hardening of the bitumen—are not allowed to take place. Moisture movements during freezing and thawing pose a special problem in this connection since accelerated testing is not possible.

Other differences between in situ and RTM conditions are hydraulic load application, loads passing in both directions, time between loadings, and variations of materials, but these, like the boundary conditions, are believed to have only limited influence on the response or performance of the pavement structure.

Figure 1. Cross section of road-testing machine.

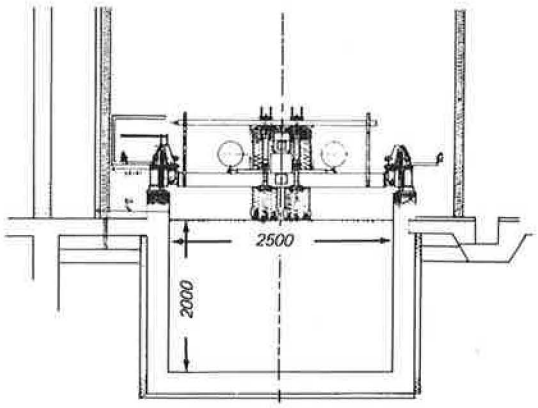

Figure 2. Longitudinal section and plan of road-testing machine showing climate chamber and arrangement of hydraulic motors.

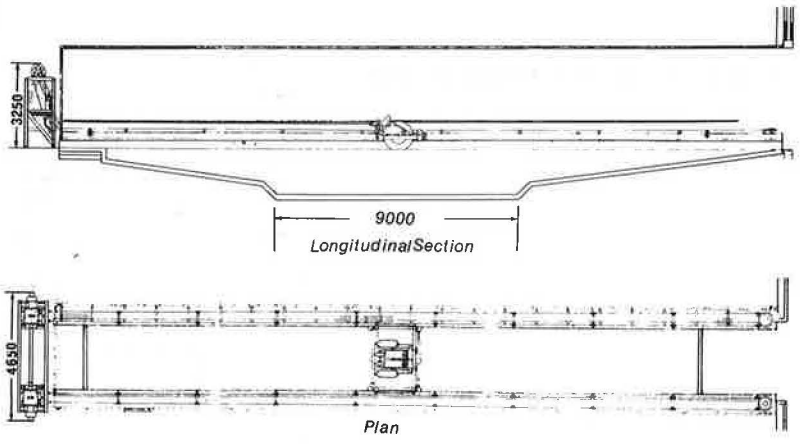

INSTRUMENTATION

For a simple two-layer road structure, such as the bituminous base on a subgrade of silty sand used for the first three test series in the RTM, the stresses or strains usually assumed to be critical to the service life of the structure are at the asphalt-subgrade interface. The horizontal strain at the bottom of the asphalt layer should be limited to avoid cracking, and the vertical stress or strain at the top of the subgrade should be limited to avoid excessive permanent deformation. To predict the performance of the pavement, therefore, these values should be measured.

To find out whether the response of the pavement can be accurately predicted from layered elastic theory, stresses and strains at other depths as well as the deflection of the structure are also of interest. In this connection, the temperature of the asphalt layer and the negative pore pressure of the subgrade soil (suction) must be known in order to determine the elastic parameters of the materials. To measure these values, the test section was instrumented as shown in Figure 3 (deflection and suction gages are not shown).

The pressure cells are of the diaphragm type, and the strains in the diaphragm, when it deflects under stress, are measured by strain gages. The cells are made of titanium. A major problem with pressure cells is that the presence of the cell alters the stress field in the soil. In Figure 4, the changes from a uniform distribution caused by cells with 1- and 2-mm diaphragms are shown. The changes are seen to be highly dependent on the soil modulus E.

Theoretical considerations showed that the error in cell registration, compared with calibration under hydrostatic pressure, would be in the range of 0 to +10 percent for the soil moduli to be expected in the subgrade.

After completion of the pavement structure, an attempt was made at in situ calibration of the pressure cells. Dynamic plate loading tests in which a falling-weight deflectometer was used were carried out at different distances from the cells to obtain the stress distribution at the depth of the cells. From this stress distribution, the total vertical force on the horizontal plane through the cell can be found; this force must be equal to the force applied on the pavement surface.

Figure 3. Instrumentation of test section.

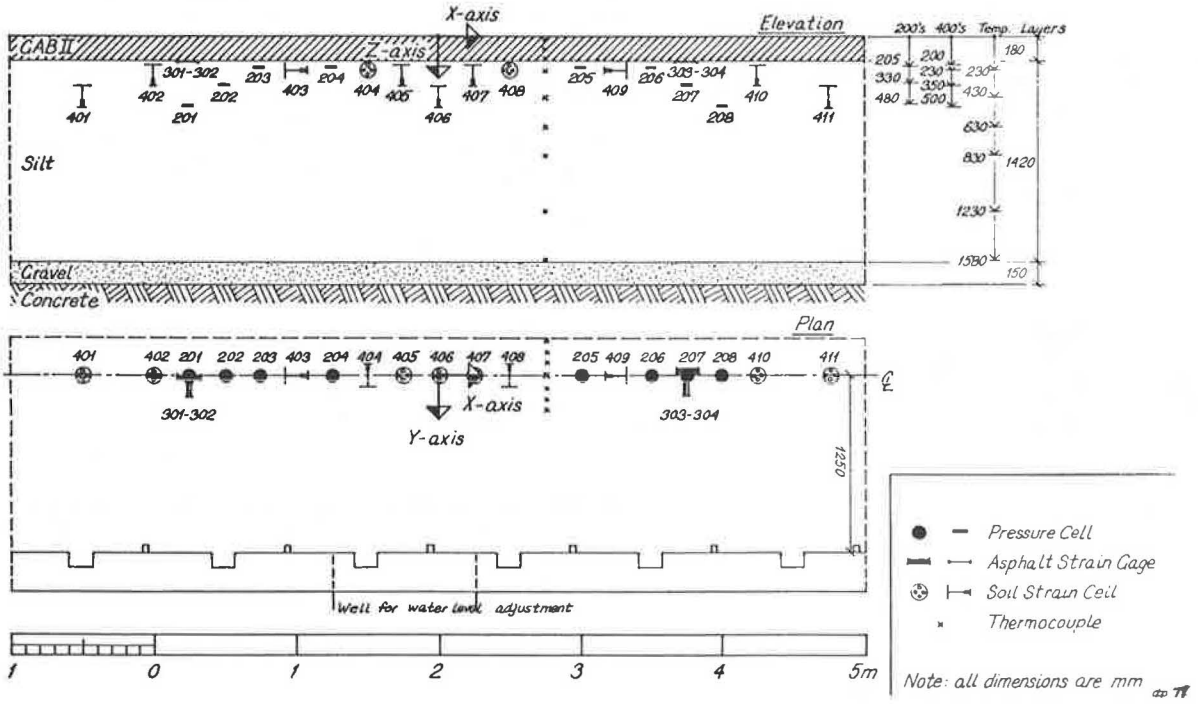

Figure 4. Excess stress distribution in diaphragm plane.

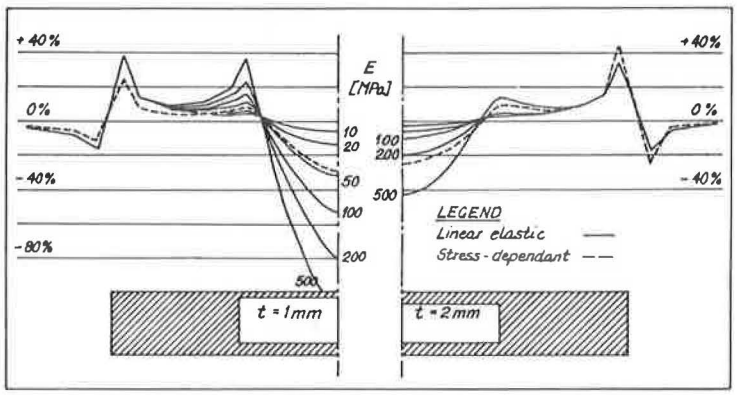

Figure 5. Soil strain cell.

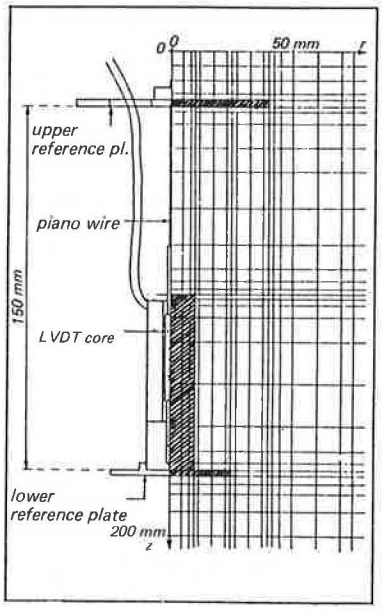

Figure 6. Installation procedure for soil strain cell.

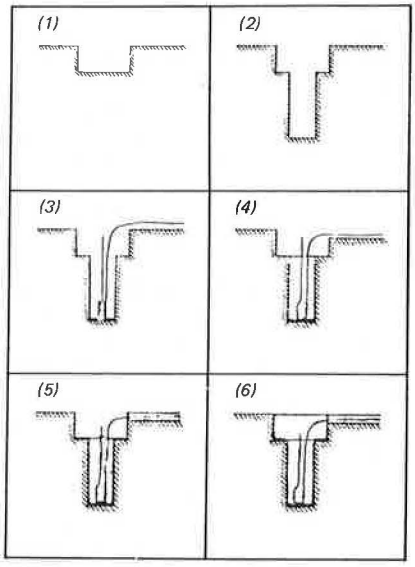

Figure 7. H-gages.

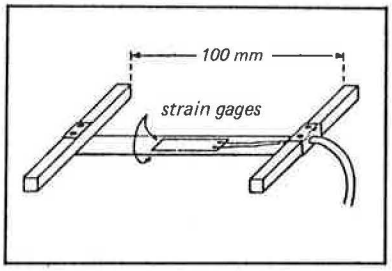

Figure 8. Asphalt gages glued to cores.

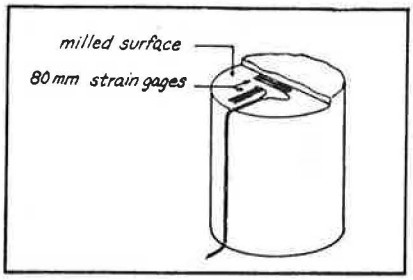

To determine the total force from the stress distribution, an integration was performed in which it was assumed that the Boussinesq stress distribution could be used and that the ratio between the observed and the actual stress was a constant (a) independent of the distance from the load because the cross sensitivity of the cells is negligible (<4 percent). By varying the depth in the Boussinesq expression, a "best" a-value (error factor) and equivalent depth were determined on the criterion that Σ (observed stress - a × calculated stress)^2 should be minimized. This resulted in equivalent depths that compared well with equivalent depths determined from the elastic moduli of the materials, but it also resulted in widely scattered error factors: from 0.9 to 3.5. For high asphalt temperatures, the mean error factor (six gages) was 1.45 and the standard deviation 0.39. The error factors were also found to be highly dependent on the temperature of the asphalt layer, which indicated that the procedure used for installing the gages—in dug-out holes after completion of the subgrade—was rather unsuccessful even though great care had been taken to fill back exactly the amount of soil dug out minus the volume of the cell. It should be noted that this calibration is correct only if the stress follows a Boussinesq distribution.

Strains in the subgrade were measured by linear variable differential transformers (LVDTs) as the relative change in length over a reference length of 100-150 mm. Finite-element calculations were made by using the net shown in Figure 5 to determine the influence from the cell on the strains in the soil. It was found that the results were much influenced by the assumption of either full friction or no friction between cell and soil. With full friction the cell would underestimate the strains by approximately 30 percent, whereas with no friction it would overestimate by 40 percent.

The effect of the installation procedure, shown in Figure 6, could not be evaluated, but it is hoped that the unsuccessful backfilling of soil found with the pressure cells will be of less importance to the strain cells because holes drilled through the upper reference plate ensure that most of this plate rests on undisturbed soil. A pair of electromagnetically coupled coils (BISON) were tried because they are much simpler to install, but they were found not to be suited for measuring dynamic strains because the signal induced by the metal masses of the loading vehicle was larger than the strain signal.

The strains at the bottom of the asphalt layer were measured by strain gages mounted on an aluminum strip anchored to the asphalt by two steel bars, or H-gages (see Figure 7). These gages functioned immediately after completion of the pavement, but they quickly deteriorated. After completion of the first test series, two gages were recovered by drilling and were found to be extensively corroded. A new attempt at measuring the strains was made by cementing strain gages to the cores drilled from the pavement (see Figure 8), and refitted in the pavement with araldite. These gages worked satisfactorily at the beginning of the second performance test, but the araldite eventually failed.

Deflections were measured by using a geophone or an accelerometer and one or two analog integrations of the signal, respectively. The geophone is the sturdier and cheaper of the two instruments. Because the signal is proportional to the velocity of the instrument and thus needs only one integration, the drift on the signal is much less than that of the accelerometer. Because the geophone does not respond to low frequencies, however, it is not very well suited for measuring deflections under a slow-moving wheel, a condition in which the accelerometer can be used, even if with some difficulty. The geophone on the other hand is an excellent deflection

gage in connection with dynamic plate loading tests.

Both psychrometers and agricultural tensiometers were installed in the subgrade at different depths. The tensiometers showed that the suction (measured in millimeters) water column was equal to the height of the tensiometer above groundwater level. The suction values were too low (maximum 1.5 m of water) to be measured with the psychrometers.

Finally, 10 thermocouples were installed to record temperature at different depths.

All signals from stress and strain transducers were amplified on direct-current amplifiers with peak detectors. The peak signals were monitored by a scanner, digitalized, and fed into a programmable desk-top calculator, which would divide each signal by the appropriate sensitivity and amplification and print out the result in the desired unit (megapascals or microstrain). A maximum of 30 signals/wheel passage could be monitored. If the shape of the signals was needed, an analog record of 12 signals could be made by a UV recorder.

EQUIPMENT

The elastic moduli of the materials in the pavement structure were evaluated in situ by using the falling-weight deflectometer (FWD) and the lightweight deflectometer (LWD). These determinations were supplemented by tests on samples of the materials that used an LWD with test tank, a triaxial apparatus, and a bending machine. Rutting and longitudinal roughness were measured by a profilometer. This equipment and the interpretation of the test results are briefly described below.

The FWD is a dynamic plate loading apparatus where the load pulse is produced by a weight falling on a system of springs (2).

The duration of the dynamic load pulse is 26 ms with a peak force magnitude of 50 kN. For asphaltic materials, where the duration of the load pulse influences the modulus, the FWD impact corresponds to vehicle velocities of 40-60 km/h.

On a linear elastic semi-infinite half space the modulus of the material will be equal to the surface modulus E_0, calculated from Boussinesq's equation (3):

$$E_0 = 2(1 - \nu^2)\sigma_0 a/d_0 \quad (1)$$

where

ν = Poisson's ratio,

σ_0 = uniformly distributed stress at the surface (contact pressure),

a = radius of the loaded area, and

d_0 = deflection at the center of the load.

If the material is nonlinear elastic or if the subgrade is layered, the surface modulus cannot be used as a materials modulus. If the nonlinearity follows the simple relation $E = C \times (\sigma_1/\sigma')^n$, the constants C and n can be determined from the surface modulus at different stress levels by using the following relation (4):

$$E_0 = (1 - 2n) \times C \times (\sigma_0/\sigma')^n \quad (2)$$

If the modulus is constant with depth, the surface modulus $E_0(r)$ at different distances r from the center of the load will be constant. For $r > 2a$, the surface modulus can be calculated from

$$E_0(r) = (1 - \nu^2)\, \sigma_0 a^2/[r \times d_0(r)] \quad (3)$$

where $d_0(r)$ is the surface deflection at distance r.

Because the compression (or extension) of the material between the surface and a depth equal to the distance from the load center is negligible, the surface modulus $E_0(r)$ will reflect the surface modulus at a depth $\cong r$.

For two-layer systems, the moduli may be determined from graphs based on surface deflections if the subgrade is either linear elastic or nonlinear with n = -0.25 or -0.5 (5). For more complex structures, a nondestructive determination of the moduli is still possible through a trial-and-error approach in which the moduli are estimated, the surface moduli calculated and compared with the measured values, and changes made to the original estimates until a reasonably good fit is obtained. Tests made directly on granular materials are avoided by using these nondestructive methods. This is important for two reasons: (a) The bearing capacity at the surface of a granular material is low—zero if the cohesion is zero—and (b) the moduli of granular materials are stress dependent and will change when the surcharge is removed.

Because the critical strain at the bottom of an asphalt layer is greatly influenced by the modulus of the material immediately below the asphalt layer, an LWD was developed (see Figure 9). The modulus of a granular material can be measured directly by the LWD because a surcharge can be applied around the loaded area.

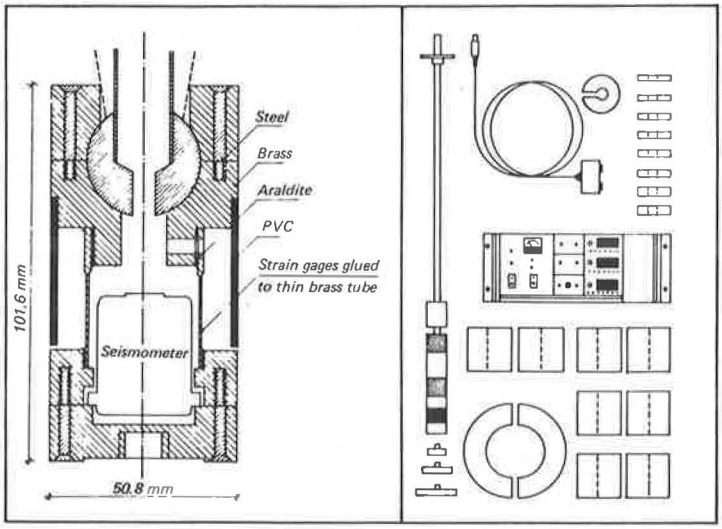

Figure 9. Lightweight deflectometer.

The LWD works on the same principle as the FWD, but the peak force and the radius of the loaded area are much smaller. The LWD is thus particularly well suited for determining moduli within a shallow depth.

Apart from in situ tests, the LWD can be used on material built into a test tank at varying moisture contents, degrees of compaction, etc. To find the elastic parameters or the constants in nonlinear elastic relations, correlations have been developed between these values and the surface deflections at varying contact pressures and surcharges (6). These correlations have been established through numerous finite-element calculations and can be used for linear as well as nonlinear elastic materials; the moduli can be dependent on either the major principal stress (in cohesive materials) or on the minor principal stress (in granular materials).

Because of the problems encountered in reproducing in situ conditions of materials and loading in the laboratory, emphasis was placed for the most part on in situ tests. Some laboratory tests have been carried out, however, partly to check on the in situ determined moduli and partly to get an estimate of Poisson's ratio.

The subgrade has been tested in a dynamic triaxial apparatus by using a simple pneumatic loading system (7). In these tests, an attempt was also made to determine the plastic characteristics of the subgrade material. The same loading system has been used for monoaxial short-term creep testing on cylindrical asphalt specimens extracted from the pavement section. Finally, three- and four-point bending tests have been carried out on prismatic asphalt specimens at temperatures between -20° C and +40° C in a frequency range of 0.01-100 Hz (8).

The performance of the pavement structure with respect to rutting and longitudinal roughness was determined by using a simple profilometer: The changes in surface level in relation to a 2-m-long aluminum rail were recorded directly on waxed paper. The slope variance was calculated from the longitudinal profile by using the slope over 225 mm at 300-mm intervals. The present serviceability index was calculated from the slope variance and rutting values by using the AASHO Road Test equation for flexible pavements (9).

MATERIALS TESTS

A number of conventional tests were made on asphalt and subgrade materials. The subgrade consisted of a nonplastic sandy silt with approximately 50 percent sand and 50 percent silt. The subgrade was constructed in 150-mm-thick lifts and compacted to 100 percent Proctor density (1700 kg/m^3) at approximately optimum moisture content (14 percent). At this density and moisture content, the California bearing ratio was found to be 18 percent and the capillary suction greater than 1 m.

The asphalt layer was a base-course material made from a well-graded, naturally occurring gravel with a maximum grain size of 20 mm. The thickness of the compacted layer varied between 170 and 180 mm. Tests made on recovered bitumen after construction of the asphalt layer showed that penetration at 25°C had dropped from the original 60 to 43. Three years later, after completion of the first test series, the penetration had dropped further to 27. The void content was rather large—11.5 percent—and compaction was 98.5 percent of the Marshall density of 2210 kg/m^3. The bitumen content was 3.65 percent by weight (standard deviation of 0.10 from five tests).

The modulus of the subgrade material was determined from dynamic triaxial tests, in situ FWD and LWD tests, and LWD tests in a test tank. The triaxial tests showed that the modulus depended on the cell pressure (σ_3), whereas the FWD tests showed a dependence on the major principal stress. In both cases, however, the nonlinearities were not very pronounced, the absolute value of the powers being in the range of 0.2 to 0.3. Thus, for the range of vertical and horizontal stresses to be expected in the subgrade, the modulus was considered to be constant in the calculation of the pavement response.

The minimum moduli were those that corresponded to a cell pressure of zero in the triaxial tests and to a contact pressure of 0.6 MPa in the FWD tests. The in situ LWD test made at a moisture content of 20 percent was carried out 800 mm below formation level. That the modulus of the subgrade decreased with depth was confirmed by FWD testing with different plate radii.

After conclusion of the first test series, the groundwater level was raised to 0.3 m below formation level. The resulting subgrade modulus was determined from FWD tests on top of the asphalt and LWD tests made in boreholes. A modulus range of 62-82 MPa was found with the FWD and 62-66 MPa with the LWD. These results agree well with the above-reported moduli at high moisture content.

Poisson's ratio, determined from dynamic triaxial tests, was found to be in the range of 0.15-0.20 for the vertical and horizontal stresses to be expected at the top of the subgrade. For large bulk stresses, Poisson's ratio decreased to about 0.1.

The modulus of the asphalt was determined through bending tests on prismatic specimens cut from the pavement. Results of tests carried out when the penetration of the bitumen was 27 are shown in Figures 10 and 11 (8). The modulus is seen to be a function of temperature, frequency, and maximum strain. Tests on specimens cut horizontally and vertically showed the asphalt to be isotropic although an analysis of the particle orientation showed a markedly horizontal orientation of the principal axes.

Figure 10. Results of bending test on bars cut vertically and horizontally.

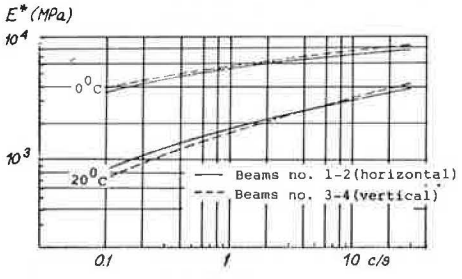

Figure 11. E* versus strain amplitude in outer fibers at different temperatures and frequencies.

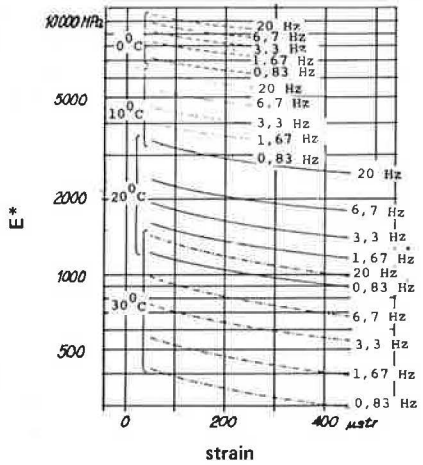

FWD tests carried out during the second test series gave asphalt moduli about 30-40 percent above the values obtained from bending tests. For comparison of calculated and measured response during the second test series, the FWD-determined values were used.

The Poisson's ratio of the asphalt, determined from short-term creep tests on cylindrical specimens mounted with strain gages, was found to be in the region of 0.3-0.35 and to increase with increasing temperature.

CALCULATION OF STRESSES AND STRAINS

Three different methods were used to determine moduli and calculate pavement response and performance. To calculate the response of the pavement, a program developed by Chevron for an n-layer, linear elastic system was used (10). To determine the influence of rigid boundaries, nonlinear stress-strain relations from plate loading tests, and errors of pressure and strain cells, an axisymmetric finite-element program (11) was used (this program is a modified version of a program developed at the University of California). Finally, the method of equivalent thicknesses was used in an attempt to predict the performance as well as the response of the pavement. The method of equivalent thicknesses is much simpler than the other two methods and is therefore very useful when a large number of calculations must be done (12-14).

The basic principle of the method of equivalent thicknesses is to transform a system composed of layers with different moduli into a semi-infinite space for which Boussinesq's equations are valid. The two kinds of transformations used (see Figure 12) are as follows:

1. For calculations of the stresses and strains above the interface or the compression of the upper layer, the system is treated as a semi-infinite space with modulus E_1.
2. For calculation of the stresses, strains, and deflections at or below the interface (including the vertical stress and the horizontal strain at the bottom of the upper layer), the upper layer is transformed to an equivalent layer with modulus E_2 but with the same stiffness as the original layer.

For the stiffness to remain the same, the equivalent thickness of the transformed layer h_e must be

$$h_e = h_1 \times \sqrt[3]{(E_1/E_2) \times (1 - \nu_2^2)/(1 - \nu_1^2)} \quad (4)$$

Because the assumptions are not quite correct, a correction factor is often introduced to obtain the same results as one would obtain with exact elastic theory.

Besides being very simple to use, the method of equivalent thicknesses can be used with nonlinear elastic materials. Finite-element calculations (4) have shown that a nonlinear relation of the type $E = C \times (\sigma_1/\sigma')$ has a negligible influence on the stress distribution. When the stress distribution is known, the modulus can be calculated at any point, and from this the strains and deflections can be found.

Because the plastic characteristics of road-building materials can often be expressed by the above nonlinear relation, even the permanent (or plastic) deformations can be calculated. To do this, the separative method (15) is used—i.e., stress state and equivalent thicknesses are determined from the elastic parameters and from these the permanent deformations are computed by using the plastic stress-strain relations.

DETERMINATION OF SERVICE LIFE

If a structural design is to make sense, the limit(s) between acceptable and unacceptable pavement conditions must be defined. The limit should preferably be based on the functional characteristics of pavements, such as safety, riding comfort, and effects on the environment. One of the most widely used criteria is the present serviceability index (PSI), a riding comfort criterion mainly influenced by the longitudinal roughness (slope variance) of the pavement surface. Roughness, expressed in centimeters per kilometer and measured with a "bump integrator", is a similar criterion, and for a regular sinusoidal pavement surface (without rutting or cracking) the approximate PSI value can be found by using

$$PSI = 3.262 \log [(2 \times 10^5)/\text{roughness}] - 7.25 \quad (5)$$

Rutting does not have much influence on riding comfort, but because of its importance in relation to safety it ought to be included as a separate criterion. When ruts measure 15-25 mm (depending on camber), ponding of water is a risk.

Structural failure is often, but not always, related to functional failure. An indication of structural failure is increasing surface deflection under a given load—an easily measured factor that is often used as a design criterion. However, since overall surface deflection does not tell in which layer the failure is occurring, it is sometimes supplemented by a determination of the radius of curvature of the deflection bowl. An even better localization of failure can be obtained if several points on the deflection bowl are determined and the previously described method of fitting computed to measured surface moduli is used.

Prediction of pavement performance was attempted by using several different methods. Two methods were used to predict cracking of the asphalt layer: the Danish methods developed by Kirk (16, 17, 18) and the Nottingham method (19). Both methods relate fatigue life, in terms of number of load repetitions N, to critical tensile strain in the asphalt layer. Failure caused by excessive deformation in the subgrade was predicted by using five methods, some of which were based partly on the AASHO Road Test and all of which relate service life to either

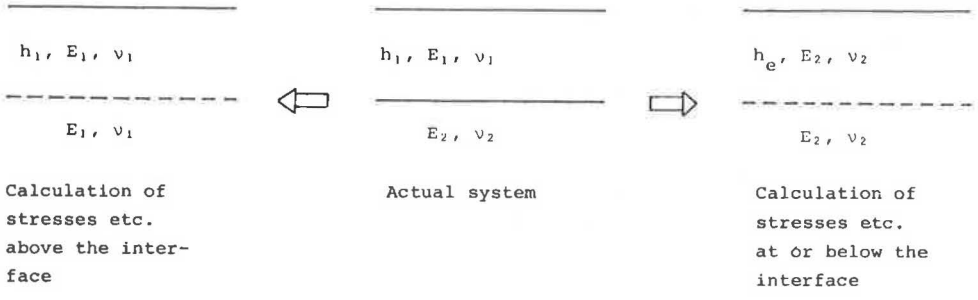

Figure 12. Transformations used with the method of equivalent thicknesses.

critical vertical stress or vertical strain at the top of the subgrade. Rutting was calculated by using the Shell method (20) for the asphalt layer and the previously described nonlinear elastic theory with the plastic stress-strain relation for the subgrade. In the plastic stress-strain relation, two zones were used: A decreasing strain rate was assumed for strains below a critical level and a constant strain rate above that level (see Figure 13). Finally, the PSI value was predicted by using a simulation program developed at the Technical University of Denmark (21).

This program uses a modified random walk to generate important input parameters at points with given spacing (0.3 m). Both materials and structural parameters are generated to given mean values and standard deviations. The increase of permanent deformation with number of load applications is calculated at each point and, from these values, mean rut depth and slope variance are evaluated. A fatigue model is used to estimate crack propagation and, finally, the PSI value is calculated. The program has facilities for using static (constant) or dynamic loading and for varying the climatic conditions with respect to temperature changes during the year and changes in the moduli of unbound layers caused by the spring thaw.

RTM TESTING

Three test series were run on the first pavement in the RTM. The first two series consisted of response and performance tests, and the third was a freeze-thaw test.

In the response test during the first series, stresses, strains, and deflections were measured at temperatures of 0.5°C, 10°C, 20°C, and 30°C; at wheel velocities of 2.5, 5, 10, and 20 km/h; and at wheel loads of 10, 20, 30, and 40 kN. For some of these combinations, the effects of single versus dual wheel load, lateral wheel position, and tire pressure were also examined. The measured quantities were then compared with values calculated by using layered elastic theory.

During the first performance test, loading was done in two tracks 1 m apart by using a 20-kN and a 30-kN load, respectively. The tests were made at a temperature of 30°C and a wheel velocity of 20 km/h. In each track, a lateral wheel-load distribution that approached a normal distribution was used and, for each 30-kN load, five loads of 20 kN were applied to get equal damage in the two tracks if the AASHO load-equivalency factors were applicable. The groundwater level was kept at the bottom of the pit during this first test series but was then raised to 0.3 m below formation level for the second and third series.

In the second series, response tests were repeated at 10, 20, and 30 kN at temperatures of 10°C and 30°C, and measured and calculated values were again compared. This time, the performance test was carried out at a temperature of 25°C at the centerline of the pit, which made it possible to follow changes in critical stresses and strains. Longitudinal roughness was measured in addition to rutting, and the change in PSI values was calculated from the difference between these values and the original surface profiles.

In the third test series, the pavement was frozen to a depth of approximately 0.5 m. This resulted in a frost heave of 40 mm and longitudinal cracking of the asphalt layer. During thawing, a brief performance test of 5000 loads was made. It did not produce any additional cracking of the asphalt or any appreciable increase in permanent deformation.

ANALYSIS OF RESULTS

The objectives of the first tests in the RTM can be summarized as (a) the running in of the machinery, (b) qualitative and quantitative evaluation of pavement response, and (c) prediction of pavement performance.

The main parts of the machinery were brought into line during the first two years, but improvements are still being made, especially in the system for measuring and recording stresses, strains, and deflections.

The qualitative evaluation of pavement response confirmed that the RTM is well suited to simulating heavy traffic loadings. The variations of stresses and strains with variations in, for instance, wheel load, velocity, and tire pressure were the same as those measured in situ under heavy traffic. The performance in the RTM should also be compared with the performance of in situ pavements, but this has not yet been possible.

The quantitative evaluation of pavement response consists of (a) evaluation of the accuracy of the measured values and (b) comparison of measured and calculated values. To measure the critical vertical stress and strain in the top of the subgrade, four pressure cells and four strain cells were installed. The typical coefficient of variation for both measured quantities was about 0.25. Even larger deviations were encountered for lower levels; the two lowest pressure cells typically showed a difference of a factor of four. Most of the variations are likely to be caused by an inappropriate installation procedure, as indicated by the in situ cali-

Figure 13. Permanent strain model.

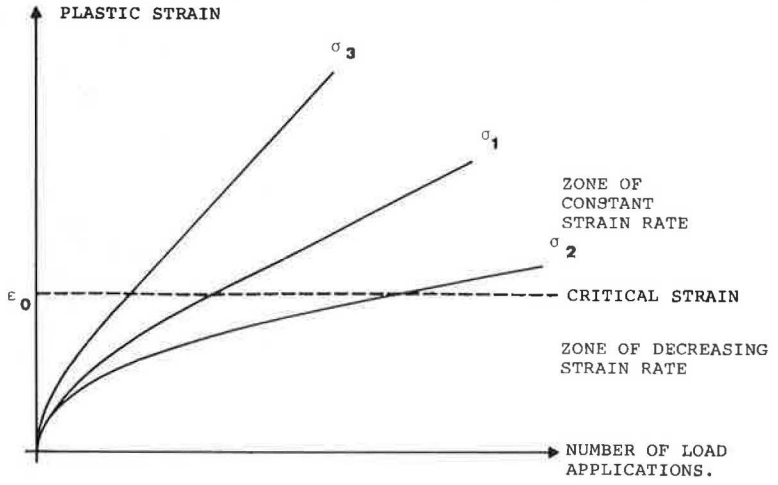

bration of the pressure cells, but part of the variation is definitely the result of varying materials and structural characteristics and thus cannot be avoided. Severe problems were encountered in attempting to measure the horizontal strain at the bottom of the asphalt layer, and this was only achieved in a few of the tests. For this quantity, a coefficient of variation of up to 0.8 was found.

These large variations in the measured values must be kept in mind in comparing measured and calculated quantities. Figure 14 shows the variation with distance from the center of the load of the measured vertical stress and strain at the top of the subgrade. The stress and strain were measured in FWD tests at a peak force of 30 kN and an asphalt temperature of 30°C. Superimposed on the measured values are calculated values found by using the Chevron program and the method of equivalent thicknesses. The agreement between the measured and calculated values is seen to be reasonably good. The variation of the measured vertical strain, however, indicates a horizontal variation of the subgrade modulus, which was not included in any of the theoretical methods.

Four kinds of performance prediction were attempted: (a) cracking of the asphalt layer, (b) excessive deformation of the subgrade, (c) amount of permanent deformation, and (d) PSI.

The two previously mentioned methods of crack prediction were used. For series 1, the prediction was based on calculated critical strains; for series 2, it was based on measured values plus and minus one standard deviation. There was some indication from the measured stresses and strains for test series 2 that crack initiation might have taken place in the asphalt, but no visible cracks were detected nor did FWD tests in any of the test series show any decrease in the asphalt modulus. It can be concluded that either both fatigue criteria are somewhat conservative or the assumption of a standard (weighted) asphalt temperature is too simple a model of the real fatigue performance.

Five different methods were used to test for excessive deformation of the subgrade. The only criterion that did not predict a fair amount of permanent subgrade deformation was that of Witczak (23). The actual permanent deformation of the subgrade was found to be 4 mm of a total pavement deformation of 11 mm.

The AASHO-based criteria were somewhat conservative, perhaps because most of the damage during the AASHO Road Test was caused by longitudinal roughness (85 percent) and the variation in permanent deformation was therefore more important than the average deformation. The first few tests, therefore, supported the criteria suggested by Witczak with respect to average permanent deformation of the subgrade. If, however, a riding comfort criterion is accepted, the variations in permanent deformation may be more relevant than the average deformation. In Figure 15, four of the predictions used are compared with the experimental PSI values. The agreement between observed and predicted life is seen to be better when a limiting value of PSI = 2.5 is used, but the scatter in the predicted values is considerable.

The amount of rutting during the first test series was calculated as previously described. For the asphalt, the following relation between mixture stiffness E and bitumen stiffness S_{bit} (both in megapascals) was used:

$$E = 63 \times S_{bit}^{0.31} \quad (6)$$

This relation was obtained from three-point bending tests that were carried out at high temperature and low frequencies before the first test series. Two calculations were done, one using a softening point (ring and ball) of 57°C and a penetration index (PI) of 0 found in August 1973 before the first test series and another with a softening point of 65.5°C and a PI of 0.5 found in May 1976 after completion of the first test series. In Figure 16, the calculated rut depths are compared with the measured values. The agreement appears to be reasonably good. Part of the discrepancy in predicting the rutting caused by the 20- and 30-kN wheel loads results from the fact that the real load distributions are not circular as assumed in the calculations.

Finally, an attempt was made to predict the PSI value through a computer simulation of pavement performance. Parts of the input, such as the standard deviations of the materials and the structural characteristics, were not known and had to be estimated.

Ten computations were done. The range of calculated values is shown in Figure 17 superimposed on the experimental results. The predicted life is seen to be rather longer than the observed life. Cracking of the asphalt layer was not predicted in any of the simulations. A few additional simulations were carried out for yearly temperature variations between +20°C and -2°C and a spring thaw reduction of the subgrade modulus of 70 and 90 percent. In neither case was any cracking produced, nor did the PSI value decline to 2.5 within the first million axle passages (30-kN wheel load) applied during the first four years. This, at least, does not contradict the results of the freeze-thaw test.

Figure 14. Measured and calculated stress and strain values.

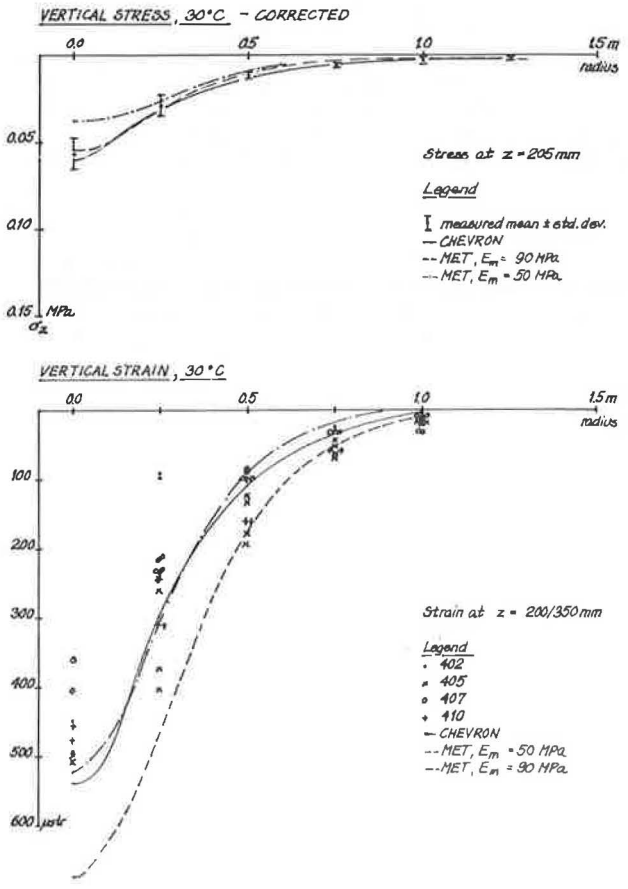

Figure 15. Subgrade criteria versus PSI values.

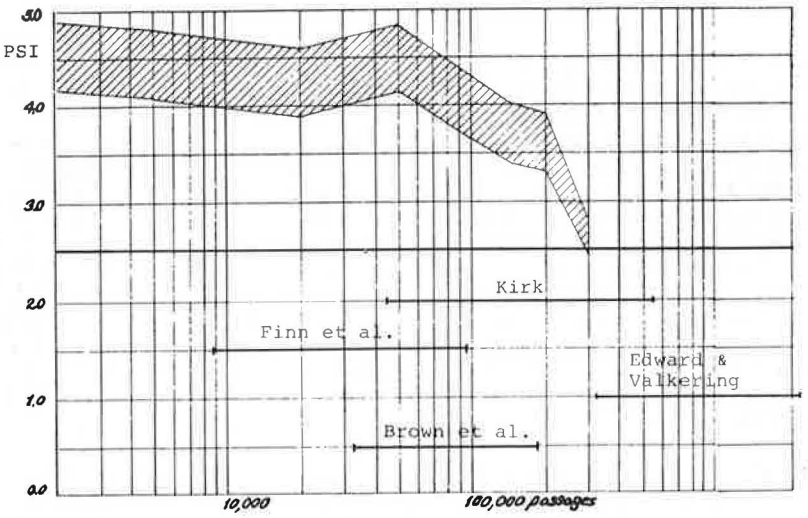

Figure 16. Computed rutting versus measured rutting.

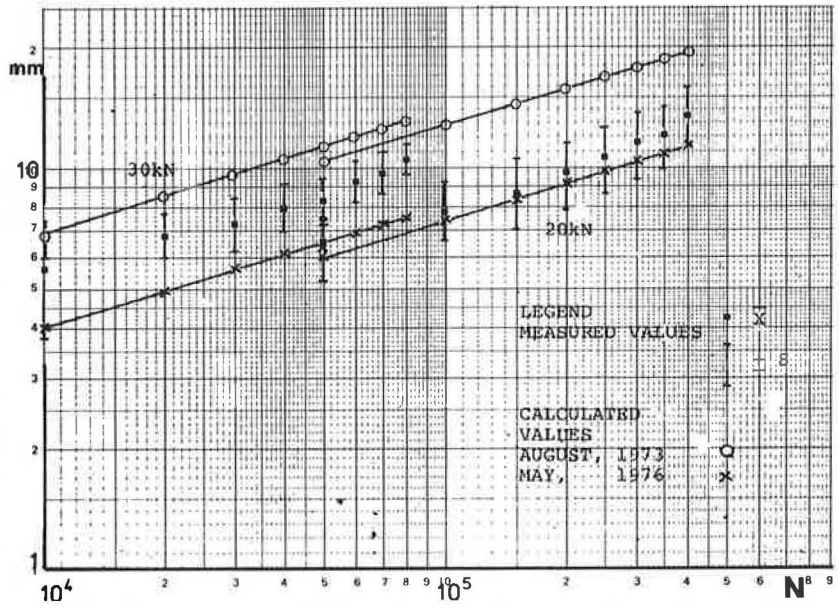

Figure 17. Computed PSI values versus measured PSI values.

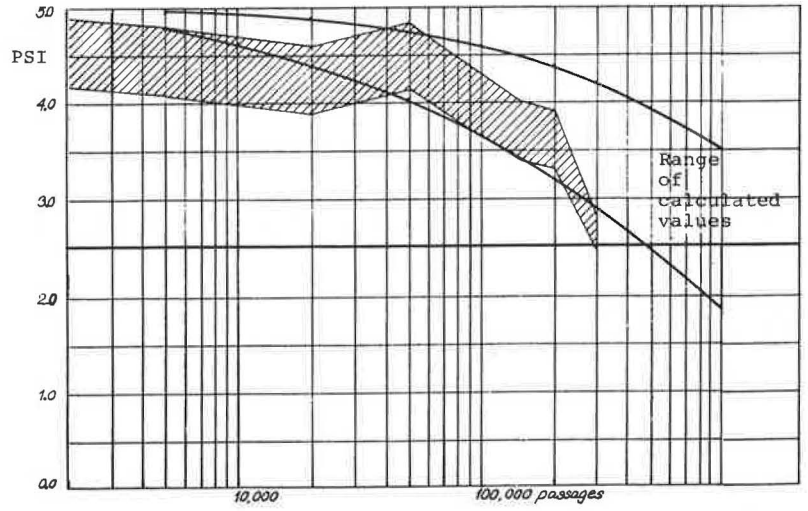

CONCLUSIONS

The main conclusion of the first few test series is that the RTM appears to be well suited to simulating the effects of heavy traffic loadings and climatic variations on full-scale pavement structures. As a result, a five-year research program jointly sponsored by the National Danish Road Laboratory and the Technical University of Denmark has been initiated. In this research program, nonconventional pavement structures and materials will be tested under varying climatic conditions simultaneously with more traditional structures. It is hoped that these tests will also contribute to the development of a predictive design procedure that will be superior to the deterministic procedures currently being used.

REFERENCES

1. P. Simonsen and A. Sørensen. Et Fuldskalaforsøg på en Asfaltvej i Laboratoriet. Tech. Univ. of Denmark, Lyngby, Ph.D. dissertation, Rept. 1, 1976.
2. A. O. Bohn, P. Ullidtz, R. Stubstad, and A. Sørensen. Danish Experiments with the French Falling Weight Deflectometer. 3rd International Conference on the Structural Design of Asphalt Pavements, London, 1972.
3. J. Boussinesq. Application des Potentiels à l'Étude de l'Équilibre et du Mouvement des Solides Élastiques. 1885.
4. P. Ullidtz. Some Simple Methods of Determining the Critical Strains in Road Structures. Tech. Univ. of Denmark, Lyngby, Ph.D. dissertation, 1976.
5. P. Ullidtz. Overlay and Stage by Stage Design. 4th International Conference on the Structural Design of Asphalt Pavements, Ann Arbor, MI, 1977.
6. C. Busch-Petersen. The Stress Dependent Moduli of Unbound Materials. Tech. Univ. of Denmark, Lyngby, Ph.D. dissertation, Rept. 10 (in preparation).
7. K. O. Møgelvang and S. H. Jensen. Silts Egenskaber. Tech. Univ. of Denmark, Lyngby, M.Sc. dissertation, 1974.
8. A. O. Bohn, R. N. Stubstad, A. Sørensen, and P. Simonsen. Rheological Properties of Road Materials and Their Effect on the Behavior of a Pavement Section Tested in a Climate Controlled, Linear Track Road Testing Machine. AAPT, Minneapolis, 1977.
9. The AASHO Road Test: Report 5—Pavement Research. HRB, Special Rept. 61 E, 1962.
10. H. Warren and W. L. Dieckmann. Numerical Computation of Stresses and Strains in Multiple Layered Asphalt Pavement System. Chevron Research Co., San Francisco, 1963.
11. J. M. Duncan, C. L. Monismith, and E. L. Wilson. Finite Element Analysis of Pavements. HRB, Highway Research Record 228, 1968, pp. 18-33.
12. N. Odemark. Undersökning av Elasticitetsegenskaperna hos Olika Jordarter Samt Teori för Beräkning av Belägningar Enligt Elasticitetsteorien. Statens Väginstitut, Meddelande 77, 1949.
13. J. M. Kirk. Vurdering af Befæstelsers Bæreevne. Dansk Vejtidsskrift, Vol. 38, No. 5, 1961.
14. P. Ullidtz. En Studie af to Dybdeasfaltbefæstelser. Tech. Univ. of Denmark, Lyngby, Ph.D. dissertation, 1973.
15. E. N. Thrower. Methods of Predicting Deformations in Road Pavements. 4th International Conference on the Structural Design of Asphalt Pavements, Ann Arbor, MI, 1977.
16. J. M. Kirk. Relations Between Mix Design and Fatigue Properties of Asphaltic Concrete. 3rd International Conference on the Structural Design of Asphalt Pavements, London, 1972.
17. J. M. Kirk. Revideret Metode til Dimensionering af Bituminøse Befæstelser. Asfalt, No. 42, 1973.
18. A. Skjoldby. Styrkeparametre i Statens Vejlaboratoriums Dimensionering af Bituminøse Belægninger. Dansk Vejtidsskrift, No. 5, 1976.
19. S. F. Brown, P. S. Pell, and A. F. Stock. The Application of Simplified, Fundamental Design Procedures for Flexible Pavements. 4th International Conference on the Structural Design of Asphalt Pavements, Ann Arbor, MI, 1977.
20. J. F. Hills, D. Brien, and P. J. van de Loo. The Correlation of Rutting and Creep Tests on Asphalt Mixes. Journal of the Institute of Petroleum, Paper IP 74-001, Jan. 1974.
21. P. Ullidtz. Computer Simulation of Pavement Performance. Tech. Univ. of Denmark, Lyngby, Rept. 18, 1978.
22. F. N. Finn, K. Nair, and C. L. Monismith. Applications of Theory in the Design of Asphalt Pavement. 3rd International Conference on the Structural Design of Asphalt Pavements, London, 1972.
23. M. W. Witczak. Design of Full-Depth Asphalt Airfield Pavements. 3rd International Conference on the Structural Design of Asphalt Pavements, London, 1972.
24. J. M. Edwards and C. P. Valkering. Structural Design of Asphalt Pavements for Road Vehicles: The Influence of High Temperature. Shell, 1974.

Publication of this paper sponsored by Committee on Strength and Deformation Characteristics of Pavement Sections.

Utility Decision Model for Pavement Recycling

Telimoye M. Oguara, College of Science and Technology, Port Harcourt, Nigeria
Ronald L. Terrel, Department of Civil Engineering, University of Washington, Seattle

A decision model developed by using utility theory to evaluate various techniques for recycling of pavement materials is described. The model is quantified by using subjective opinions of experienced engineers who are familiar with pavement rehabilitation. Limited objective field data

are also required. The analysis involves identification of various recycling techniques and decision criteria and development of utility data. The optimum recycling technique is determined based on the maximum expected utility associated with the technique. The decision model provides a systematic and rational means for evaluating all of the various criteria that should be considered in a decision on pavement recycling.

In the existing institutional framework, transportation officials make decisions on the recycling technique to be used in a given scheme of pavement rehabilitation. In almost all of the recycling projects that have been undertaken, cost and the availability of equipment have been the main factors in the choice of a recycling technique. Although these factors are extremely important, other factors or criteria also have an important influence on the decision to recycle. For instance, in recent years, highway engineers have become aware of energy and environmental considerations in their decisions. They would rather not consider techniques that use excessive energy or pollute the environment.

The decision to recycle pavement should therefore be based on a thorough analysis of possible recycling techniques by considering all of the various decision criteria and selecting the technique that would yield the greatest satisfaction to the decision maker. One way to achieve this is by using utility theory in the decision process.

Utility is a measure of individual preferences that can range from zero to one. The utility of any object or activity is the degree to which it or its consequences are perceived by the individual as satisfying his or her preferences in a given situation. The utility value need not be the same for two or more individuals or for a particular individual at all times or in all situations. Utility theory has been used successfully in the analysis of a variety of engineering problems. Examples include the study of the development of the Mexico City airport (1) and the determination of the optimum configuration for the supersonic transport (2).

Figure 1. Utility decision process in pavement recycling.

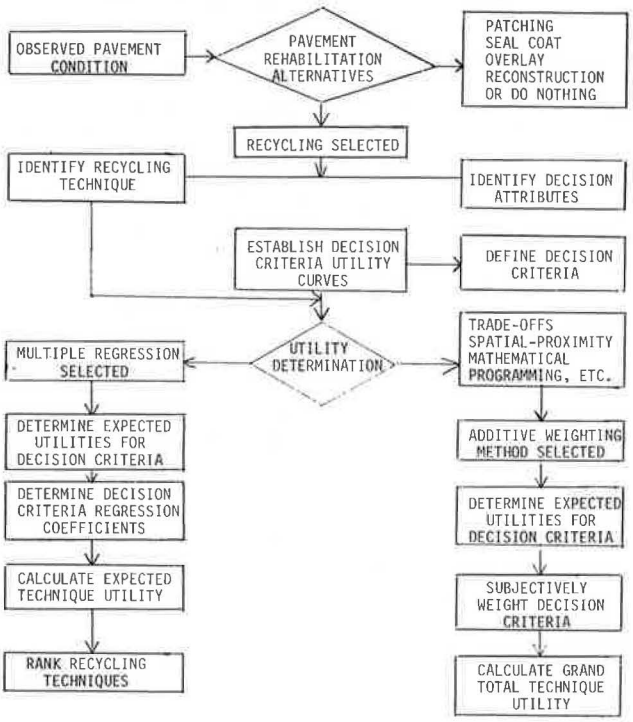

The utility approach can be used whenever a systematic analysis of possible alternatives requires the consideration of various decision criteria in the choice of an alternative. Such criteria include human values or preferences, uncertainty, and other judgmental elements as well as objective operational and technological considerations. Once recycling is selected as the pavement rehabilitation alternative, several possible recycling techniques are available. Utility theory can be applied to provide the information needed in making a rational decision on the choice of a recycling technique. The best technique for a particular scheme of pavement rehabilitation can be chosen on the basis of the relative power (or utility) of that technique to satisfy the decision maker.

This paper describes a decision model that uses utility theory to evaluate various techniques for pavement recycling and is based on material presented in detail elsewhere (3). A schematic diagram of the model is shown in Figure 1. The following basic components of the decision model are discussed:

1. Structuring the decision problem, which includes identification of the decision maker, definition of the decision problem, generation of recycling alternatives, and establishment of decision attributes and criteria;
2. Utility analysis, which includes establishment of utility functions and determination of decision-criteria utilities and technique utilities; and
3. Implementation of the decision model, which includes a discussion of the Use Estimates 1 (USEE1) computer program, data generation, and evaluation results.

STRUCTURING THE DECISION PROBLEM

The decision to use a particular recycling technique in a scheme of pavement rehabilitation is generally made by one or more state, federal, or local transportation officials. These officials can be identified here as the decision makers or simply the decision maker. The problem can be stated as follows: For a defined pavement condition and in view of various decision criteria or factors, what recycling technique(s) would yield the greatest satisfaction to the decision maker? The decision maker's first task in structuring the decision problem is to identify the various recycling techniques available.

Recycling Techniques

From a wide variety of recycling approaches, the Federal Highway Administration Demonstration Project 39 Technical Advisory Committee has identified three main categories of recycling (4):

1. Surface recycling involves reworking of the pavement surface to a depth of less than 25 mm (1 in) by heater-planer, heater-scarifier, and surface milling devices. This operation is a continuous single-pass, multistep process that may involve the use of new materials, including aggregate, modifiers, and/or mixtures. Several recycling techniques can be identified in this category based on the device used and whether or not additional aggregate and thin or thick overlay is used in the process.
2. In-place surface and base recycling involves in-place pulverization to a depth greater than about 25 mm (1 in) followed by reshaping and compaction. This operation can be performed with or without the addition of new binder or stabilizer. In-place recycling techniques can be identified based on (a) whether in the asphalt-concrete thickness of the existing pavement is less than 50 mm

(2 in) (thin asphalt concrete) or more (thick asphalt concrete) and (b) whether the in-place technique used is an equivalent method for minor or major structural improvement.

3. Central plant recycling involves the scarification of the pavement, removal of the pavement material from the roadway before or after pulverization, processing of material with or without the addition of a stabilizer or modifier, followed by laydown and compaction to the desired grade. Depending on the type of material recycled and the stabilizer used, this operation may involve the addition of heat (hot process) or no heat (cold process). Several techniques can be identified in this category based on whether heating is used and whether the technique is an equivalent method for a minor or major structural improvement.

Decision Attributes and Decision Criteria

In the decision to recycle a pavement in a particular condition, the broad objective is to be able to select the best technique or techniques that can provide optimum satisfaction to the decision maker. More specifically, the recycling technique that will be selected is the one that best meets a set of multiple objectives, such as

1. Minimize cost,
2. Maximize expected performance,
3. Minimize energy use,
4. Minimize environmental pollution and noise, and
5. Maximize safety.

This set of objectives can be considered the attributes of the recycling decision. But, because these attributes may be too general to be of practical use, subobjectives can be developed and associated with each attribute as a measure of effectiveness. These subobjectives can be considered the decision criteria. Their measurement can be quantitative or qualitative depending on the convenience or cost of measurement to the decision maker. A possible set of attributes, decision criteria, and measures of effectiveness for a pavement-recycling decision is given below (because the data used in the model developed in this study are in U.S. customary units, no SI equivalents are given):

Attribute	Decision Criterion	Measure of Effectiveness
Cost	Recycling cost	Dollars per square yard-inch
	Future maintenance cost	Dollars per lane mile per year
	Ride quality	Present serviceability index (PSI)
Expected performance	Expected distress	Distress deduct points
	Pavement life	Years
	Expected traffic	Relative traffic value
Energy	User energy savings	Btu per year
	Process energy	Btu per square yard-inch
Environment	Pollution	Qualitative rating
	Noise	Qualitative rating
Safety	Safety during recycling	Qualitative rating
	Safety performance	Qualitative rating

The qualitative rating scale for environmental and safety-related decision criteria is as follows: 1 = excellent, 2 = good, 3 = fair, 4 = poor, 5 = very poor, and 6 = unacceptable. Whereas the decision criteria specified under cost, expected performance, and energy attributes are measured quantitatively, those under environmental and safety attributes are rated qualitatively. Although this list of attributes and decision criteria is not intended to be complete, it illustrates the concept. Other possible attributes or decision criteria considered significant enough to influence the choice of a technique for pavement recycling can be identified by the decision maker.

UTILITY ANALYSIS

The decision-making process requires that value judgment be effectively exercised at the level of the individual decision criterion to provide an explicit quantitative relation between the magnitude of the decision criterion and the relative preference or utility derived by the decision maker. Such a relation, termed the utility function, can be used to determine the expected utility of each alternative.

Characteristics of Utility Functions

Utility functions possess some qualitative characteristics, and each characteristic implies a certain attitude of the decision maker with regard to his or her preference for consequences and lotteries. One of the characteristics of utility functions is monotonicity (5). This concept can be explained in terms of lotteries as follows: A standard reference lottery is preferred to a second standard lottery if and only if the first lottery's probability of receiving the most preferred prize is greater than that of the second (6). To illustrate this in a pavement context, a decision maker may assess performance in terms of ride quality x of the pavement. If $x_1 > x_2$, then the utility $u(x_1) > u(x_2)$. In this case, the utility function is said to be monotonically increasing.

If we now consider process energy as a decision criterion, use of more process energy does not yield a preferable prize in comparison with use of less process energy. So, if the process energy $x_1 > x_2$, then the utility $u(x_2) > u(x_1)$. In this case, the utility function is said to be monotonically decreasing. There are also situations in which the utility function is not monotonic.

Another characteristic of utility functions is risk aversion. This can be described by the various basic attitudes of decision makers toward risk. Consider a decision maker facing a lottery that yields a consequence x', or a less preferable consequence x'' with equal probability. The expected consequence $\bar{x}$ of this lottery is $\bar{x} = 0.5\,(x' + x'')$. Suppose the decision maker is asked to state a preference between receiving $\bar{x}$ for certain or the lottery. If the certain consequence $\bar{x}$ is preferred, the decision maker is actually saying that he or she prefers to avoid the risk associated with the lottery. A decision maker who has this type of attitude toward lotteries is "risk averse". From a mathematical derivation, it can be shown that a decision maker is averse to risk if and only if his or her utility function is concave in shape (5).

On the other hand, a decision maker who prefers any lottery to the expected consequence $\bar{x}$ is more than willing to accept the risks associated with the lottery and is said to be "risk prone". The utility function of a risk-prone decision maker is convex in shape.

Between the risk-averse and risk-prone cases is the "risk-neutral" case, in which the utility of the expected consequence equals the utility of the lottery and the utility function is linear.

In the determination of utility functions, a decision maker's utility function should not always be described as risk averse or risk prone for the entire length of the curve. In most decision situations, it is found that, up to a certain point in the utility function, the decision

maker's preference is risk prone or risk averse and beyond that is risk averse or risk prone. So, instead of wholly convex or concave functions, we have functions that are part convex and part concave. This S-shaped function, which has a point of inflection where the preferences turn from prone to averse or averse to prone, can be used for determining utility functions in pavement recycling.

Assessment of Utility Functions for Decision Criteria

The assessment of utility functions can be considered as much an art as a science. Therefore, there are no set rules that invariably result in a utility function. In general, the assessment of utility functions requires conducting repeated interviews with carefully phrased questions that reveal, by determining levels of indifference, the actual shape of the functions. The approach suggested here involves several steps, including the following:

1. Determine whether or not the utility function for a decision criterion is monotonic. This might be done by asking questions such as, If an amount of the decision criterion x_k is greater than x_j, is x_k always preferable to x_j? If the answer to such a question is yes, it implies that the utility function for this decision criterion is monotonically increasing; if no, then the utility function should be monotonically decreasing.
2. Determine boundary limits for the utility function. Since utility is a measure of the relative preference of the decision maker on a scale from zero to one, the lower bound and upper bound can be set at a utility of zero and one, respectively. The values of zero and one can be assigned to the least desirable and most desirable magnitudes of the decision criterion.
3. Determine the expected consequence or magnitude of the decision criterion x for which the decision maker would feel like assigning a mean utility value $\bar{u}(x) = 0.5$.
4. Determine the expected consequence of the decision criterion for which the decision maker would assign a utility of 0.66 or 0.34 [$\bar{u}(x) \pm 0.16$].
5. Determine which portion of the utility function is risk averse, risk neutral, or risk prone. This can be done by asking questions that reveal values of the decision criterion that would make the decision maker indifferent as to his or her satisfaction with using pavement recycling as a rehabilitation alternative. This helps fix inflection points on the utility function. Then the decision maker's preference can be tested before and beyond this value of decision criterion to determine his or her willingness to take risk.

In this approach, a five-point assessment procedure at utility values of 0, 0.34, 0.5, 0.66, and 1.0 can be made for the quantitatively measured decision criteria, and a three-point assessment at utility values of 0, 0.66 or 0.5, and 1.0 would suffice for the qualitatively rated decision criteria.

Determination of Decision-Criterion Utility

The utility functions determined from the foregoing discussion can be used to determine the utility of any decision criterion once a particular value of the criterion is known. But, in predicting the magnitude of each decision criterion, no one can predict with certainty the outcome at the time the decision is to be made. The uncertainty associated with estimates of outcomes is relatively rarely described in an explicit way; it is even more rarely included explicitly and quantitatively in the evaluation of outcomes. The riskiness associated with an alternative is usually handled subjectively or implicitly. However it is handled, uncertainty is present in recycling decisions.

The uncertainty concerning the estimates of a decision criterion (recycling cost, ride quality, pollution, etc.) can be explicitly and quantitatively represented by a probability density function. This representation ensures more confidence in the decisions made under uncertainty since the decision variables are described as a distribution of values instead of being treated as single values.

One of the most versatile probability density functions (pdfs) is the beta pdf, given by

$$f(x) = \Gamma(a + b)\, x^{a-1}\, (1 - x)^{b-1} / [\Gamma(a) \cdot \Gamma(b)] \qquad (1)$$

for $0 < x < 1$, $a > 0$, $b > 0$, and where $\Gamma(a)$ and $\Gamma(b)$ are gamma functions of a and b, which are distribution constants.

The beta pdf is a useful tool whenever a variable x is bounded at both upper and lower ends. Another advantage is the wide variety of shapes that can be obtained by varying a and b. The beta pdf is very convenient for determining the means and standard deviations of decision-criteria estimates. For optimistic or low (o), most probable (m), and pessimistic or high (p) estimates of the decision variable, the mean μ is given by

$$\mu = (0 + 4m + p)/6 \qquad (2)$$

and the standard deviation $\sigma = (p - o)/6$. The distribution parameters a and b are then given as

$$a = \mu\{[\mu(1 - \mu)/\sigma^2] - 1\} \qquad (3)$$

and

$$b = \{[\mu(1 - \mu)/\sigma^2] - 1\}\, (1 - \mu) \qquad (4)$$

These values of a and b are used to calculate the distribution function f(x) for any value of the decision criterion x.

The expected value of the decision-criterion utility is given by

$$U(x) = \int_{x\,min}^{x\,max} f(x)\, u(x)\, dx = \bar{u} \qquad (5)$$

and variance $\sigma(x)^2$ is given by

$$\sigma(x)^2 = \int_{x\,min}^{x\,max} f(x)\, u^2(x)\, dx - \bar{u}^2 \qquad (6)$$

where u(x) = utility function.

The decision-criteria utilities obtained are used in determining the recycling-technique utilities.

Determination of Recycling-Technique Utility

A variety of methods are available for determining utilities, including weighting, sequential elimination, mathematical programming, and spatial proximity methods. Each type has its own merits, but weighting methods have received the most attention and been most widely applied in the determination of utility. Of the various weighting methods available, simple additive weighting and linear regression have been chosen in this paper to

weight the individual decision-criteria utilities in the process of determining the recycling-technique utility.

Additive Weighting

In additive weighting, the individual utilities for each decision criterion must be weighted and added together to give an overall utility for the recycling technique. This can be found from the relation

$$E(u)_i = \sum_{i=1}^{n} W_i\, U_i(x) \tag{7}$$

where

$E(u)_i$ = overall or grand total value of utility for the technique i,
$U_i(x)$ = expected value of utility of the ith decision criterion, and
W_i = normalized weight of the ith decision criterion.

The weights of the decision criteria are normalized so that their sum is one; i.e.,

$$\sum_{i=1}^{n} W_i = 1 \tag{8}$$

The overall variance of the technique $\sigma^2(u)$ is given by

$$\sigma^2(u) = \sum_{i=1}^{n} W_i\, \sigma_i^2(x) \tag{9}$$

where $\sigma_i^2(x)$ is the variance of the utility of the ith decision criterion.

The additive weighting model assumes that even though there might be situations in which interaction among the various criteria is possible, the expected decision-criteria utilities are independent of each other.

Multiple Linear Regression

The general linear regression model is given by

$$y_i = a_0 + a_1\, x_{i1} + a_2\, x_{i2} + a_n\, x_{in} \tag{10}$$

where

y_i = value of response (dependent) variable in the ith trial,
$a_0, a_1, a_2, \ldots, a_n$ = regression coefficients, and
$x_{i1}, x_{i2}, \ldots, x_{in}$ = known independent variables.

In some situations, the variables can be transformed, yet the model can be treated as a general linear regression model. One version of a transformed model is

$$\ln y_i = a_0 + a_1 \ln x_{i1} + a_2 \ln x_{i2} + \ldots a_n \ln x_{in} \tag{11}$$

This model is equivalent to

$$y_i = e^{a0}\, x_{i1}^{a1}\, x_{i2}^{a2} \ldots x_{in}^{an} \tag{12}$$

This transformed model can be called a log multiple regression model.

By using the decision-criteria utility values as independent variables, this regression model can be used to determine technique utilities from the relation

$$E(u)_i = e^{a0}\, U_{i1}^{a1}\, U_{i2}^{a2} \ldots U_{in}^{an} \tag{13}$$

where $E(u)_i$ = expected utility for recycling technique i and U_{ij} = expected utility for the jth decision criterion for technique i.

The regression model assumes that, even though utility independence is a necessary condition in utility decisions, there can be some interaction among the various decision-criteria values. It therefore provides a means of transforming the decision-criteria utilities in order to use the concepts of utility independence.

IMPLEMENTATION OF DECISION MODEL

USEE1

The USEE1 computer program (3) uses the utility concepts discussed above to evaluate various recycling techniques for any defined pavement condition. Several decision criteria can be considered; for each criterion, the program input requires optimistic (low), most likely, and pessimistic (high) estimates, utility function data, weighting factors, and regression constants. The program fits a utility curve to the utility function data for each decision criterion and also fits a beta distribution curve to the three estimates. It then multiplies the two curves and integrates to come up with the expected decision-criteria utility U(x). It uses the weighting factors w_i to weight and sum the expected decision-criteria utilities to come up with a grand total technique utility E(u). The program also uses the regression constants ai with the expected decision-criteria utilities, assuming a log model to come up with expected technique utility E(u).

Data Generation

Since there are not many performance data available on pavement recycling, to implement the decision model, data generation in this study was geared toward subjective data and only limited objective field data. In this process, the subjective opinions of engineers who are familiar with pavement recycling were incorporated with objective data in the decision process. Assessment of utility thus implied that some procedure for extracting subjective data from individuals was necessary.

The procedure used in this study involved setting up a decision panel and getting the responses of individual decision makers to various questionnaires. The decision panel then met and, after they discussed their individual responses, a consensus value was taken for the decision analysis.

By this process, the utility data summary given in Table 1 was obtained. Questionnaires were also developed so as to obtain some useful information about the values of the decision criteria, the decision makers' implied preferences for the various recycling techniques under certain pavement conditions, and weighting factors for the decision criteria. Regression coefficients for the decision criteria were obtained by using a SELECT regression computer program (7).

Results of Evaluation

The USEE1 program was used to evaluate 24 recycling techniques for a pavement with moderate alligator cracking. The program output included utility functions for each decision criterion from the data given in Table 1, beta distribution plots for decision-criteria estimates, a weighting table, and a final output table.

Figures 2 and 3 show utility curves for the decision criteria of recycling cost and expected life. Figures 4 and 5 show distribution plots of decision-criteria estimates for recycling cost and expected life. The final

Table 1. Summary of decision criteria, utilities, and characteristics.

Attribute	Decision Criterion	Utilities	Values	Utility Characteristic[a]
Cost	Recycling cost ($/yd^2-in)	1.0, 0.66, 0.50, 0.34, 0.0	0.10, 0.30, 0.60, 1.2, 2.0	Monotonically decreasing
	Maintenance cost [$/(lane mile/year)]	1.0, 0.66, 0.50, 0.34, 0.0	100, 250, 400, 1000, 3000	Monotonically decreasing
Expected performance	Ride quality (PSI)	0.0, 0.34, 0.50, 0.66, 1.0	1.2, 2.5, 3.5, 4.0, 4.8	Monotonically increasing
	Distress deduct points	1.0, 0.66, 0.50, 0.34, 0.0	0, 10, 20, 50, 100	Monotonically decreasing
	Life (years)	0, 0.34, 0.50, 0.66, 1.0	0, 3, 5, 7, 15	Monotonically increasing
	Relative traffic value	0, 0.34, 0.50, 0.66, 1.0	0.5, 0.70, 0.8, 1.0, 1.5	Monotonically increasing
Energy	User energy savings (Btu/year)	0, 0.50, 1.0	10^5, 10^9, 10^{11}	Monotonically increasing
	Process energy (Btu/yd^2-in)	1.0, 0.66, 0.50, 0.34, 0.0	200, 2000, 20 000, 25 000, 50 000	Monotonically decreasing
Environment	Pollution rating	1.0, 0.66, 0.0	1, 2, 6	Monotonically decreasing
	Noise rating	1.0, 0.66, 0.0	1, 2, 6	Monotonically decreasing
Safety	Safety during recycling rating	1.0, 0.66, 0.0	1, 2, 6	Monotonically decreasing
	Safety performance rating	1.0, 0.50, 0.0	1, 3, 6	Monotonically decreasing

[a]All S-shaped.

Figure 2. Results of recycling technique 24: recycling cost versus utility values.

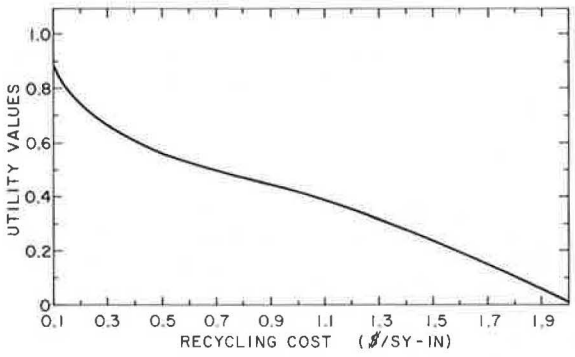

Figure 3. Results of recycling technique 24: expected life versus utility values.

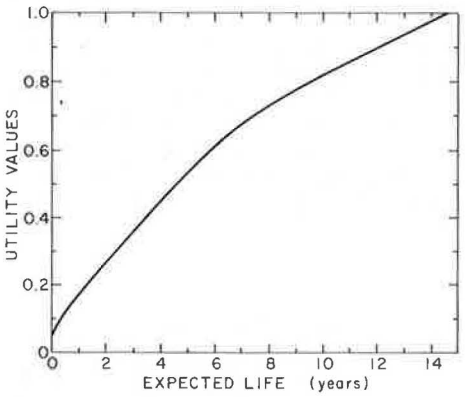

Figure 4. Results of recycling technique 24: recycling cost versus distribution frequency.

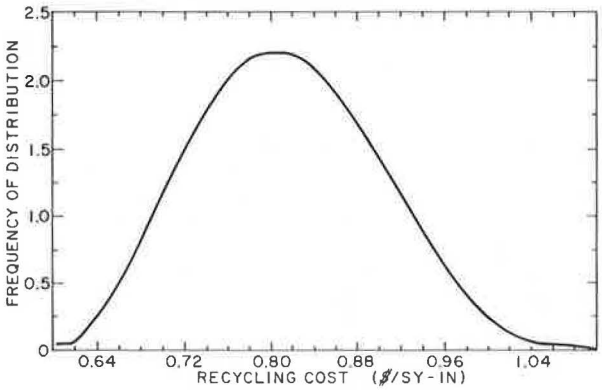

Figure 5. Results of recycling technique 24: expected life versus distribution frequency.

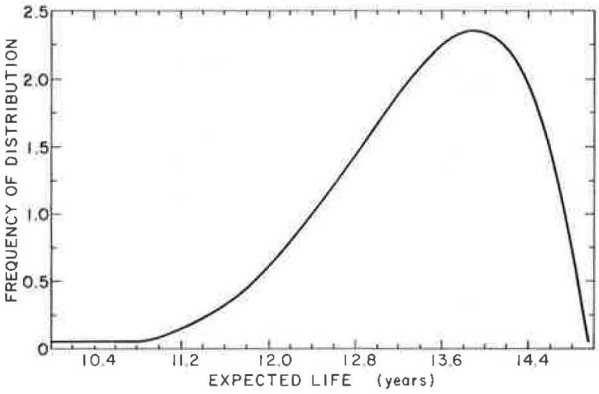

output table consists of displays of the three estimates, calculated means, standard deviations, expected decision-criteria utilities, variances, and weighted utilities and variances. At the bottom of the table is given grand total utility and variance for the additive weighting approach. Table 2 gives the final output for technique 24. The expected technique utility for the multiple regression approach is 0.928. Table 3 gives a summary of the utilities and rankings obtained from the analysis of the 24 recycling techniques by the decision panel set up for the model implementation.

The results indicated that, for these decision makers,

1. The possible range of technique utilities was smaller for the additive weighting model (0.429-0.716) than for the multiple regression model (0.095-0.928).
2. Techniques with low utilities in both models had considerably higher values in the additive weighting model than in the multiple regression model. On the other hand, utility values for the best techniques were considerably higher in the multiple regression approach than in the additive weighting approach.
3. Ranking of the techniques, although not exactly the same for both models, tended to result in good correlation for the two models. The techniques with low utilities were ranked low and those with high utilities were ranked high for both models.
4. Either model or both models can be satisfactorily used to select an optimum recycling technique for a pavement rehabilitation scheme.

Sensitivity analysis of the decision model also showed that

1. The utility values obtained for the recycling tech-

Table 2. Final output for recycling technique 24.

Decision Criterion	Estimate			Mean	Standard Deviation	Expected Decision Criterion Utility	Variance	Weighted Utility	Weighted Variance
	Low	Most Probable	High						
Recycling cost	0.60	0.80	1.10	0.82	0.08	0.458	0.000 45	0.068	0.000 01
Maintenance cost	100.00	150.00	200.00	150.00	16.67	0.818	0.001 27	0.073	0.000 01
Ride quality	4.00	4.50	4.80	4.47	0.13	0.852	0.003 31	0.101	0.000 05
Distress	1.00	3.00	5.00	3.00	0.67	0.827	0.000 48	0.061	0.000 00
Expected life	10.00	14.00	15.00	13.50	0.83	0.945	0.000 99	0.126	0.000 02
Traffic	1.10	1.30	1.50	1.30	0.07	0.868	0.002 00	0.051	0.000 01
User energy savings	5[9]	5[10]	1[11]	5.083[10]	1.583[10]	0.897	0.002 13	0.020	0.000 00
Process energy	20 000.00	23 000.00	25 000.00	22 833.00	833.33	0.390	0.000 47	0.012	0.000 00
Pollution	2.00	3.00	4.00	3.00	0.33	0.461	0.003 70	0.041	0.000 03
Noise	2.00	3.00	4.00	3.00	0.33	0.461	0.003 70	0.014	0.000 00
Safety during recycling	2.00	3.00	4.00	3.00	0.33	0.461	0.003 70	0.041	0.000 03
Safety performance	1.00	2.00	3.00	2.00	0.33	0.707	0.005 76	0.084	0.000 08
Weighted total								0.691	0.000 24
Grand total								0.691	0.000 24

Note: Data for central plant, hot process, major structural improvement with new binder, moderate alligator cracking.

Table 3. Summary of utilities and rankings obtained for 24 recycling techniques.

Technique	Additive Weighting Model		Multiple Regression Model	
	Utility	Ranking	Utility	Ranking
1	0.429	24	0.095	23
2	0.446	23	0.134	22
3	0.472	21	0.198	21
4	0.508	20	0.325	20
5	0.679	9	0.680	11
6	0.460	22	0.094	24
7	0.510	19	0.352	19
8	0.677	10	0.725	9
9	0.540	18	0.435	18
10	0.622	11	0.595	13
11	0.693	5	0.739	8
12	0.716	1	0.753	7
13	0.555	17	0.497	16
14	0.621	12	0.564	14
15	0.694	4	0.780	5
16	0.713	2	0.762	6
17	0.561	16	0.489	17
18	0.615	13	0.541	15
19	0.687	7	0.861	4
20	0.707	3	0.896	2
21	0.599	15	0.695	10
22	0.607	14	0.659	12
23	0.686	8	0.893	3
24	0.691	6	0.928	1

niques could change slightly but not significantly with an increase or decrease in one of the decision variables and this change could be higher for the additive weighting model than for the multiple regression model.

2. There can be considerable variation in the expected decision-criteria utilities because of changes in the values of the decision criteria. These changes could be more significant in the utilities of the qualitatively rated decision criteria than the quantitatively measured decision criteria.

3. Changes in the weighting factors or regression constants can result in differences in the utility values. However, this was found not to significantly affect the rankings of the recycling techniques in this study.

4. Because the uncertainties associated with the expected utility values can be small, this model could be used to compare recycling techniques without taking variances into consideration.

5. The expected performance of the pavement was considered to be the most sensitive attribute and ride quality the most important decision criterion in the decision panel's selection of an optimum technique. Cost was also important. Energy considerations were the least important. These results, however, are not absolute since they reflect only the preferences of the decision panel used.

CONCLUSIONS

This paper has demonstrated the applicability of utility theory to the decision-making process in selecting optimum recycling strategies for pavements. The model requires the identification of the various possible recycling techniques and the significant decision criteria that can affect the decision maker's choice of a technique. For each of these criteria, the decision process requires the determination of a utility function. It then considers the uncertainties associated with the estimates of decision-criteria values and determines expected decision-criteria utilities. Weighting factors and regression constants are used to weight the decision-criteria utilities, and the optimum recycling technique is defined based on the maximum expected utility associated with a technique.

Probably the major benefit derived from the application of utility theory to decisions on pavement recycling is that it provides a logical and consistent method for systematically evaluating all the various factors that should be considered before a recycling decision can be made.

ACKNOWLEDGMENT

This study was conducted as part of a Ph.D. dissertation at the University of Washington. We wish to express our appreciation to R. L. Lytton of Texas A&M University for his guidance and helpful advice during the course of the study.

REFERENCES

1. R. de Neufville and R. L. Keeney. Use of Decision Analysis in Airport Development in Mexico City. In Analysis for Public Systems, MIT Press, Cambridge, MA, 1972.
2. Request for Proposals for the Development of a Commercial Supersonic Transport. Federal Aviation Administration, U.S. Department of Transportation, Aug. 15, 1963; Addendum 1, Oct. 4, 1963.
3. T. M. Oguara. Optimum Decision Making in Recycling of Pavement Materials. Univ. of Washington, Seattle, Ph.D. dissertation, 1978.
4. Recycling Materials for Highways. NCHRP, Project 20-5, Topic 8-01, draft, Dec. 1977.
5. R. L. Keeney and H. Raiffa. Decisions with Multi-

ple Objectives: Preferences and Value Trade Offs. Wiley, New York, 1976.
6. J. N. Vedder. Multiattribute Decision Making Under Uncertainty Using Bounded Intervals. In Multiple Criteria Decision Making, Univ. of South Carolina Press, Columbia, 1973.
7. D. A. Debose. Variable Selection Procedure: Implementing the Hocking-LaMotte-Leslie Method. Institute of Statistics, Texas A&M Univ., College Station, 1970.

Publication of this paper sponsored by Committee on Theory of Pavement Design.

Seasonal and Short-Term Variations in Skid Resistance

S. H. Dahir and J. J. Henry, Pennsylvania Transportation Institute, Pennsylvania State University, University Park

Preliminary results of a three-year program to investigate possible causes of seasonal and short-term variations in skid resistance are presented. The program was initiated in 1976 at the Pennsylvania State University to develop a method for predicting the lowest skid number a pavement is expected to attain during the year from a skid-resistance measurement made at any time during the year. Results of two years of testing indicate that skid-resistance variations of 15-30 SN_{40} occur at the changes of season from early to late fall and early to late spring. Higher numbers occur in the winter season. Skid numbers vary by about 25 percent between rainfall periods whether or not the surface is subject to significant traffic. Higher skid numbers are observed after heavy rainfall. Where traffic is low (average daily traffic < 1000), only minor macrotexture changes are noted from one season to another. On these pavements, therefore, microtexture changes are expected to cause the variations in skid resistance. Bituminous surfaces containing sandstone gravel aggregate are subject to small variations in skid resistance over time, whereas surfaces containing limestone and dolomite are subject to large variations. Temperature has been found to have insignificant effects on skid resistance.

Seasonal and short-term variations in skid-resistance measurements made according to the ASTM E 274 test method have been observed on Pennsylvania and other public highways (1, 2). These variations make it difficult to establish a maintenance management program in which skid resistance is an important factor. Day-to-day variations, apparently caused by rainfall patterns and local weather conditions, are superimposed on an annual cycle. At least in northern states, this annual cycle tends to be higher in winter through spring than in summer through fall. Frequent tests during the period from spring through fall reveal that the skid resistance of pavements may vary by as much as 25 percent during a single week.

To establish a means of interpreting skid-resistance data subject to seasonal and short-term variations, in 1976 the Pennsylvania Department of Transportation (PennDOT) initiated a three-year research program at the Pennsylvania Transportation Institute (PTI). The primary objective of the research is to investigate the possible causes of the variations and to develop a method for predicting the lowest skid number a pavement is expected to attain during the year from a skid-resistance measurement made at any time during the year. This paper summarizes the data and preliminary findings obtained during the first two years of the study.

TEST SITES

Six pavements on public roads in the State College, Pennsylvania, area were selected for the study according to the following criteria:

1. The pavements should be in a sufficiently small geographic area so that each could be tested within a short period of time by using the same skid tester.
2. As far as possible, the pavements should be subject to the same weather conditions.
3. The pavements should be at least three years old so that their surface characteristics would have stabilized.
4. The pavements should contain a variety of aggregates and mix designs and include at least one portland cement concrete pavement.
5. The pavements should have as wide a range of average daily traffic (ADT) as possible.

The selected pavements met all of these criteria. Their characteristics are summarized in Table 1.

During the 1976 test season, local weather conditions were monitored by rain gauges that were read at the time of skid tests. Since weather variations among the sites were small, the weather records provided by the Pennsylvania State University weather station were subsequently used as representative of the weather at all sites. Available daily weather data include the amount of rainfall, maximum and minimum temperatures, relative humidity, wind speed and direction, and cloud cover. In addition, the temperature of the pavement and the tire and ambient temperatures are measured at the time of skid testing.

Five test locations at each site are marked with a fluorescent orange square to assist the driver in conducting the daily skid tests at the same locations each day. A series of three nails have also been placed in the surface at each location so that pavement texture can be measured at the same spot each month.

At all locations, skid tests are made in the wheel tracks. At one site, skid tests are also made between the wheel tracks to verify whether skid-resistance variations occur where no significant tire traffic passes. Although skid resistance is expected to be higher between the wheel tracks, the behavior of short-term variations between the wheel tracks may provide further insight into the mechanisms involved.

DATA COLLECTION AND ANALYSIS

Daily Skid Testing

Skid-test measurements according to ASTM E 274 are made on all days when the pavement is dry. In addition, tire and pavement temperatures are continuously monitored by using radiometers mounted on the tester. Ambient and water temperatures are measured with appropriate thermometers. Skid tests are made at each of five marked locations at each site. The data are reported as the average of the five tests. Locked-wheel skid numbers at 64.5 km/h (40 mph) (SN_{40}) are shown in Figures 1-4. Also shown in the figures are the daily rainfall (in millimeters per 24-h period) and a five-day weighted rainfall function (WRF), which is defined as

$$WRF = R_1 + (R_2/2) + (R_3/3) + (R_4/4) + (R_5/5) \quad (1)$$

where

R_1 = rainfall on the day in question (mm),
R_2 = rainfall on the previous day (mm), and
R_n = rainfall (n - 1) days before the day in question ($1 < n < 5$).

From Figures 1-4, it can be seen that the short-term skid-resistance variations have a behavior qualitatively similar to that of the WRF. During the testing season, the variations between wheel tracks, where traffic is light, followed a pattern similar to that of variations in the heavily traveled wheel tracks (see Figure 5).

During the 1977 test season, skid tests were performed in the transient slip mode (3). Although this method provides SN_{40} data according to the ASTM E 274

Table 1. Description of road surfaces selected for testing.

Item	Test Section					
	University Drive	PA-45E	US-322N	PA-26N	PA-26S	PA-871
April 1976 ADT	6500	800	7000	2500	2500	1200
Construction year	1966	1961	1968	1969	1969	1973
Pavement Description	Base 20 cm limestone, surface 5 cm limestone	Pennsylvania 1B limestone, natural sand	Pennsylvania 1B limestone, natural sand	Pennsylvania 1B limestone, natural sand	Gravel, natural sand	Reinforced cement concrete, silica sand, 2B limestone, PDH design
Type	ID-2	ID-2	ID-2	SR-1A	SR-1A	Class AA RCCP
Asphalt (%)	6.2	6.2	5.8	6.0	7.5	
Percentage passing 2.36-mm sieve	45	45	45	17	17	
Sand-patch texture depth (mm)	0.50	1.35	0.46	1.4	1.6	0.69

Notes: 1 cm = 0.39 in; 2.36-mm sieve = no. 8 sieve.
PDH = Pennsylvania Department of Highways.

Figure 1. Skid-test and rainfall data for 1976 test season: University Drive, PA-45, and PA-26S.

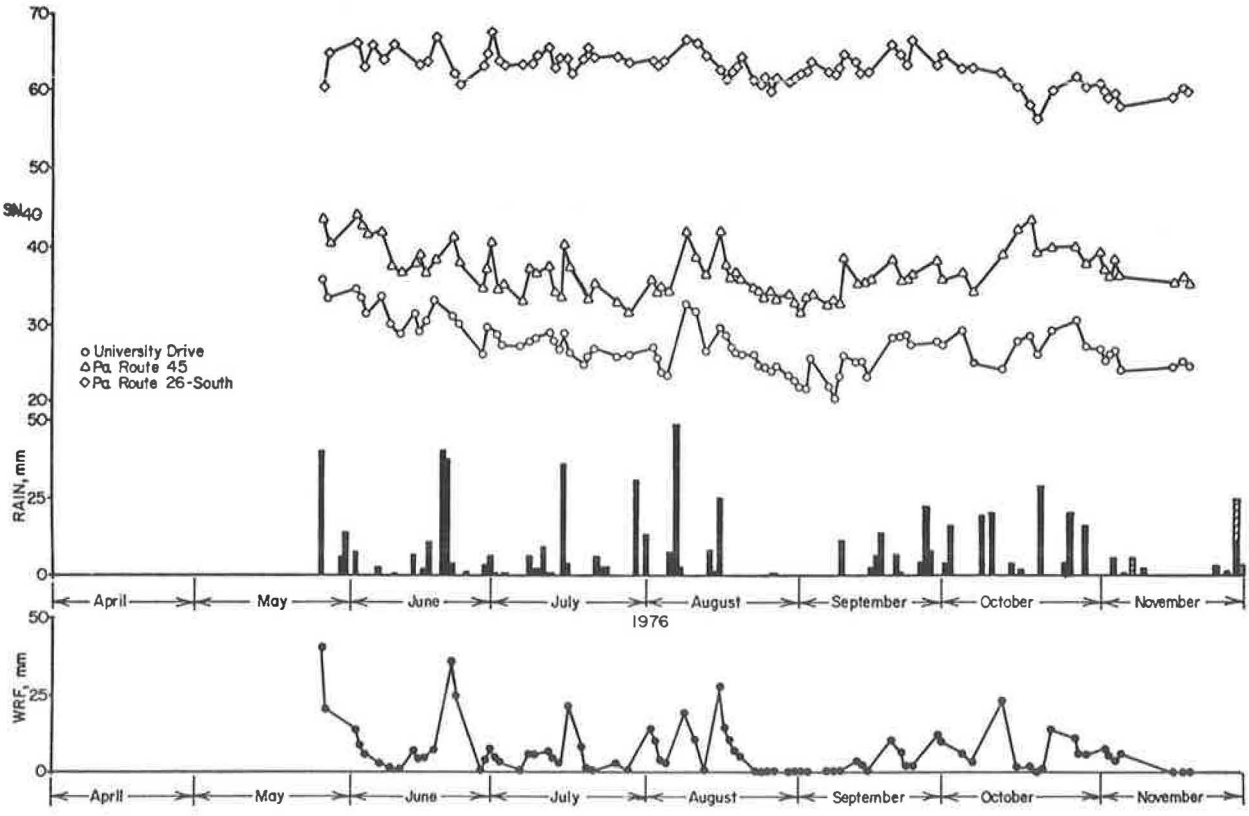

test method, it also provides brake slip numbers at 16, 32, and 48 km/h (10, 20, and 30 mph) that can be used to approximate SN_{10}, SN_{20}, and SN_{30}. These data, together with the locked-wheel skid number SN_{40}, were regressed to the Penn State model for the behavior of skid resistance (SN) with speed (V) (4):

$$SN = SN_0\, e^{(-PNG/100)V} \quad (2)$$

where SN_0 is the zero-speed intercept of a curve for skid number versus velocity and PNG is the percentage normalized gradient (4). The daily values for SN_0 and PNG are plotted versus rainfall data in Figures 6 and 7, respectively.

Figure 2. Skid-test and rainfall data for 1976 test season: PA-871 (concrete), US-322, and PA-26N.

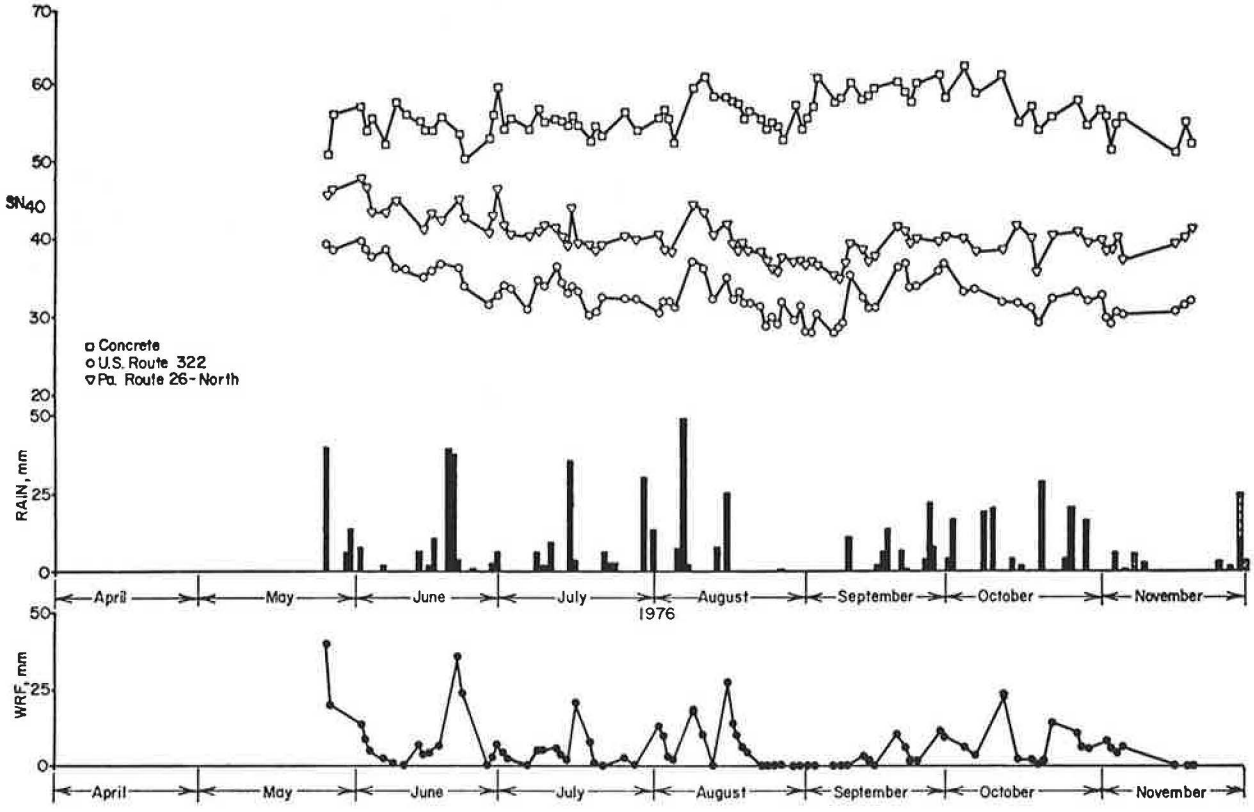

Figure 3. Skid-test and rainfall data for 1977 test season: University Drive, PA-45, PA-26S, and US-322 (between wheel tracks).

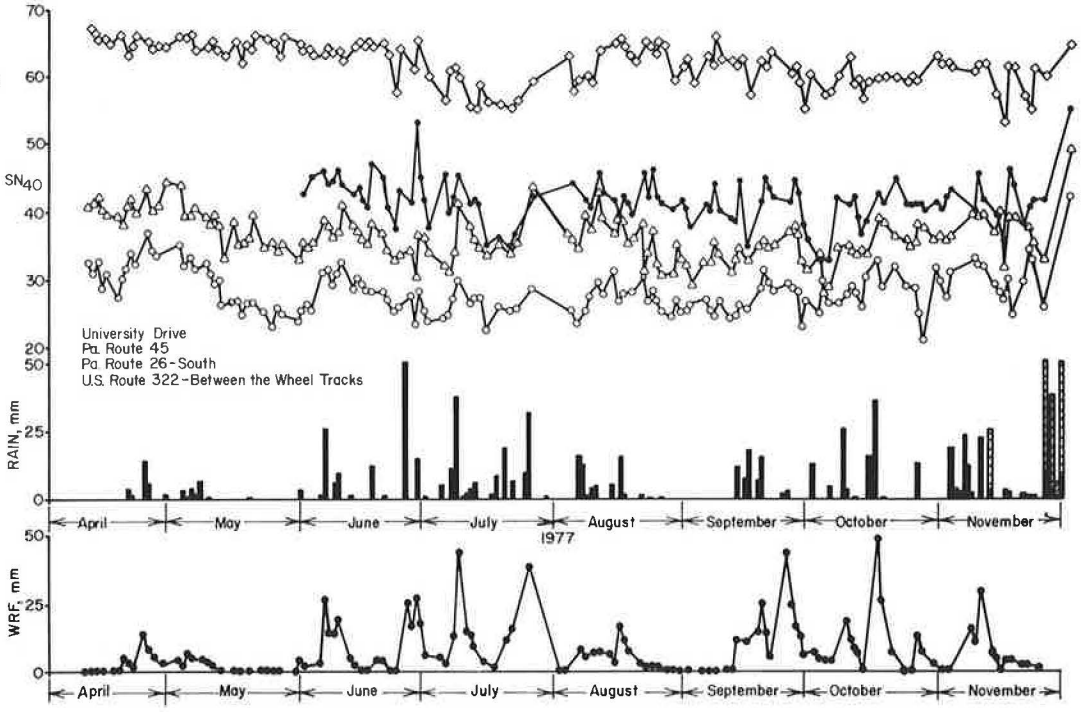

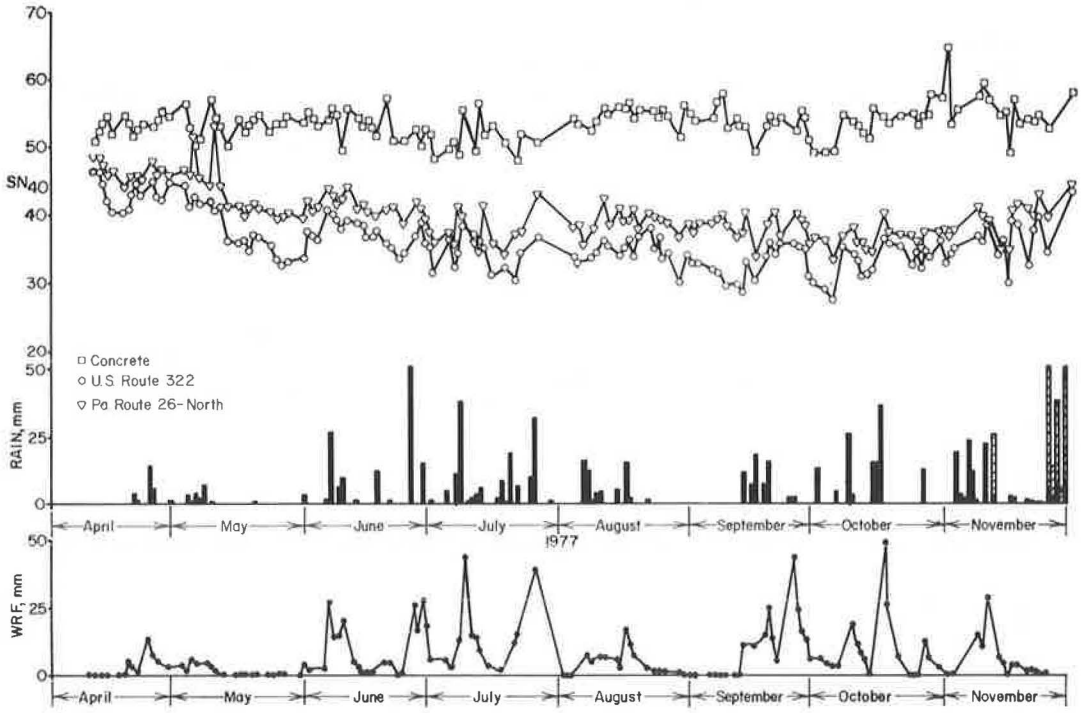

Figure 4. Skid-test and rainfall data for 1977 test season: PA-871 (concrete), US-322, and PA-26N.

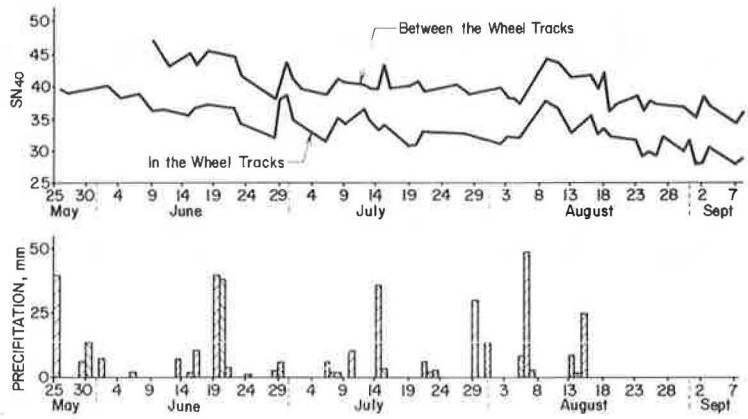

Figure 5. Skid-number history (1976) for US-322 between and in wheel tracks.

It is significant that the short-term variations of SN_0 amplify the variations noted in SN_{40}. In addition, the level of SN_0 decreases from early spring to a more or less stable level by mid-July for the seven surfaces tested. Since SN_0 correlates well with microtexture, one can conclude that early-season polishing for the pavements in this study reaches its terminal level by mid-July. The time required to reach terminal polishing is expected to depend on ADT and type of aggregate.

The variations in PNG that do exist have not yet been explained but, unlike the variations in SN_0, they do not appear to be related to rainfall history.

Texture Measurements

Texture measurements and other examinations of each test pavement have been conducted on a monthly schedule during the test season. During the 1976 season, four sets of measurements were obtained from July to October; in the 1977 season, six measurements were made from May to November. Two days were required to complete these measurements; each pavement section was closed to traffic for about 2 h each day. The tests were performed at the same spots on the pavements each month by referring to nails driven into the pavement during the first test session.

The following data were obtained on a monthly basis:

1. Macrotexture profile recordings;
2. Microtexture profile recordings;
3. Sand-patch texture depth;
4. British pendulum data (a) in the wheel track, (b) out of the wheel track before polishing, and (c) out of the wheel track after polishing with various abrasives;
5. Stereophotographs; and
6. Extracted aggregates for petrographic analysis and observation of particle surface changes.

The texture recordings were made by using PTI profile tracers that produce electrical signals proportional to the profile height. These signals were recorded on magnetic tape and were subsequently processed to provide data on root-mean-square profile height (RMSH). It has been determined that, for purposes of skid-resistance prediction, microtexture is best defined as consisting of asperities that have a wavelength of less than 0.5 mm (0.02 in) [or a space frequency greater than 2000 cycles/m (600 cycles/ft)] (4).

During the first two seasons, sand-patch tests were performed according to the American Concrete Paving Association method (5) but by various operators, and there is considerable variation in the data because of differences in operator technique. During 1978, these tests were performed by a single operator in strict adherence to the method.

British pendulum tests were performed according to ASTM E 303 in and out of the wheel tracks. In addition, the PTI modified portable reciprocating pavement

Figure 6. SN_0 data for 1977.

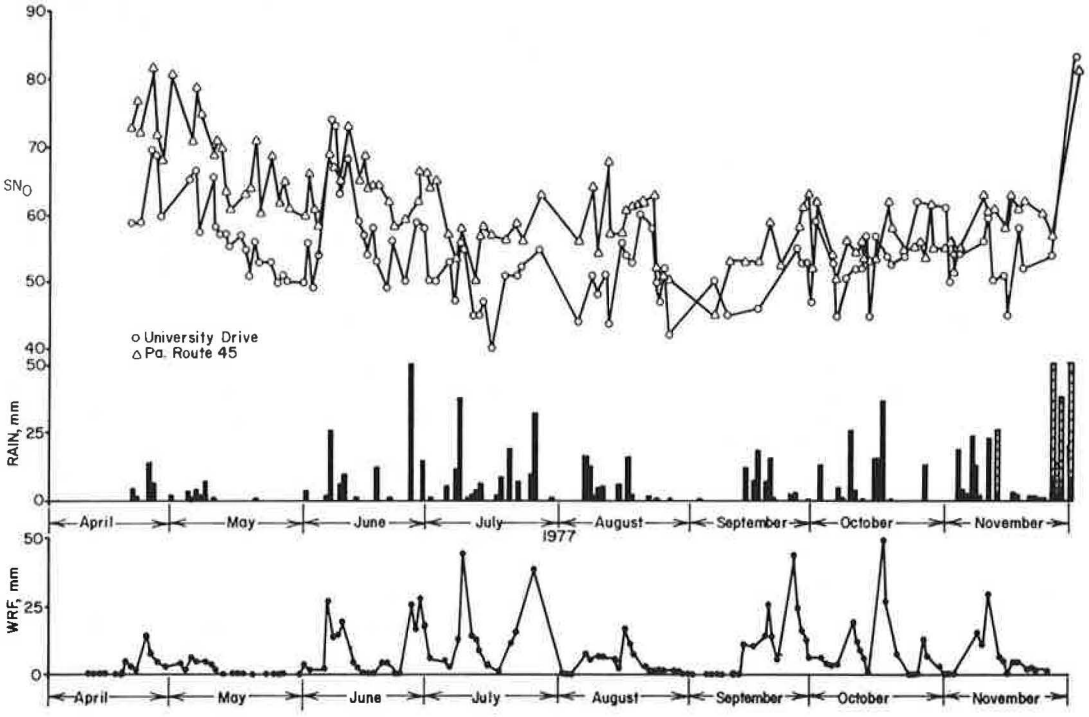

Figure 7. PNG data for 1977.

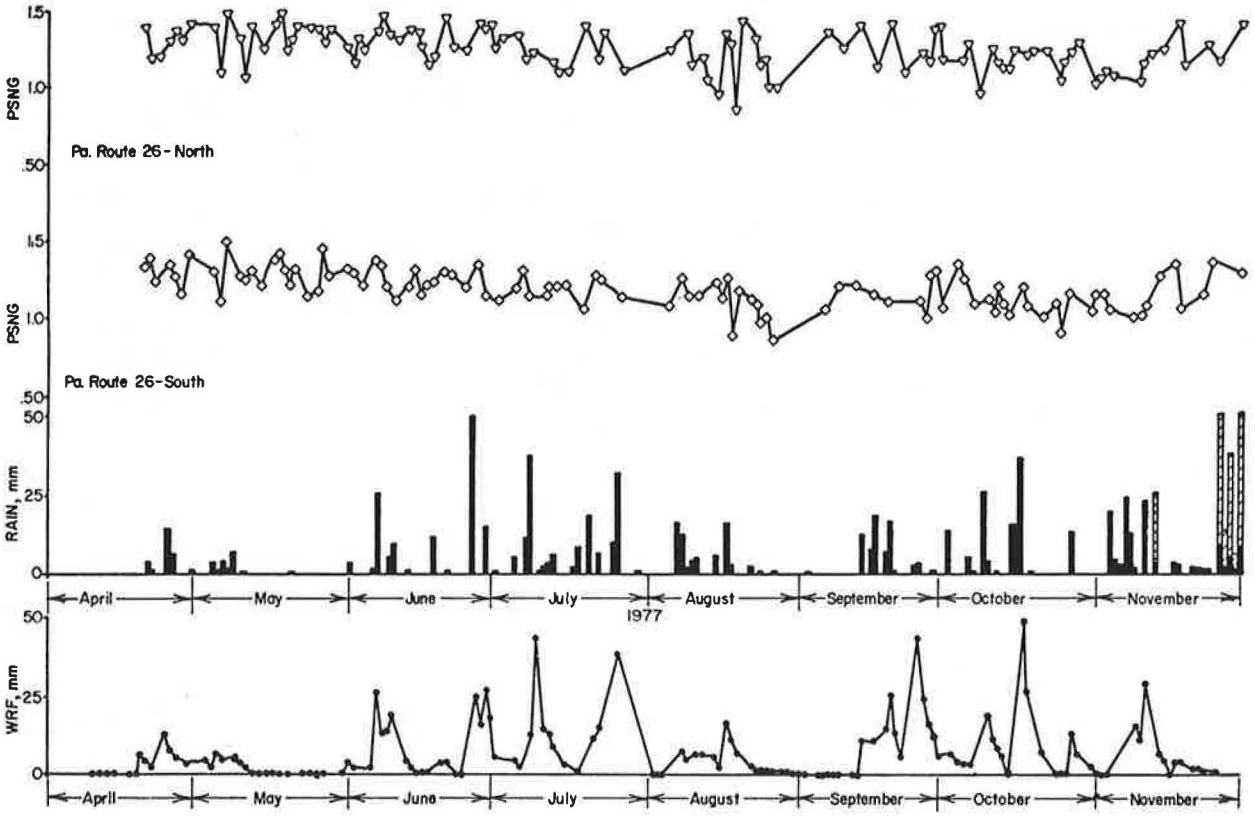

polisher (6) was used to polish spots on the pavement out of the wheel track with abrasives of various sizes. The polishing data are discussed later in this paper.

Stereophotographs of 35-mm slide pairs were taken by using the Schonfeld procedure as described in ASTM E 559. The stereophotographs provide a record of the surface condition. Although they are interesting and provide qualitative insight into pavement weathering and polishing, no quantitative analysis of these photographs appears promising at this time.

Visual Inspection and Petrographic Analysis of Aggregates

Individual stones taken from the five bituminous sections were inspected under magnifications of 4X and 10X. Stones taken from the same road section but in different months of the same year and in different months a year apart were compared, as were stones from different locations. The stones were inspected for (a) type, (b) appearance and cleanliness, and (c) texture and texture changes.

After many hours of inspection, it was difficult to detect any systematic, significant changes in texture. The stones did appear to have relatively clean surfaces in May but in June or July were fully or partially coated with an asphalt film. The surfaces tended to be cleaner but more shiny in August and September and still cleaner but less shiny in November. Based on this experience, it appears that quantitative texture information cannot be obtained through visual inspection of individual stones lifted from the pavement.

After inspection of the stones under magnification, thin sections were prepared from each set of stone samples. At least two thin sections from the stones taken from each of the five bituminous test locations were prepared and analyzed.

The petrographic analysis showed that the sandstone gravel used in the PA-26S section is superior to the limestone and dolomite used in the other sections. The gravel contained about 60 percent quartz grains and 40 percent sericite, clay, and other rock fragments. This combination permitted the gravel to maintain a high level of skid resistance after nine years in service (average SN_{40} = 63). An adjacent test section (PA-26N), in which the coarse aggregate was 30 percent dolomite, 5-10 percent quartz, and 60 percent limestone, had an average SN_{40} of 40. Both sections PA-26S and PA-26N were placed simultaneously, and the same design—an open-graded friction course—was used. The other three bituminous sections that contained limestone coarse aggregate averaged SN_{40} = 36, 35, and 27. The lowest value was on the surface where the coarse aggregate was practically pure limestone and contained only 10-15 percent dolomite but no hard siliceous minerals. In addition, the grain size was small: 10-100 μm (0.0004-0.004 in). These results confirmed previous observations on the polishing characteristics of surface aggregates (7).

Table 2. Results of 1977 pavement polishing.

Test Surface	Date	Particle Size at 3000 Cycles (μm)	Polished BPN	Actual Wheel-Track BPN (11/1/77)
University Drive	6/28	5	65	58
PA-45	6/28	15	59	58
PA-871	6/28	105	71	77
US-322	6/28	30	64	57
PA-26N	7/27	44	70	66
PA-26S	7/27	44	82	84

Note: 1 μm = 0.039 x 10^{-3} in.

Pavement Polishing

The British portable tester (ASTM E 303) was used to take measurements on the test sections in the wheel path and outside the wheel path next to the shoulder. The location out of the wheel path was then polished by using the Penn State portable pavement polisher (6) and water and silica abrasives of varying gradations to aid in the polishing process. Generally, 3000 cycles of the polisher were used. After polishing, the British portable number (BPN) was measured again, and the change from the prepolished number was observed. In addition, the BPN on the polished surface was compared with the BPN taken in the adjacent wheel path. The size of abrasive that caused the polished surface to attain a BPN close to that measured in the wheel path was assumed to be the abrasive closest in gradation or effect to the road dust that was causing the polishing by tires in the wheel path.

Abrasive sizes found in 1976 to produce polished-pavement BPNs close to those caused by tire polishing in the wheel path were retested on June 28, 1977. The abrasive sizes and their results are given in Table 2, where the BPN of the polished pavement in June is compared with the BPN measured on November 1, 1977, in the wheel path. The BPN of the polished pavement was used to predict terminal polish by traffic, which was assumed to have been reached by November 1.

Road Contamination

The friction characteristics of the road surface vary throughout the year because of factors such as pavement polishing and wear, amount of precipitation, and road-surface contamination. The size of contamination particles is mostly in the microtexture range, and they provide a form of lubrication for the road surface by preventing intimate tire-pavement contact. During rainfall, the action of water escaping from the tire-pavement interface causes a cleansing of the road surface. This cleansing washes away the fine dust created by road polishing and, soon after a heavy rainfall, increases the skid resistance of the road surface.

To determine the nature of pavement contamination, a vehicle-mounted device was designed and constructed to collect the loose contamination particles and classify them according to size. In 1977, the particles were collected daily, weather and equipment permitting, during the last week in September and through the month of October. The vacuum device was attached to the front bumper of the PTI road-friction tester. Collection was carried out in the inner wheel track of a 150-m (500-ft) section of the PA-45 test pavement, on which daily skid tests were conducted. The dust-collection data are given in Table 3.

Before the dust collection started, four impaction collection filters, a backup filter, and a preseparator cup were weighed to the nearest 10 000 th of a gram on a Mettler balance. After they were weighed, the filters were placed in the cascade impactor, and the collection device was assembled on the truck. The speed was maintained at 20 km/h (12.5 mph) through the test area. At the end of the test section, the impactor was removed from the bumper and stored in the truck. The impactor was then taken to the laboratory, where the filters and preseparator were weighed.

In addition to loose particulate contamination, which can be removed and analyzed, there were oils or lubricants, which cannot be easily removed. The effect of oils was investigated in the laboratory by using the British portable tester. A small amount [2 ml (0.0005 gal)] was applied to a Society of Automotive Engineers

vary by about 11°C (20°F). But the skid resistance (also plotted in Figure 10) shows a very slight, insignificant variation. From these results it may be concluded that temperature variations of the magnitude experienced in the tests do not significantly affect skid-resistance measurements.

CONCLUSIONS

Based on the findings of the first two years of the test program, the following preliminary conclusions have been reached.

1. Significant variations in the skid resistance of pavement surfaces (15 to 30 SNs) occur in Pennsylvania from one season to another, particularly as the seasons change from early fall to late fall and from early spring to late spring. Periods of cold, rainy, and snowy weather improve skid resistance, whereas warm, dry periods reduce the friction characteristics of the surface. The zero-speed skid-number intercept SN_0, which is related to microtexture, appears to be highest in early spring and to decrease gradually to a stable level by mid-July, after which its level remains fairly constant until the next cold, snowy season starts in late November or early December. This behavior would indicate that the test pavements reach a stable level of polishing by July.
2. Within any season, particularly within the period from April to December, daily or weekly variations in skid resistance of as much as 25 percent occur according to changes in rainfall. Higher skid numbers follow an abundance of rainfall whether traffic is heavy or light. In addition, the greatest changes appear to be caused by the amount and/or the duration of rainfall immediately before a measurement. The proposed WRF appears promising as a predictor of short-term cycles.
3. Temperature changes within short periods—e.g., within 30 h—appear to have little or no effect on pavement skid resistance.
4. Minor changes in the macrotexture may occur from one season to the next, but on stable pavements (three years or older) these changes and their effects appear to be negligible.
5. Surfaces made from aggregates that exhibit differential wear (sandstone gravel, for example) exhibit relatively small variations in skid resistance. Surfaces made from polish-susceptible aggregates such as limestones and dolomites undergo pronounced seasonal and short-term, rain-related variations in skid resistance.
6. BPN values are strongly correlated with values of the zero-speed skid-resistance intercept SN_0 measured after periods of rain. It is believed that the BPN conditioning procedure (ASTM E 303) produces data that correspond to the clean condition of the pavement.

ACKNOWLEDGMENT

This paper is based on research sponsored by PennDOT in cooperation with the Federal Highway Administration, U.S. Department of Transportation. The research has been conducted at the Pennsylvania Transportation Institute, Pennsylvania State University. Personnel from PennDOT and Pennsylvania State University have assisted in the research. Particularly valuable assistance was contributed by W. L. Gramling, R. K. Shaffer, and R. H. Howe of PennDOT.

The contents of this paper reflect our views, and we are responsible for the facts and accuracy of the data presented. The contents do not necessarily reflect the official views or policies of the Pennsylvania Department of Transportation or the Federal Highway Administration. This paper does not constitute a standard, specification, or regulation.

REFERENCES

1. W. L. Gramling and J. G. Hopkins. Skid Resistance Studies—Aggregate Skid Resistance Relationships as Applied to Pennsylvania Aggregates. Pennsylvania Department of Transportation, Harrisburg, Final Rept., 1974.
2. J. M. Rice. Seasonal Variations in Pavement Skid Resistance. Public Roads, Vol. 40, No. 49, March 1977.
3. V. R. Shah and J. J. Henry. Determination of Skid Resistance-Speed Behavior and Side Force Coefficients of Pavements. TRB, Transportation Research Record 666, 1978, pp. 13-18.
4. M. C. Leu and J. J. Henry. Prediction of Skid Resistance as a Function of Speed from Pavement Texture Measurements. TRB, Transportation Research Record 666, 1978, pp. 7-11.
5. Interim Recommendation for Construction of Skid Resistant Concrete Pavement. American Concrete Paving Assn., Oak Brook, IL, Tech. Bull. 6, 1976.
6. S. H. Dahir, W. E. Meyer, and R. R. Hermon. Laboratory and Field Investigation of Bituminous Pavement and Aggregate Polishing. TRB, Transportation Research Record 584, 1976, pp. 1-13.
7. S. H. Dahir. Petrographic Insights into the Susceptibility of Aggregates to Wear and Polishing. TRB, Transportation Research Record 695, 1978, pp. 20-27.

Publication of this paper sponsored by Committee on Surface Properties-Vehicle Interaction.

Table 3. Data on 1977 dust collection on PA-45.

Date	Weight (g)						
	Preseparation Stage	First Stage	Second Stage	Third Stage	Fourth Stage	Backup	SN_0
9/21	0	0.087	0.030	0.028	0.007	0.021	58.7
9/29	0	0.147	0.049	0.034	0.007	0.061	53.2
9/30	0	0.115	0.056	0.033	0.011	0.035	58.8
10/3	0.27	0.101	0.033	0.025	0.007	0.028	58.5
10/4	0.518	0.140	0.048	0.025	0.009	0.043	53.6
10/5	0.314	0.122	0.036	0.022	0.007	0.027	54.6
10/7	0.525	0.104	0.033	0.021	0.006	0.029	58.6
10/10	1.545	0.189	0.046	0.038	0.010	0.041	53.2
10/11	0.491	0.049	0.025	0.014	0.003	0.016	60.6
10/12	1.481	0.181	0.053	0.027	0.009	0.038	52.5
10/13	0.696	0.154	0.052	0.033	0.014	0.029	52.2
10/14	0.188	0.066	0.027	0.022	0.009	0.011	60.3
10/17	0.320	0.050	0.032	0.016	0.007	0.025	61.4
10/18	0.451	0.051	0.030	0.018	0.014	0.023	59.7
10/21	0.602	0.126	0.052	0.033	0.010	0.033	55.9
10/24	1.014	0.239	0.083	0.052	0.033	0.058	54.4
10/25	0.782	0.254	0.080	0.050	0.015	0.052	54.2
10/26	0.486	0.213	0.073	0.046	0.011	0.032	53.5
10/28	0.249	0.082	0.032	0.018	0.007	0.013	56.7
10/31	0.195	0.109	0.049	0.023	0.009	0.015	56.2
11/2	0.211	0.092	0.022	0.013	0.003	0.011	60.1
11/14	0.471	0.296	0.091	0.048	0.014	0.051	53.7

Note: Particle sizes = preseparation stage, 50 μm; first stage, 7-50 μm; second stage, 3.3-7 μm; third stage, 2-3.3 μm; fourth stage, 1-2 μm; backup, <1.1 μm.

Figure 8. Effects of SAE 30 oil on BPN.

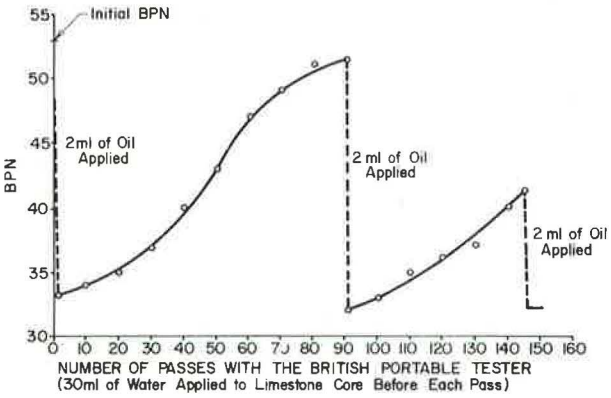

SAE 30 oil of 150-mm (6-in) diameter core sample, which dramatically reduced the BPN. Subsequent repeated tests were made until the oil was removed by the action of the slider and water. Reapplication of oil reproduced the low value. The results of the experiment are shown in Figure 8.

By cleaning the surface and by "conditioning" the slider when BPN is measured in accordance with ASTM E 303, the effects of contaminants can be eliminated. During the 1978 season, British pendulum tests were conducted on a monthly schedule, and the values obtained before the cleaning and conditioning of the pavement were also recorded. Only "clean" BPN values are available for 1976 and 1977. One would expect them to be related to the skid resistance of the clean pavement after a rainfall. To test this hypothesis, the mid-summer high levels of SN_0 for each pavement were noted from the data in Figure 4. These high levels were reached after rainfall during the months after the pavements were polished to a stable level. The BPN data from September 1977 and the high-level SN_0 data for the seven test sites are correlated in Figure 9. A high coefficient of correlation (r = 0.97) was obtained.

Temperature Effects

To investigate the effects of temperature, a test was performed in September 1976 in which the skid resistance

Figure 9. High-level SN_0 versus September BPN for 1977.

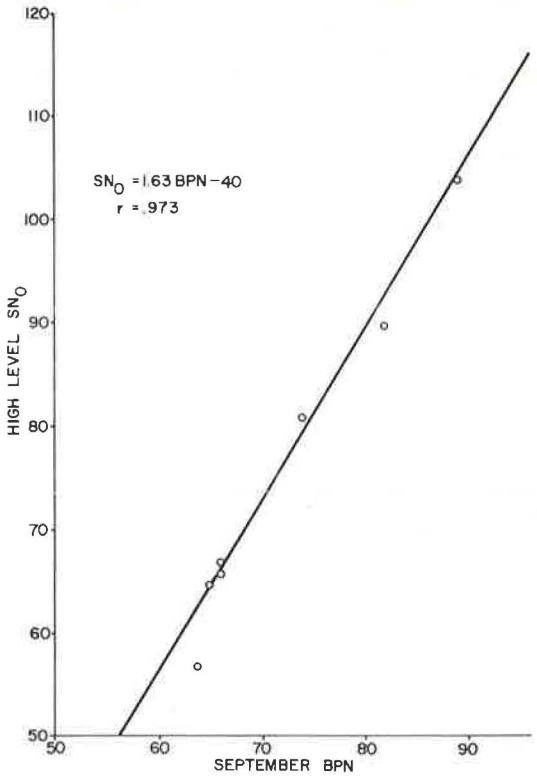

Figure 10. Temperature effects of SN_{40} on test surfaces.

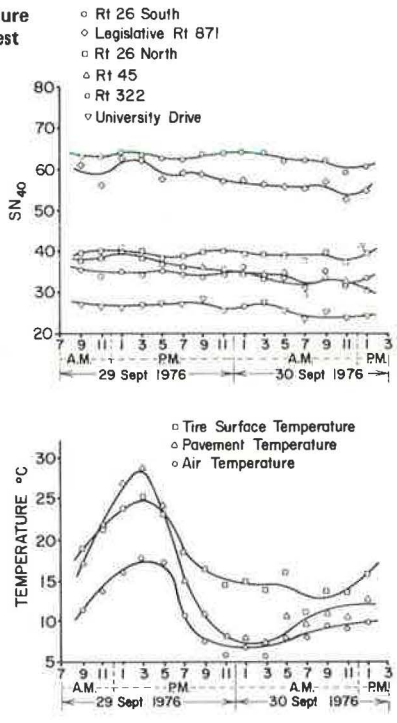

of each test surface was measured every 2 h for a period of 30 h. During such a short period of time, the only major test parameters that are expected to change significantly are the temperatures of the air, the pavement, and the tire. Air, pavement, and tire temperatures measured during this test are shown in Figure 10. The pavement shows a temperature variation of about 22°C (40°F); the air and tire temperatures